

Editor-in-Chief B.E.Paton

Editorial board:

Yu.S.Borisov	V.F.Grabin
A.Ya.Ishchenko	V.F.Khorunov
B.V.Khitrovskaya	I.V.Krivtsun
S.I.Kuchuk-Yatsenko	
Yu.N.Lankin	V.K.Lebedev
V.N.Lipodaev	L.M.Lobanov
V.I.Makhnenko	A.A.Mazur
O.K.Nazarenko	I.K.Pokhodnya
I.A.Ryabtsev	Yu.A.Sterenbogen
N.M.Voropai	K.A.Yushchenko
A.T.Zelnichenko	

International editorial council:

N.P.Alyoshin	(Russia)
U.Diltey	(Germany)
Guan Qiao	(China)
D. von Hofe	(Germany)
V.I.Lysak	(Russia)
N.I.Nikiforov	(Russia)
B.E.Paton	(Ukraine)
Ya.Pilarczyk	(Poland)
P.Seyffarth	(Germany)
G.A.Turichin	(Russia)
Zhang Yanmin	(China)
A.S.Zubchenko	(Russia)

Promotion group:

V.N.Lipodaev, V.I.Lokteva
A.T.Zelnichenko (exec. director)

Translators:

I.N.Kutianova, V.F.Orets,
T.K.Vasilenko, N.V.Yalanskaya

Editor

N.A.Dmitrieva
Electron galley:
I.S.Batasheva, T.Yu.Snegiryova

Address:

E.O. Paton Electric Welding Institute,
International Association «Welding»,
11, Bozhenko str., 03680, Kyiv, Ukraine

Tel.: (38044) 287 67 57

Fax: (38044) 528 04 86

E-mail: journal@paton.kiev.ua

http://www.nas.gov.ua/pwj

State Registration Certificate
KV 4790 of 09.01.2001

Subscriptions:

\$324, 12 issues per year,
postage and packaging included.
Back issues available.

All rights reserved.

This publication and each of the articles
contained herein are protected by copyright.
Permission to reproduce material contained in
this journal must be obtained in writing from
the Publisher.

Copies of individual articles may be obtained
from the Publisher.

CONTENTS

SCIENTIFIC AND TECHNICAL

- Lankin Yu.N.** Automatic control of the MAG welding process
with periodic short circuiting of arc gap (Review) 2
- Kulik V.M. and Savitsky M.M.** New procedure for evaluation
of cold cracking resistance of hardening steel welded joints 8
- Nazarenko O.K. and Lanbin V.S.** Analog and microprocessor
control of the welding electron beam current 14
- Labur T.M., Poklyatsky A.G. and Grinyuk A.A.**
Improvement of fracture resistance of joints of alloy 1420
produced by nonconsumable-electrode argon-arc welding
with forced oscillations of the weld pool 18
- Dyadin V.P.** Influence of pre-deformation on impact
toughness of Charpy sample in fracture 22

INDUSTRIAL

- Shelyagin V.D., Khaskin V.Yu., Siora A.V., Bernatsky
A.V., Goncharenko E.I. and Chizhskaya T.G.** Gas-shielded
laser and laser-arc welding of steels 27

NDT OF WELDED JOINTS

- Kuchuk-Yatsenko S.I., Radko V.P., Kazymov B.I.,
Zyakhor I.V. and Nikolnikov A.V.** Peculiarities of detection of
defects in FBW joints on pipes by ultrasonic inspection 31

ECONOMY OF WELDING PRODUCTION

- Bernadsky V.N. and Makovetskaya O.K.** Welding
fabrication and welding equipment market in modern economy 35

BRIEF INFORMATION

- Sidorets V.N. and Zhernosekov A.M.** Computer simulation
of pulsed-arc systems 40
- Savitsky M.M., Savichenko A.A., Kulik V.M., Lupan A.F.,
Melnichuk G.M., Chertorylsky L.A., Golub N.A. and
Suprunenko V.A.** Light-weight welded cylinders for motor
transport 43
- News 44
- Thesis for a scientific degree 45

NEWS

- Our congratulations 46
- Developed at PWI 39



AUTOMATIC CONTROL OF THE MAG WELDING PROCESS WITH PERIODIC SHORT CIRCUITING OF ARC GAP (REVIEW)

Yu.N. LANKIN

E.O. Paton Electric Welding Institute, NASU, Kiev, Ukraine

A review of publications on automatic control of the process of CO₂ welding with short circuiting of the arc gap and control algorithms at each stage of the welding cycle is done.

Keywords: CO₂ welding, short circuits, automatic control, self-regulation, process stability, spattering, transfer of drops, current pulse

The main mechanized method of welding is a semi-automatic gas-shielded consumable electrode welding. Carbon dioxide is widely used as a shielding gas due to its cheapness. At low current and fall of voltage across the arc CO₂ welding proceeds with periodic short circuits (SC) of the arc gap, during which molten metal of the electrode is transferred into the weld pool. Due to low heat input, contact mass transfer, small size of the drops and the pool, this method is widely used in welding of low-thickness metals in all spatial positions, and medium- and high-thickness metals in the position, different from the downhand one. For CO₂ welding the simplest rectifiers with a flat dipping external characteristic and a choke, serially connected to the welding circuit, are used. Flat dipping characteristic of the rectifier stipulates self-regulation of the arc, and the choke limits rate of current increase during SC. Typical oscillograms of the current and the voltage (Figure 1) are of a pulsing character. Energy, accumulated in the choke during SC, is used for melting of the electrode at arcing. Open-circuit voltage of the rectifier, consumable electrode feed rate and inductivity of the choke are used as regulated parameters. However, besides advantages the welding process has significant shortcomings. Be-

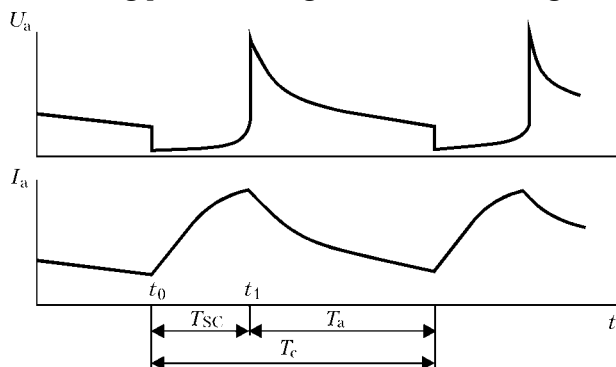


Figure 1. Characteristic oscillograms of voltage and current in CO₂ welding

© Yu.N. LANKIN, 2007

cause of SC in the arc gap significant spattering of the metal occurs, and low heat input is characterized by low penetration capacity.

Significant efforts were applied within last decades for removal of shortcomings of CO₂ welding with SC. First of all, they concern development of a new class of pulsed power sources, characterized by increased response rate and equipped with systems for controlling shape of the current and the voltage within each cycle of formation and transfer of the drop, according to the information received from the process. Such sources are almost 2 times more expensive than traditional ones, but they ensure quality of welding, comparable with welding in argon.

By now the idea about «ideal» welding cycle has been developed (Figure 2), which should be ensured by the automatic control system. At different stages of the cycle different control algorithms are required.

Main tasks of control systems for CO₂ welding with SC of the arc gap are reduction of the metal spattering more than 2 times; increase of the welding process stability; compensation of excitations, which act on the welding process.

Control at initial moment of the arc gap SC. In initial stage of SC t_0 (Figure 2), the smallest radius of formed bridge of molten metal is in the place of contact of the drop with the pool. Electrodynamic forces of the current, which passes through the bridge, prevent transfer of the drop into the pool under action of the surface tension forces. Moreover, they may even cause throw off of a drop from the pool surface, and a passing current may cause overheating and explosion of the bridge being formed. Whereby, as shows high-speed filming [1], a drop, when it tears off from the electrode, flies away in the form of spatter or remains on the end of the electrode and transits into the pool during one of the following SC. It follows from the theoretical analysis that the lower is radius of a drop and the higher is the current, the higher is possibility of the drop throw-off [2].

For reducing spattering, when a drop touches surface of the pool, and increasing stability of the welding process, welding current is reduced before SC of the arc gap or at once after its origination. A signal, in-



dicating beginning of SC, is sharp reduction of arc voltage by the total of anode and cathode voltage fall, which for CO₂ welding constitutes $U_{an-c} = 19\text{--}20\text{ V}$ [3]. Change of the arc voltage at SC occurs very quickly --- within $20 \cdot 10^{-9}\text{ s}$ [4].

Prof. I. Zaruba was the first to implement idea of SC current limiting in 1970 [5] and later repeatedly addressed to it [1]. In [6] base current of the arc and SC current were established at a very low level (6--12 A) in such way that transition of a drop mainly occurred under action of surface tension forces. Melting of the electrode was performed under action of a short high-current pulse.

The authors of [7] were the first to perform short-term reduction of current at the beginning of SC in 1980 (Figure 3). According to their data, reduction of current down to 2--10 A for the period of 0.7--1.0 ms at the beginning of each SC allows practical removing of short-term SC and increasing 2--3 times stability of the process, estimated by variation coefficient of the SC duration. Later this algorithm was used by different researchers without any changes [8--17]; difference consisted only in the equipment, which was used for its implementation. First thyristors were used, which bridged welding torches, or a serially connected resistor. At present quick-response transistorized inverter power source is used or instead of the thyristor a transistor is used, which bridges a serially connected to the welding circuit resistor.

Control of metal transfer at SC stage. Metal of a drop, having rather big size (in comparison with diameter of the electrode), may be transferred into the weld pool even without current --- only under action of surface tension forces. According to estimates of authors of [6], critical height and diameter of a drop constitute $1.2d_{el}$ and $1.4d_{el}$ respectively (the authors practically implemented such process in CO₂ welding). In [18] critical height of the bridge is estimated as $1.4d_{el}$.

For reducing SC time and guarantying rupture of the bridge, current is passed through it, interaction of which with its own magnetic field causes force, directed inside to the bridge axis. This force, proportional to the square of current density in this section, enables reduction of diameter of the bridge. If shape of the latter is different from cylindrical one, axial forces occur in addition to the radial ones, which cause flow of metal in the direction from a smaller diameter to a bigger one and lead to reduction of diameter of the narrowest place in the bridge (pinch effect).

Time of the current pulse application after beginning of SC is of high significance. At the first stage the smallest diameter of molten bridge is near the contact with the weld pool. In this case pinch effect is harmful, because it decelerates increase of the area of the drop contact with the pool and thus delays transfer process. Moreover, diameter of the bridge neck may even reduce down to zero, and transfer of the drop material into the pool will not take place. By means of flow of the bridge material into the weld

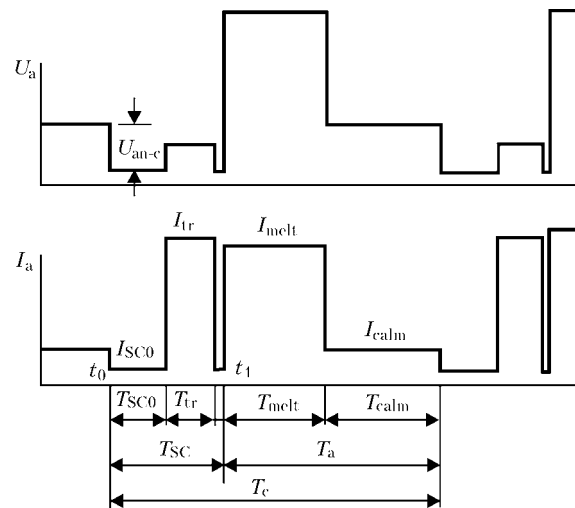


Figure 2. «Ideal» cycle of CO₂ welding

pool, minimum diameter of the bridge increases from zero (at the instant of contact) up to a certain maximum, and then again reduces down to zero (rupture of the bridge occurs), whereby position of minimum radius shifts in direction of the item (Figure 4) [19]. Only at this stage electromagnetic forces enable transfer of a drop. Usually pulse of SC current is fed with a fixed delay time $T_{SC0} = 0.6\text{--}1.0\text{ ms}$ after beginning of SC (see Figure 3) [7, 8, 12, 15, 17, 20]. In our opinion, it is most advisable to apply transfer current pulse after radius of the bridge neck achieves maximum value (Figure 4) or, which is the same, at minimum resistance of the electrode-part circuit (zone B, Figure 5 [19]). In this case transfer current maximally reduces SC time. This conclusion is confirmed experimentally [8] and by physical [9] and computer simulation of the molten bridge rupture (Figure 6) [10].

As far as electromagnetic forces are proportional to square of the current, it is advisable to set SC current at maximum allowable for this power source level. It is evident that in this case the shortest time of the drop transfer is ensured by rectangular pulse of SC current. The only positive feature of saw-tooth [12, 21, 22] and trapezoidal [7, 15, 21] current pulses is that they have reduced current at initial stage of

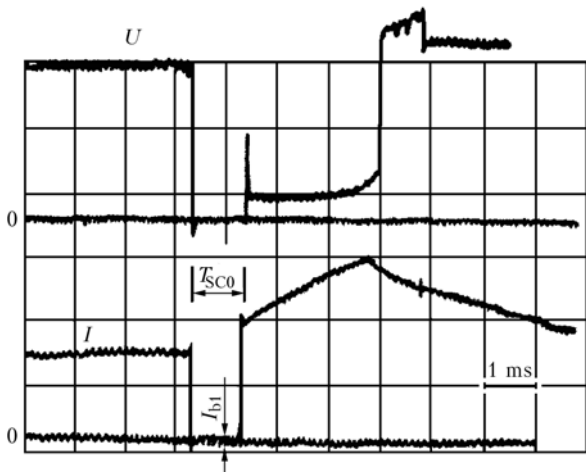


Figure 3. Oscillograms of voltage and current in CO₂ welding with switching of current at beginning of SC [7]

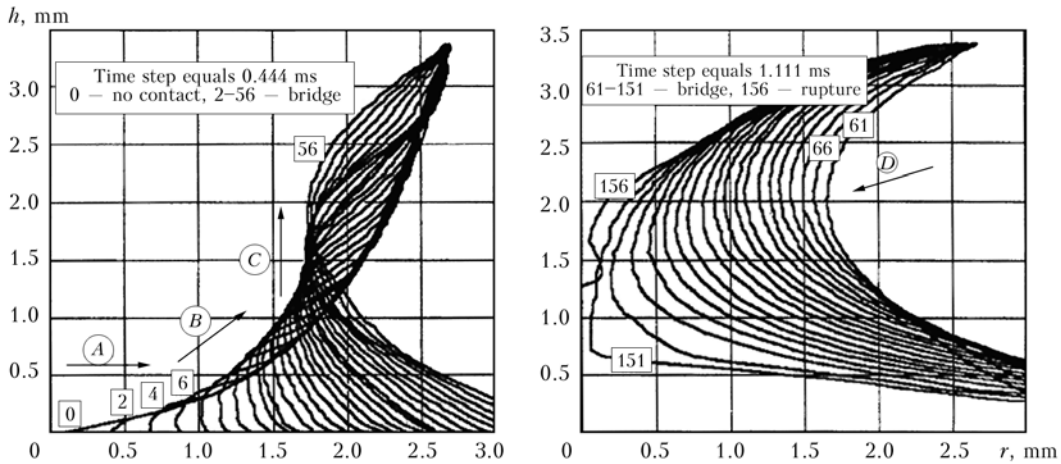


Figure 4. Dynamics of molten bridge profile change (flowing over of water drop) [19]

SC at $T_{SC0} \sim 0$, when the current just prevents transfer of the drop.

Control of the process of the molten bridge rupture. Rupture of the molten bridge under current is accompanied by electric explosion and is the main reason of splashing in CO₂ welding with SC of the arc gap. For reducing this shortcoming it is necessary to reduce as much as possible current through the bridge during its rupture.

The first, who announced in 1970 about this method of reducing spattering, was I.I. Zaruba [23], and in 1971 he published results of its practical implementation [5]. According to this method, SC current pulse of fixed duration started with a delay after occurrence of SC and terminated before rupture of the bridge (Figure 7). Later authors of [20] used transfer pulse of variable duration. It was automatically disengaged, when voltage fall across the bridge increased up to the assigned level due to thinning of the bridge before its rupture.

The next step was made by S.I. Pinchuk et al. [24] in 1976. A device was designed, which reduced at a fixed time interval SC current down to 2–10 A immediately before rupture of the bridge, when voltage on it started to quickly increase and achieved values 8–12 V (Figure 8) (in [5, 20] minimum SC current remained at the level 100–130 A).

Since that time nothing principally new was proposed, and in all subsequent publications method of I.I. Zaruba was used in its pure form or in the form,

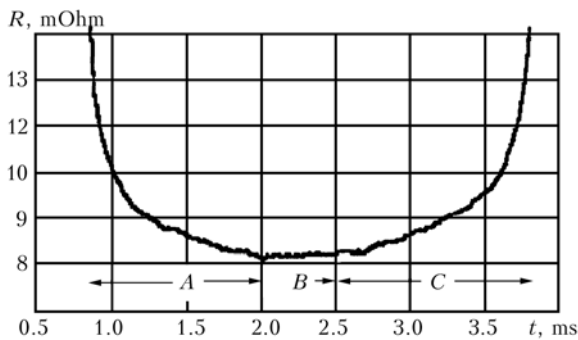


Figure 5. Change of resistance of the electrode-part circuit during SC ($I = 190$ A, $v_w = 5.2$ m/min, $L = 14$ mm, wire of 1.2 mm diameter) [19]

improved by S.I. Pinchuk [7, 12, 16, 22, 25, 26]. Main improvements concerned equipment, by means of which this method was implemented. Only E.K. Stava [15] used not the voltage fall within the spacing current lead-component part for determining the instant of launching command for reduction of SC pulse current, but the rate of its change. It makes the hardware or software more complex, but reduces influence of resistance of the electrode extension and the component part. Voltage fall within the spacing current lead-component part has the form

$$U_{c-p}(t) = I(R_{el} + R_{br}(t) + R_p). \quad (1)$$

As far as during SC only $R_{br}(t)$ changes, then

$$\frac{dU_{c-p}}{dt} = \frac{d(IR_{br})}{dt} \quad (2)$$

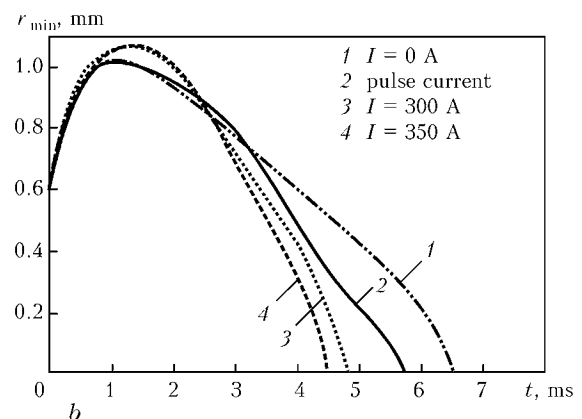
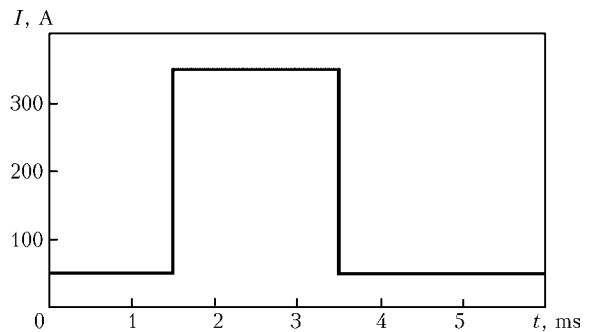


Figure 6. Influence of transfer current (a) and minimum radius of bridge r_{min} (b) on SC duration [10]

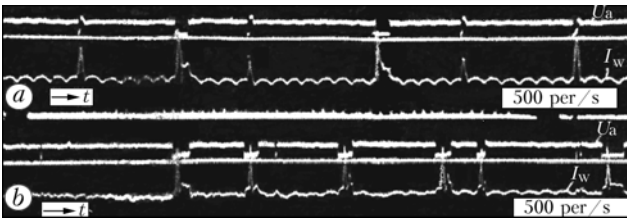


Figure 7. Oscillograms of voltage and current in CO₂ welding: a, b — current pulses are fed at beginning and in middle of long SC respectively [5]

and state of the bridge before its rupture is determined more accurately (however, beginning of the analysis dU_{c-p}/dt has to be delayed by 100 μ s after engagement of SC current pulse [27]). Otherwise control scheme may disengage SC current pulse not immediately before rupture of the bridge, but at once after its engagement.

In our opinion, for determining instant of disengagement of the transfer current pulse it is best of all to use rate of change of the bridge resistance as a parameter, which does not depend upon the current.

Sharp reduction of diameter of the bridge neck before its rupture lasts for about $10 \cdot 10^{-6}$ s, and avalanche-like reduction of the neck (its rupture) — for about $0.1 \cdot 10^{-6}$ s [4]. If SC current starts to be reduced too late and rate of its reduction is low, rupture of the bridge will occur at a significant current with high probability of spattering. If SC current is reduced too early, the probability increases that the bridge will not disrupt at all. So, the control system should ensure reliable determination of the instant, when irreversible reduction of diameter of the bridge neck begins, and significantly reduce SC current before its rupture. This task, probably, is not completely solved till now.

Control of the electrode melting, growth and size of a drop. After rupture of the bridge arc is ignited and starts melting of the electrode by the energy, which is supplied both from the arc and from the electrode extension due to the current, passing in it. Task of the control system at this stage is ensuring of producing an assigned volume of the drop irrespective of excitations, acting on the process (fluctuations of the electrode feed rate, voltage of the network, electrode extension, distance from the torch to the item, etc.).

Usually for CO₂ welding with SC and constant wire feed rate, sources with flat dipping characteristic are used. Stability of the process in this case is ensured due to self-regulation property of the system of voltage source–consumable electrode–arc. When length of the arc reduces, current automatically increases, which causes increase of the arc gap, and vice versa. On similar principle state-of-the-art Japanese inverter power sources for CO₂ welding with SC [8, 13, 16] are based. The source is switched over in them during SC into the current control mode, and for the arcing period — into constant voltage mode (Figure 9) [13].

The most perfect sources use pulse mode for controlling formation of the molten metal drop. At the

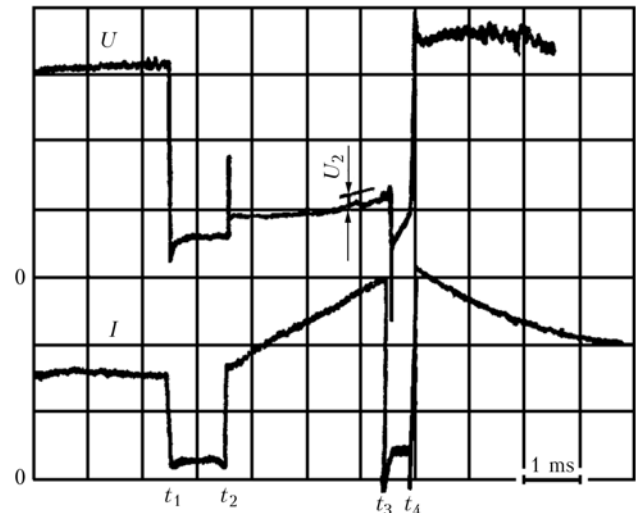


Figure 8. Oscillograms of voltage and current in stabilized transfer of metal with limitation of bridge explosion energy [24]

first stage of the arcing, intensive melting of the electrode by high current occurs till achievement of the assigned drop volume, and then the current significantly reduces. Forces, which act on the drop located on the electrode end and try to displace it to side surface of the electrode, reduce, and the drop occupies coaxial with the electrode position. Under action of the surface tension forces shape of the drop approaches the form of a correct sphere, which creates favorable conditions for smooth transfer of the drop into the weld pool.

In order to minimize chaotic movement of the drop, its size should be small, for example, not more than diameter of the electrode [28]. In opinion of specialists of the Lincoln Electric [15], average size of the molten spherical drop on the electrode end should be $1.2d_{el}$ for good transfer. Authors of [29] consider that optimum diameter of the drop is $(1.4-1.7)d_{el}$ for $d_{el} = 1.6$ mm, and $(1.56-1.88)d_{el}$ for $d_{el} = 2$ mm.

Two options for producing drops of assigned mass are possible. According to the first one, control of the metal melting is performed by means of current pulses of constant amplitude I_p and duration t_p . According to the second option, the arc is powered from the voltage source, and duration of the pulse is automat-

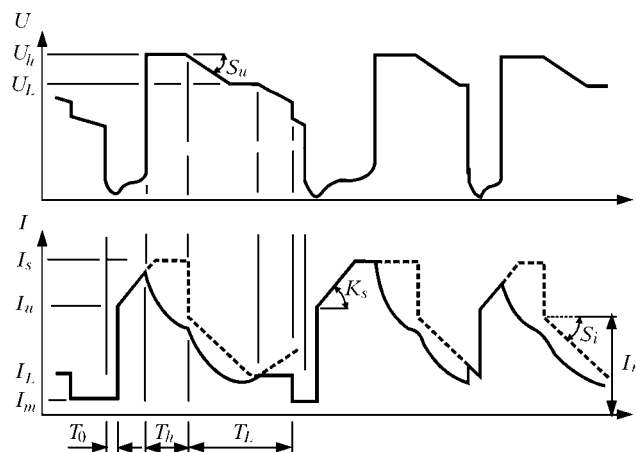


Figure 9. Oscillograms of voltage and current of inverter power sources in CO₂ welding [13]

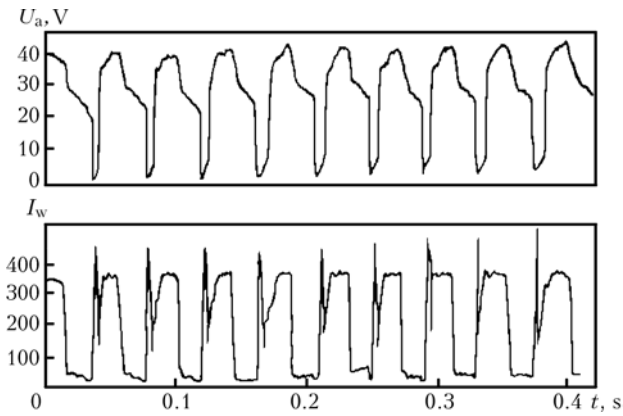


Figure 10. Oscillograms of voltage and welding current in case of arc feeding with current pulses of constant amplitude and duration [12]

ically set in the function of certain parameters of the welding process. The first principle is described in [12, 15, 21], and version of the second one --- in [30, 31].

Authors of [12] consider the arc (Figure 10) powered from controllable source of current with rigidly assigned amplitude I_{melt} and duration T_{melt} of the melting pulse. Duration of the drop «calming» pause T_{calm} with low current of the arc before SC, I_{calm} , is set automatically. The system has self-regulation property at disturbances on arc length and wire feed rate till duration of the pause is different from zero. Disturbances on the electrode extension length are not compensated and cause change of the drop volume.

In the STT source [15] a certain compensation of the electrode extension length is performed by automatic correction of pulse duration of the current with constant amplitude. It is done as follows. During SC the system measures voltage drop at the electrode, proportional to the electrode extension. It is averaged and fed to the integrator. The latter starts integration with zero initial conditions at the time of the arc ignition. When voltage at the integrator output equalizes with a regulated reference voltage (it is set by the knob «heat» on front panel of the source), the melting pulse stops and arc current starts to slowly reduce down to the base current of the pause. So, duration of the melting current pulse is inversely proportional to the arc length.

In majority of cases such compensation just worsens size stability of the drops when length of the electrode extension changes. Usually energy, emitted

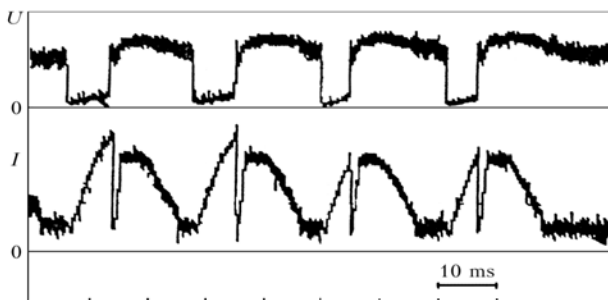


Figure 11. Oscillograms of voltage and current. Current pulses of electrode melting with smooth droop of rear front [21]

in the electrode, is relatively low (less than 15–20 %), that's why overcompensation of disturbance occurs.

For melting of the electrode shape of the current pulse does not play a special part, but in the STT and «Tekhnotron» sources (Figure 11) [21] a regulated smooth droop of the melt current pulse is envisaged. It is assumed that this will cause damping of the drop and the weld pool fluctuation. Neither theoretical no experimental data are presented in favor of this assumption.

In the sources, suggested by A.F. Knyazkov and Yu.N. Saraev, duration of the melting pulse (flat dipping output characteristic of the source) is set as follows:

- proportionally to the arc gap duration by the time, when the melting current pulse starts to act [32]. Counting of the arc gap duration being measured is performed from the instant of the arc ignition till reduction of voltage in it down to a certain reference value U_{ref} ;
- proportionally to integral of the arc voltage at the stage of a parametrically assigned pause by the time of the bridge destruction [33];
- proportionally to duration of the pause before SC [34].

In all these sources the most important factors are not requirements of the drop size stability, but requirements of the process stability, taking into account behavior of the weld pool depending upon spatial position of a weld. Melting of a consumable electrode and formation of the molten metal drop is determined by a complicated complex of electromagnetic and hydrodynamic forces in the gravity field and, therefore, may be described to a full degree only with application of the laws of thermal physics, electrostatics, electrodynamics, electromagnetism, and hydrodynamics. By now this task is not completely solved, but some of its aspects are theoretically and experimentally investigated. Using method of heat balance and experimental data, relations between such important welding parameters as welding current $I(t)$, rate of a consumable electrode melting $U_{melt}(t)$, electrode extensions $l_{el}(t)$, etc. [35] were proposed. Generalizing all these models we come to the following model:

$$U_{melt}(t) = aI(t) + bl_{el}(t)I^2(t), \quad (3)$$

where a, b are the proportionality factors.

Rate of the drop volume growth is

$$\frac{dV_{drop}(t)}{dt} = S_{el}U_{melt}(t), \quad (4)$$

where $V_{drop}(t)$ is the drop volume; S_{el} is the area of the electrode cross section.

Having substituted (3) into (4) we obtain

$$V_{drop}(t) = S_{el} \int_0^t [aI(t) + bl_{el}(t)I^2(t)] dt. \quad (5)$$

For stabilization of the drop volume the control system must solve equation (5) in real time relative

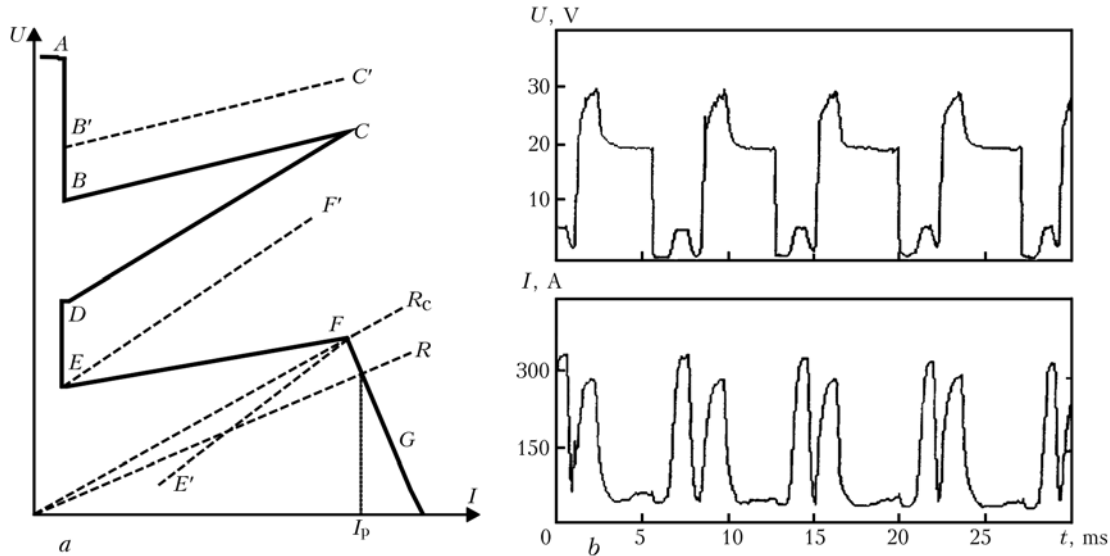


Figure 12. External characteristic of source in CO₂ welding with SC (a), and oscillograms of voltage and current (b) [36]

T_{melt} for the given $V_{drop}(t)$, $I(t)$, a , b and $I_{el}(t)$. Volume of the drop V_{drop} is determined when conditions of welding are assigned, $I(t)$ ---- during welding, a ---- proportionally to the cathode voltage drop and in first approximation is a constant value. Product bl_{el} is determined from voltage drop in the welding circuit at SC of the arc gap. SC voltage at the instant of the biggest diameter of the bridge neck equals

$$U_{c-p} = bl_{el}I_{SC},$$

from which bl_{el} is found. So, all components of equation (3) are known, which makes it possible to calculate in real time volume of the growing drop. When integral (5) achieves assigned value, the control system disengages melting current pulse, finishing interval T_{melt} . Using this algorithm, the control system ensures production of each drop of assigned volume irrespective of majority of disturbances, which act on the process.

Quite new concept of implementation of the «ideal» welding cycle (see Figure 2) was proposed by Chinese scientists [36, 37]. Instead of the program assignment of shape of the welding current pulses a power source with a complex external characteristic is used. For CO₂ welding with SC, external characteristic of the power source has seven segments (Figure 12, a) [36]. In addition, external characteristic automatically adapts to instant changes of the arc current and voltage (segments $B'C'$ and EF'). As a result welding cycle close to the «ideal» one is formed irrespective of disturbances, acting on the process (Figure 12, b). Connected in parallel transistors, working in linear mode, were used as regulating elements. External characteristic of the source is formed by the control scheme with non-linear current and voltage drop feedback on the load [37]. Linear mode of transistors' operation allows achieving extremely fast precision control of the welding process, but requires for dissipation on the power transistors, comparable with power of the welding.

Stage of the drop «calming» (interval T_{calm}).

After termination of the melting pulse the control system must reduce current down to the value, which still ensures stable arcing, but is insufficient for noticeable melting of the electrode. Arc pressure on the drop significantly reduces, it occupies coaxial with the electrode position and shape, close to the axial-symmetrical one. In a certain time due to feeding of the electrode and return movement of excited surface of the weld pool they'll meet, SC will occur, and welding cycle will be repeated.

Presence of the time interval for «calming» of the drop is necessary for removal of disturbances on the arc gap length. In case of sudden change of the latter, time till SC, T_{calm} , automatically increases or reduces by means of the electrode extension change. As a result by the next cycle length of the arc gap gets equal to the assigned one, i.e. in contrast to traditional systems with self-regulation this system has top speed of optimization of disturbances on the arc length.

1. Zaruba, I.I., Bargamen, V.P., Andreev, V.V. et al. (1973) Influence of method of short circuit current limiting on formation of vertical and overhead welds in CO₂ welding. *Avtomatch. Svarka*, **4**, 64–67.
2. Lebedev, V.K., Zaruba, I.I., Andreev, V.V. (1975) Conditions of formation of liquid bridge in drop metal transfer with short-circuiting of the arc gap. *Ibid.*, **9**, 1–3, 8.
3. Lenivkin, V.A., Dyrgerov, N.G., Sagirov, Kh.N. (1989) *Technological properties of gas-shielded welding arc*. Moscow: Mashinostroenie.
4. Rehfeldt, D., Bollmann, A., Niemann, M. et al. (1989) Untersuchungen zum Metall-Schutzgasschweißen mittels Ultraschwindigkeitsskinematografie und schneller Erfassung elektrischer Schweißparameter. *Schweissen und Schneiden*, **3**, 139–141.
5. Zaruba, I.I., Dymenko, V.V. (1971) Control of parameters of short-circuiting welding process. *Avtomatch. Svarka*, **8**, 43–45.
6. Potapievsky, A.G., Lifshits, M.G., Kassov, D.S. et al. (1976) On problem of short-circuiting metal transfer. *Svarochn. Proizvodstvo*, **6**, 53–54.
7. Pinchuk, I.S., Khejfets, A.L., Postaushkin, V.F. et al. (1980) Stabilization of transfer and decrease of metal spatter in CO₂ short-arc welding. *Ibid.*, **6**, 9–10.
8. Yamamoto, H., Okazaki, K., Harata, S. (1986) The effect of short circuiting current control on the spatter generation in CO₂ arc welding. *IIW Doc. 212-649-86*.



9. Maruo, H., Hirata, Y., Goto, N. (1992) Bridging transfer phenomena of conductive pendent drop. Report 3: The effects of electromagnetic pinch force on the bridging transfer. *Quarterly J. JWS*, **2**, 251–258.
10. Choi, S.K., Yoo, C.D., Kim, Y.-S. (1988) Dynamic simulation of metal transfer in GMAW. Part 2: Short-circuit transfer mode. *Welding J.*, **1**, 45–51.
11. Knyazkov, A.F., Mazel, A.G., Dedyukh, R.I. et al. *Short-circuiting arc gap welding process and device for its realization*. USSR author's cert. 930824. Int. Cl. B 23 K 9/11. Publ. 23.04.85.
12. Paton, B.E., Lebedev, A.V. (1988) Control of electrode metal melting and transfer in CO₂ welding. *Avtomatich. Svarka*, **11**, 1–3.
13. Matsuda, F., Ushio, M., Mita, T. (1988) Wellenformsteuerungsmethode im CO₂ Schweißen. *Transact. of JWRI*, **2**, 11–17.
14. Yamamoto, H., Harada, S., Yasuda, H. (1990) The development of welding current control system for spatter reduction. *Welding Int.*, **4**, 398–407.
15. Stava, E.K. (1993) The surface-tension transfer power source: A new, low-spatter arc welding machine. *Welding J.*, **1**, 24–29.
16. Ushio, M., Yamamoto, H., Nishida, Y. et al. (1994) Recent advances in welding power systems for automated welding. *Transact. of JWRI*, **1**, 1–6.
17. Nacey, T.Y. (1993) Fourth-generation inverters add artificial intelligence to the control of GMA welding. *Welding J.*, **1**, 31–34.
18. Pinchuk, I.S., Postaushkin, V.F., Kulikov, G.D. et al. (1974) Comments to article on determination of stability of bridge between consumable electrode and weld pool. *Svarochn. Proizvodstvo*, **10**, 49–50.
19. Orszech, P., Kim, Y.C., Horikawa, K. (1997) Short-circuit transient phenomena in GMA/CO₂ welding (I). *Transact. of JWRI*, **1**, 49–67.
20. Boughton, P., MacGregor, G.I. (1974) Control of short circuiting in MIG-welding. *Welding Res. Int.*, **2**, 31–53.
21. Poloskov, S.I., Ishchenko, Yu.S., Lebedev, V.A. et al. (2001) Control of drop transfer in consumable electrode arc gap short-circuiting welding. *Svarochn. Proizvodstvo*, **6**, 6–9.
22. Khejfets, A.L. (1986) Comparative evaluation of some processes of metal spattering decrease in CO₂ welding. *Avtomatich. Svarka*, **3**, 58–60.
23. Zaruba, I.I. *Consumable electrode electric arc welding*. USSR author's cert. 271680. Int. Cl. B 23 K 9/00. Publ. 26.05.70.
24. Pinchuk, I.S., Postaushkin, V.F., Kulikov, G.D. et al. (1976) Decrease of spattering in short-circuiting welding by limiting of bridge explosion energy. *Svarochn. Proizvodstvo*, **11**, 52–54.
25. Gornov, O.M. (1975) About decrease of spattering by short-circuiting current decrease in CO₂ welding. In: *Transact. of Perm Polytechnic Institute*, **164**, 115–118.
26. Gornov, O.M., Chumak, L.F. (1972) Influence of stage current decrease in short-circuiting moment on spattering in CO₂ welding. *Ibid.*, **116**, 101–103.
27. Parks, J., Stava, E. *Method and device for controlling a short circuiting type welding system*. Pat. 4,954,691 US. Publ. 04.09.90.
28. Voropaj, N.M., Lavrishchev, V.Ya. (1976) Conditions of metal transfer in CO₂ welding. *Avtomatich. Svarka*, **5**, 8–11.
29. Poloskov, S.I., Ishchenko, Yu.S., Lebedev, V.A. et al. (2002) Specifics of controlled heat mass transfer in consumable electrode welding with arc gap short-circuiting. *Svarochn. Proizvodstvo*, **7**, 6–13.
30. Saraev, Yu.N. (2001) Adaptive pulse-arc methods of mechanized welding in construction of main pipelines. *Ibid.*, **1**, 4–11.
31. Saraev, Yu.N. (1988) Control of electrode metal transfer in CO₂ welding with arc gap short-circuiting (Review). *Avtomatich. Svarka*, **12**, 16–23.
32. Knyazkov, A.F., Saraev, Yu.N., Dedyukh, R.I. *Arc gap short-circuiting welding method*. USSR author's cert. 768108. Int. Cl. B 23 K 9/00. Publ. 15.01.84.
33. Knyazkov, A.F., Saraev, Yu.N., Timoshenko, A.K. *Consumable electrode arc welding*. USSR author's cert. 951810. Int. Cl. B 23 K 9/00. Publ. 23.12.83.
34. Knyazkov, A.F., Saraev, Yu.N., Timoshenko, A.K. *Method of arc gap short-circuiting welding and device for its realization*. USSR author's cert. 1168364. Int. Cl. B 23 K 9/00. Publ. 23.07.85.
35. Lesenewich, A. (1958) Control of melting rate and metal transfer. Part 1: Control of electrode melting rate. *Welding J.*, **8**, 334–353.
36. Ou, Z., Wuang, Y., Ushio, M. et al. (1999) New concept for the characteristic of an arc welding power source (Report 2). *Transact. of JWRI*, **1**, 5–8.
37. Pan, J. (2003) *Arc welding control*. Cambridge: Woodhead Publ.

NEW PROCEDURE FOR EVALUATION OF COLD CRACKING RESISTANCE OF HARDENING STEEL WELDED JOINTS

V.M. KULIK and M.M. SAVITSKY

E.O. Paton Electric Welding Institute, NASU, Kiev, Ukraine

A method is suggested for tensile testing of flat specimens of butt joints with decreasing load. Peculiarities of delayed fracture of the joints, depending on the thickness of the steel welded, as well as welding parameters and technique, are considered. It is established that delayed fracture of homogeneous or close to homogeneous butt joints occurs primarily in the weld. The possibility is shown of determining the time of microplastic deformation, stress and delayed fracture energy, as well as time and frequency of microcrack initiation. The procedure can be applied for development of a welding technology.

Keywords: arc welding, high-strength steels, butt joints, weld, thermal cycle of welding, delayed fracture, microplastic deformation, stresses, crack resistance, evaluation procedure

Critical products with a low metal content are made of high-strength carbon and alloyed sheet steels with application of tungsten electrode argon-arc welding. The produced joints of hardening steels are prone to formation of cold cracks [1], which initiate during

relaxation of inner stresses at soaking [2], and are located both in the HAZ and weld metal (Figure 1). Crack formation is influenced by the composition and thickness of welded steel, welding mode and other factors, predetermining the importance of application of quantitative evaluation of cold cracking resistance by specialized mechanical testing of welded joints.

Methods of implant testing have become the most widely accepted [3–7]. According to the traditional method [3], a cylindrical polished sample of 8 mm



diameter is inserted into a matching through-thickness hole in a technological strap of 20 mm thickness, welded from the surface by bead deposition or incomplete penetration, and is subjected to long-term tension to fracture in the fusion zone. Delayed cracking resistance is evaluated by force (σ_{cr} , $\sigma_{cr\ max}$, σ_{cr}/σ_y) and energy a_{red} indices, where σ_{cr} is the minimum stress below which no delayed fracture occurs; $\sigma_{cr\ max}$ is the maximum stress, at which the sample does not fail for 24 h; σ_y is the proof stress of tested steel; a_{red} is the reduced (referred to sample cross-sectional area) work.

A.M. Makara and A.A. Khriplivy found that a flat sample-insert of 3 mm thickness can be used instead of the cylindrical sample. In upgraded implant methods [4–7] a sample-insert of 3×14 mm section is used.

It should be noted that welding of the above samples is performed in the modes essentially different from the modes of welding sheet steel, and the direction of action of the applied force (normal to the welded joint) does not correspond to the direction of residual stress action. In addition, a composite sample is rather massive, complex and labour-consuming. These methods are unacceptable for evaluation of crack resistance of the weld and welded joint on the whole, and their application is limited by comparative evaluation of steel weldability. Deviation from the recommended sample thickness leads to a change of σ_{cr} and violation of the stability of test results [8, 9].

Correspondence of the direction of load action at testing and of welding stresses is achieved at implementation of the procedure of [7]. A sample of 3×14 mm section is placed into a side rectangular hole, created by superposition of slots of two technological straps plane-parallel to the surface, is welded by a consumable electrode with technological straps (along the transverse groove) and is loaded by a constant tensile force (lateral relative to the weld). The work of fracture is determined by the values of load and displacement during testing, and the fracture energy content --- by the area of the section under the curve of deformation (work) changing in time in the diagram.

Difference in the thicknesses of the tested sample and technological straps is unacceptable for nonconsumable electrode welding, and the physical essence of energy content of fracture is not understood. A composite sample is more massive, complex and labour-consuming than the composite sample for the implant procedure.

A.M. Makara and his disciples N.A. Mosendz and V.G. Gordony and others, were of the opinion [10] that a valid assessment of crack resistance is achieved at testing of butt joints. Samples 12–14 mm thick of the total length of more than 500 mm were joined by consumable electrode single-pass welding, loaded by a wedge device up to the specified tensile stresses, which were determined by a mechanical deformer with 100 mm base, and soaked at these stresses up to fracture in the HAZ. Taken as the index of delayed

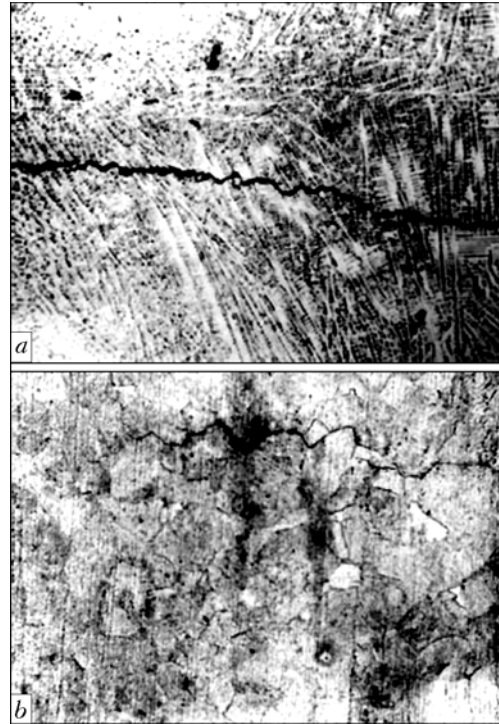


Figure 1. Microstructure of a high-strength steel TIG-welded joint with microcracks: a --- weld ($\times 100$); b --- HAZ metal ($\times 320$)

fracture susceptibility of the joint was the minimum stress, at which no fracture occurred for 24 h. This procedure is quite simple, and can be used in the shop for evaluation of crack resistance of welded joints, depending on the applied materials and welding conditions. In this case, however, similar to implementation of the above procedures, stress relaxation is not taken into account, and the samples are quite massive and large-sized.

Development of a more perfect procedure of evaluation of cold cracking resistance in welded joints of hardening steels is the purpose of this work.

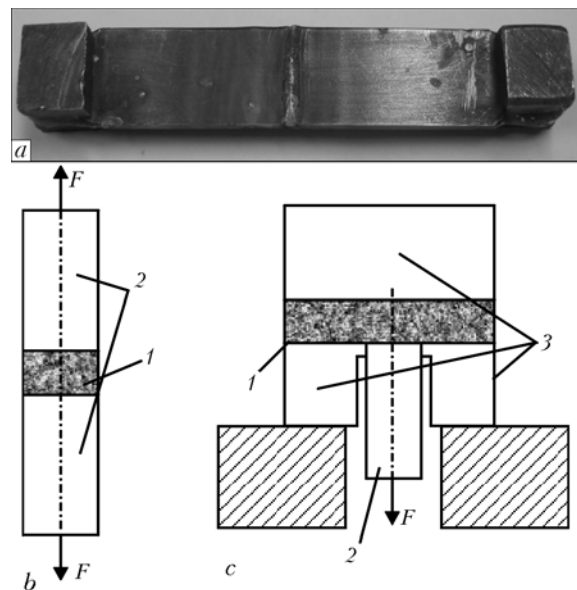


Figure 2. Sample of the main type (a), and schematics of delayed fracture testing of this sample (b) and special sample (c) of butt joint: 1 --- weld; 2 --- working (tested) part; 3 --- auxiliary parts



Crack resistance of joints on steels of different compositions and thicknesses, depending on the mode, method and parameters of one-sided argon-arc welding ($\sigma_s = 380\text{--}390$ MPa)

No.	Welded steel			Welding process	I_1/I_2 , A	v_w , m/h	q/v_w^4 , W·h/m	$q/(v_w\delta)^4$, W·h/m ²	$\bar{f} RC^5$ of weld	τ_{fr} , min
	Grade	\bar{N}_{eq}	δ , mm							
1	30KhGSA	0.65	3.1	A-TIG	85–120/--	7–12	90–110	29–35	–	1–3
2				A-TIG + TIG	130/90–110	12–13	70–95	23–31	50.5–52.5 48.0–50.0	2–19
3				A-TIG + TIG ³	130/110		100–110	32–35	–	5–20
4				A-TIG + A-TIG ¹	100/80	12	60	19	–	4
5				TIG + TIG ¹	110/110		85	27	–	750–did not fail
6				30Kh2GS2MV	1.0	3.7	A-TIG + TIG	190/130	6	240
7	140/110	12	95					26		– 49
8	42KhGSNM		1.1	2.8	TIG ²	115/--	12	95	34	–
9		A-TIG + TIG			120/80	65		23	– 48.0–50.0	< 1
10		TIG + TIG			90/120	100		36	---	< 1
11	16KhG2M	0.64	5.0	A-TIG + TIG ³	160/130	8	195	39	38.0–45.0 27.5–38.0	Did not fail
12	20G	0.35	3.0	A-TIG + TIG ¹	100/80	13	61	20	–	Did not fail

¹Two-sided two-pass welding; ²single-pass welding with incomplete penetration; ³with filler wire melting; ⁴last welding pass; ⁵the numerator gives the data obtained from ($\sigma_s = 380\text{--}390$ MPa), and the denominator --- from the reverse side; for No.12 $\sigma_s = 280$ MPa.

Crack resistance was evaluated* by testing for delayed fracture with a decreasing load in keeping with the procedure and welded samples suggested by the authors of [11]. Sample of the main type consists of two tested parts and butt joint between them (Figure 2, a, b), as a sample for static rupture testing. A special sample (Figure 2, c) includes one tested part, three auxiliary parts and one common butt joint. Bev-

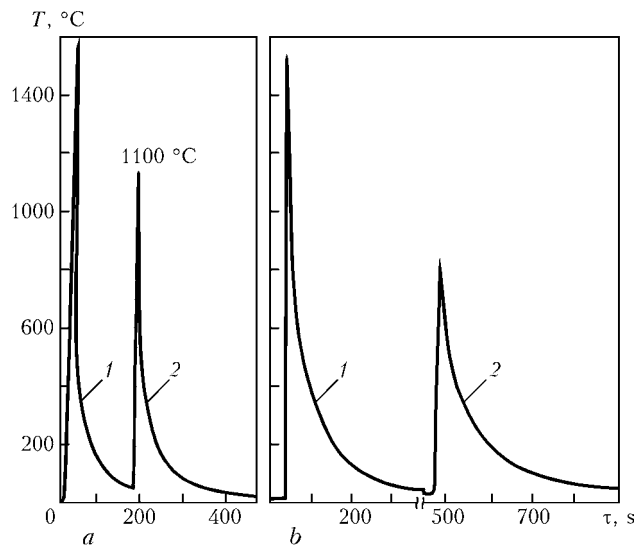


Figure 3. Thermograms of two-pass argon-arc welding of steel 3 (a) and 6 (b) mm thick: 1 — first; 2 — second pass

*Eng. G.V. Bursky participated in this work.

els or recesses are made on the side auxiliary parts to avoid jamming of the tested part because of weld shrinkage. The cross-sectional dimensions of the tested parts were equal to (14–27) × (50–90), those of auxiliary parts were 40 × 35 and 40 × 90 mm.

One- and two-pass butt A-TIG and TIG welding of samples of low- and medium-alloyed steels 2.8–6.0 mm thick with carbon equivalent of 0.35–1.10 was performed in ARK-1 unit in combination with VSVU-315 rectifier. Welding was conducted without melting and with melting of filler wire Sv-18KhMA following the specified or actual possible modes (Table). Thermal cycles of welding were recorded by KSP-4 potentiometer using VR 20/5 thermocouple of 0.35 mm diameter from the reverse side of the weld in the abutted reference-sample at 10 mm distance from the tested part.

After welding, the sample was loaded by an elastically-bent beam with rigidity $K = 8$ kg/μm in a modified LTP-1-1-6 unit by a tensile force up to the stress of 380 and 280 MPa, close to the yield point of the used steel. The sample is soaked in the loaded state without additional external impacts. The specified stress σ_s is set by deflection λ_s of elastically bent beam $\sigma_s = K\lambda_s/S$, where S is the cross-sectional area of the sample. KSP-4 potentiometer (using induction displacement transducer) records the change of sample length as the change of beam deflection, and also registers AE signals from the transducer on the sample surface [5, 6, 12].

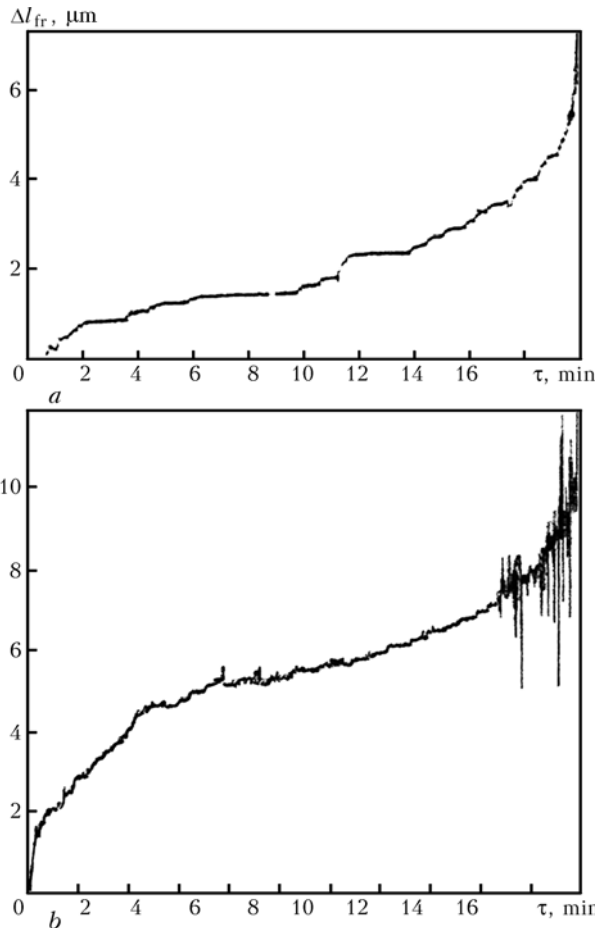


Figure 4. Delayed fracture diagrams of two-pass butt joints on steel 30KhGSA 3 mm thick welded without (a) and with (b) melting of filler metal

Typical welding thermograms, delayed fracture diagrams, and fracture location are given in Figures 3--5, and data on crack resistance of butt joints depending on the features of welding steel of different chemical compositions and thicknesses --- in the Table.

When the first and second passes of argon-arc welding of steel 2.8--3.7 mm thick are made in the given modes, the metal of the weld and the HAZ is heated above critical temperatures across the entire thickness of the joint (Figure 3, a) and then is cooled at the rate of 8--27 °C/s in the temperature range of minimum austenite stability of 600--400 °C. The difference in the cooling rates is due to the difference of the welding modes and processes, thicknesses of welded steels, temperature before deposition of the next welding pass, as well as the features of transformations at cooling. Metal of 30KhGSA steel joint develops a martensite-bainite structure, that of steels 30Kh2GS2MV and 42KhGSNM --- a martensite structure.

When making joints on 6 mm thick steel at a lower welding speed, and with a greater specific welding heat input, metal cooling from supercritical temperatures at lower rates $w_{6/4} \leq 3$ °C/s is observed (Figure 3, b), this predetermining the reduction of the amount of martensite in the metal of 30KhGSA steel joint. When the second welding pass is made, the metal from the reverse side of the joint is heated up

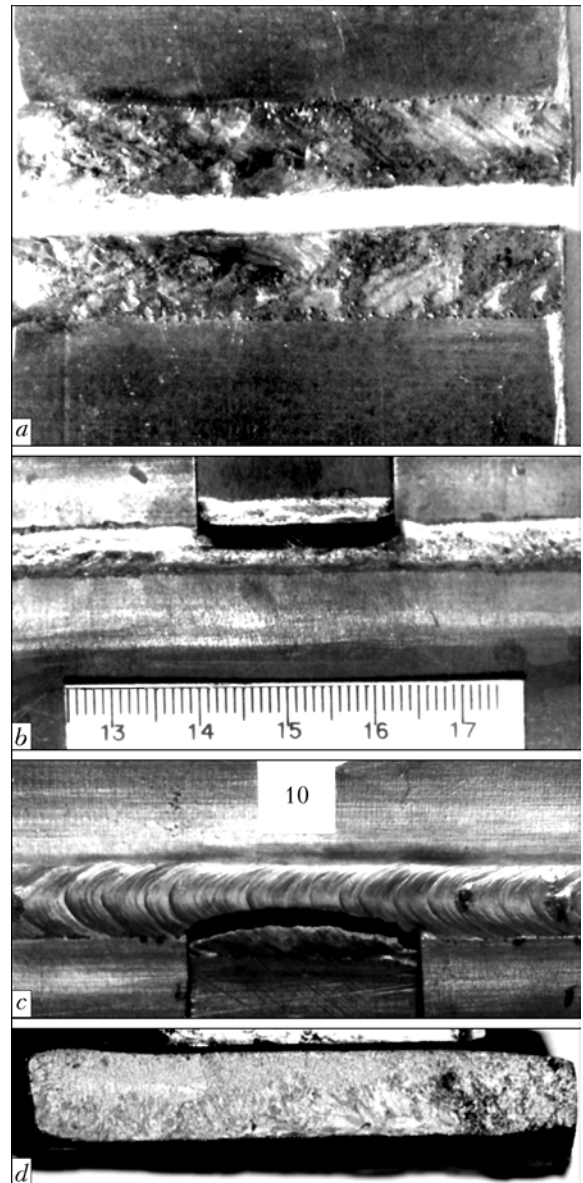


Figure 5. Appearance and location of delayed fractures of samples of joints welded in two passes without (a, b) and with (c) weld reinforcement without (a) and with (b, c) artificial stress raisers; d --- fracture surface

to temperatures close to $A_{c1} = 720\text{--}760$ °C, and goes through a short-time high-temperature tempering or repeated hardening with formation of a smaller number of hardening components of the structure. Such a thermal cycle of welding is favourable for lowering the hardness and improving the toughness of the metal of joints on 6 mm thick steel. A similar change is observed in two-pass welding of 16KhG2M steel 5 mm thick.

Welded sample loaded below the base metal yield point, goes through plastic deformation (Figure 4). At such a stress the base metal is plastically undeformed, however, microplastic deformation of the hardened alloyed steel with 0.11--0.57 % C takes place [13], and of the joint metal hardened in welding, respectively. During testing process it increases monotonically, stepwise, and in an accelerated manner before final fracture.



Step-like increases of microplastic deformation of the joint metal are accompanied by frequent low-intensity AE signals. They can be considered as a manifestation of submicrocrack development as a result of opening of local metal volumes at deformation of the crystalline lattice by not less than one interatomic distance [14]. With development of submicrocracks, stresses of the II kind decrease, metal density is lowered, and microcrack formation is facilitated. The latter is registered by AE signals of an order of magnitude greater intensity. Frequency of microcrack development during testing is lower than the frequency of low-intensity AE signals. It rises at acceleration of microplastic deformation of the hardened metal of the joint at the final stage of delayed fracture. Microcracks initiate formation of macrocracks and welded joint fracture at testing.

During testing the delayed fracture develops mostly in the weld (Figure 5). Fracture in the weld is noted also at its initiation in the fusion zone through development of a stress concentration along narrow faces of the tested part in the point of an abrupt transition to a longer weld of a special composite sample (Figure 5, *b, c*). Fracture initiating in the fusion zone propagates into the weld even when reinforcement has been made as a result of filler wire melting, while stress concentrators in the form of a lack-of-penetration of the butt and pores initiate weld fracture during sample loading (within 0.2–0.8 min). Therefore, the weld, in which the metal is identical or close to the base metal in its composition, is more prone to crack initiation and propagation than the fusion zone of the welded joint on high-strength steel. On the whole fracture is located normal to the wide faces and applied force and is of intergranular nature (Figure 5, *d*). Traces of macroplastic deformation are absent in the fracture site, this allowing the delayed fracture to be qualified as brittle.

Intergranular nature of fracture is indicative of a lowered resistance and localization of microplastic deformation along the grain boundaries of hardened metal, where maximum distortions of the atomic-crystalline structure and local increase of stresses, are observed. Localizing of microplastic deformation along the grain boundaries and lowering of the cold cracking resistance are promoted by the coarse grains of the joint metal.

Metal of a single-pass weld with a great distortion of the crystalline lattice along the grain boundaries due to cooling and hardening from the liquid state, has the highest susceptibility to delayed fracture (within a few minutes). Elongated crystallites are revealed in its fracture. The middle part of such a weld can be contaminated by liquating impurities and take on the properties of a «weak plane», particularly at a small shape factor of the weld. Avalanche cold cracks often form in single-pass welds on sheet steels with a high carbon equivalent. Naturally, incomplete penetration of the solid base metal causes a noticeable

increase of the resistance to delayed cracking in the weld.

Two-pass joints have a higher crack resistance than single-pass joints. In the penetration section when the second welding pass is made, the weld metal structure is refined (Figure 5, *d*), the shape of dendritic structure crystallites changes, the number and dimensions of second order axis nuclei are reduced, dendrite orientation to the face surface becomes more pronounced and the weak plane is eliminated. Short-time heating of the metal up to the temperatures of 980–1250 °C leads to refinement of the grain size, and higher heating promotes a reduction of the anisotropy of mechanical properties due to partial homogenizing of the metal. Impact toughness of the re-hardened steel somewhat increases. A two-layer weld structure is traced in the fracture even at a homogeneous weld composition.

When this procedure is used, an increase of the delayed fracture resistance of the welded joint is registered at lowering of welding speed, increase of the heat and specific heat input of welding, lowering of the weld cooling rate when the last welding pass is made, as well as at decrease of the carbon equivalent of the welded steel. The found features correspond to the established concepts of crack resistance. An essential increase of crack resistance of a joint of steel 5 to 6 mm thick is due to 2–3 times lowering of the cooling rate in the temperature range of minimum stability of austenite, greater duration of self-tempering in welding, lowering of the temperature of metal heating from the reverse side of the joint to or lower than the intercritical temperatures. Consequently, the non-equilibrium of the weld metal structure is reduced. In this case, the overall tearing nature of delayed fracture is preserved, although shear-type fracture (bevel to approximately 0.5 mm depth) is observed at the sample wide faces, and the fracture runs both through the weld and through the HAZ. Characteristically, the results of testing samples produced by butt welding and through-thickness penetration of the solid base metal are practically the same, this widening the possibilities of the procedure.

Elongation of the welded sample Δl_{fr} , determined at delayed fracture testing, characterizes the welded joint microductility. The metal hardened in welding, undergoes microplastic deformation by local microplastic shear along the grain boundaries. Delayed fracture of the welded joint takes place when the microductility margin of the hardened metal has been exhausted, primarily, in the weld ($\delta_{fr} = \Delta l_{fr} / l$, where l is the width of the section of hardened metal, which is by 0.5–1.0 mm greater than weld width). Considering that $\tau_{fr} = \Delta l_{fr} / v_{md} = \delta_{fr} / v_{mdr}$, where v_{md} and v_{mdr} are the averaged rates of the absolute and relative microplastic deformation, which are reduced with increase of shear resistance, the delayed fracture resistance is predetermined by a combination of the hardened metal properties.



From the delayed fracture diagrams (see Figure 4) it is seen that such a change of microplastic deformation during testing and delayed fracture in the weld are observed at close values of crack resistance τ_{fr} of butt welded joints of steel 30KhGSA welded in the same modes in two passes without melting and with melting of Sv-18KhMA filler wire. However, while the first weld not reinforced by filler metal, fails with microplastic deformation $\Delta l_{fr} = 6 \mu\text{m}$, $\delta_{fr} \approx 0.1 \%$ and averaged rate of microplastic deformation $v_{md} \approx 0.31 \mu\text{m}/\text{min}$, $v_{mndr} \approx 0.005 \%/ \text{min}$, the weld reinforced by filler material fails with $\Delta l_{fr} = 10 \mu\text{m}$, $\delta_{fr} \approx 0.17 \%$, $v_{md} \approx 0.46 \mu\text{m}/\text{min}$, $v_{mndr} = 0.008 \%/ \text{min}$. Increase of relative elongation δ_{fr} and rate of microplastic deformation v_{md} and v_{mndr} is accompanied by increase of the frequency of submicrocrack and microcrack formation at the accelerated final stage of delayed fracture. At testing of the joint produced by incomplete penetration of steel with a large carbon equivalent, $\Delta l_{fr} = 16 \mu\text{m}$ and $\delta_{fr} = 0.26 \%$. Therefore, differences in the parameters of welded joint cracking are registered with application of this procedure.

The relaxation phenomena can be considered as creep under stress which decreases in time in proportion to the growing plastic deformation [15]. Microplastic deformation at delayed fracture testing of the welded joint causes a reduction of the deflection of an elastically bent beam and applied force. Stress drop by the moment of rupture $\Delta\sigma_{fr} = K\Delta l_{fr}/S = K\delta l/S$ and rupture stress $\sigma_{fr} = K(\lambda_s - \Delta l_{fr})/S = K(\lambda_s - \delta_{fr}l)/S$ linearly depend on the value of microplastic deformation at testing. In the above examples microplastic deformation of the welded joint ($\Delta l_{fr} = 6, 10$ and $16 \mu\text{m}$) causes stress drop $\Delta\sigma_{fr} = 7, 12$ and 26MPa to rupture stress $\sigma_{fr} = 373, 368$ and 354MPa , respectively. Therefore, stress relaxation at item soaking after welding is simulated at delayed fracture testing of a butt welded joint of high-strength steel using an elastically bent beam. Compared to the time and deformation indices of delayed fracture, the force index depends on the properties of the hardened metal to a lower degree. Values σ_{cr} and σ_{cr}/σ_y can be determined at testing of a batch of samples with σ_{fr} recording.

Work is performed at delayed fracture of a welded joint. Similar to static rupture testing, specific work per a unit of volume of microplastically deformed metal, is determined as follows:

$$a_{sp} = (\sigma_s - 0.5\Delta\sigma_{fr})\delta_{fr} = (\sigma_s - 0.5K\Delta l_{fr}/S)\delta_{fr}.$$

The reduced work referred to the sample cross-sectional area, similar to impact toughness, follows from the relationship

$$a_{red} = (\sigma_s - 0.5\Delta\sigma_{fr})\Delta l_{fr} = (\sigma_s - 0.5K\Delta l_{fr}/S)\delta l_{fr}.$$

Characterizing the deformability of the welded joint and hardened metal and being more difficult to determine, the energy indices are less acceptable for evaluation of welded joint crack resistance than the deformation indices of delayed fracture.

Thus, application of the new procedure allows determination of the time, deformation, force and energy characteristics of delayed fracture of a high-strength steel welded joint.

CONCLUSIONS

1. A procedure was proposed for evaluation of cold cracking resistance of welded joints on high-strength steels of different thicknesses by delayed fracture testing with load lowering during forced microplastic deformation of the metal hardened in welding. At testing with simulation of stress relaxation small-sized samples are used and τ_{fr} , Δl_{fr} , δ_{fr} , $\Delta\sigma_{fr}$, σ_{fr} , a_{sp} are determined, as well as microcracking frequency and time. Time and deformation indices of delayed fracture are the most acceptable for fast evaluation of crack resistance.

2. It is established that the weld has the highest susceptibility to cold crack initiation and propagation, and its crack resistance rises with increase of thickness of the steel being welded. The influence of the welded steel composition, technological and thermal features of welding on crack resistance is thus confirmed.

3. The suggested testing procedure can be efficiently used when studying the crack resistance, development of welding consumables and technologies of welding various high-strength steels.

- (1978) *Welding in machine-building*: Refer. Book. Vol. 2. Ed. by A.I. Akulov. Moscow: Mashinostroenie.
- Zemzin, V.I., Chizhik, A.A., Lanin, A.A. (1982) Conditions of cracking in welding and heat treatment. Part 1: About the role of creep in cracking. *Svaroch. Proizvodstvo*, **11**, 1-4.
- Granjon, H. (1969) The implant method for studying weldability of high strength steel. *Metal Construction and Brit. Welding J.*, **11**, 509-515.
- Bursky, G.V., Sterenbogen, Yu.A. (1990) Evaluation of delayed fracture resistance of medium-alloy high-strength steel HAZ. *Avtomatich. Svarka*, **8**, 33-35.
- Bursky, G.V., Savitsky, M.M., Olejnik, O.I. et al. (1999) Improved procedure for evaluation of HAZ metal resistance to delayed fracture. *Ibid.*, **4**, 31-34.
- Kulik, V.M., Savitsky, M.M., Bursky, G.V. (2005) Evaluation of delayed fracture resistance of metal of high-strength steel HAZ with modeling of stress relaxation. *The Paton Welding J.*, **4**, 17-22.
- Sterenbogen, Yu.A., Vasiliev, D.V. (1999) Evaluation of fusion zone crack resistance by energy index of delayed fracture. *Avtomatich. Svarka*, **6**, 6-12, 17.
- Sterenbogen, Yu.A., Bursky, G.V., Savitsky, M.M. (1983) About implant procedure and its application in testing high-strength steels. In: *Proc. of 2nd Symp. of CMEA on Application of Mathematical Methods in Weldability Studies*. Sofia: VMEI.
- Inagaki, M., Tomura, H., Araki, T. (1980) Effect of testing parameters and standardization in implant cracking test in Japan. *IIW Doc. IX-1151-80*.
- Makara, A.M., Mosendz, N.A. (1971) *Welding of high-strength steels*. Kiev: Tekhnika.
- Kulyk, V.M., Savytsky, M.M. *Method for evaluation of crack resistance of hardening steel welded joint and device for its realization*. Pat. 73637 Ukraine. Publ. 15.08.2005.
- Bartenev, O.A., Kutakov, Yu.I., Khamitov, V.A. et al. (1988) Acoustic emission control of laser welded joints. *Avtomatich. Svarka*, **9**, 71-73.
- McEvily, A.J., Ku, R.C., Johnston, T.L. (1966) The source of martensite strength. *Transact. of Metallurg. Soc. of AIME*, **236**, 108-113.
- Ostakin, A.I. (1973) *Study of peculiarities of metal and alloy ductile fracture*: Synopsis of Thesis for Cand. of Techn. Sci. Degree. Leningrad.
- Oding, I.A., Ivanova, V.S., Burdunsky, V.V. et al. (1959) *Theory of creep and long-term strength of metals*. Moscow: GNTI.



ANALOG AND MICROPROCESSOR CONTROL OF THE WELDING ELECTRON BEAM CURRENT

O.K. NAZARENKO and V.S. LANBIN

E.O. Paton Electric Welding Institute, NASU, Kiev, Ukraine

Results of analog and microprocessor control of welding electron beam current in modern EBW units are discussed. It is experimentally shown that by improving the control algorithms implemented in a built-in microprocessor, it is possible to lower the value of instability of electron beam current to $\pm 1\%$ in the welding mode and to $\pm 10\%$ in the mode of low setting-up current (≤ 1 mA). Generation of current pulses of the required shape and amplitude is ensured for operation of the system of automatic guidance of the beam to the butt during welding.

Keywords: electron beam welding, welding electron beam current, NPC system, analog and digital control, noise immunity, fast reaction, accuracy, automatic guidance of the beam to the butt

Special requirements made of modern electron beam welding equipment include the ability to provide low setting-up currents of the beam and operation of secondary-emission or X-ray systems of butt following during welding [1].

Minimum programmable increment and beam current. Minimum setting-up current of the beam assigned by the operator, should not cause surface melting of the metal. As is seen from Figure 1 (ELA-60/15 gun, 60 kV accelerating voltage, 150 mm working distance), an electron beam of 60 keV power at 0.5 mA current already leaves a surface-melted zone on the sample surface, which is inadmissible for many types of commercial products. Therefore, in the equipment with accelerating voltage of 60–120 kV, both the minimum beam current and its increase increment should be limited by 0.1 mA value. In earlier practical work it was not possible to set in powerful sources the minimum current below 1 mA, as beam instability reached 100% because of the influence of capacitance leakage currents on the power source ground and electromagnetic interference in the beam current control and measurement circuit.

The actual value of beam current is determined by voltage drop on the thermally-stable resistor, connected into the current circuit. This voltage is the

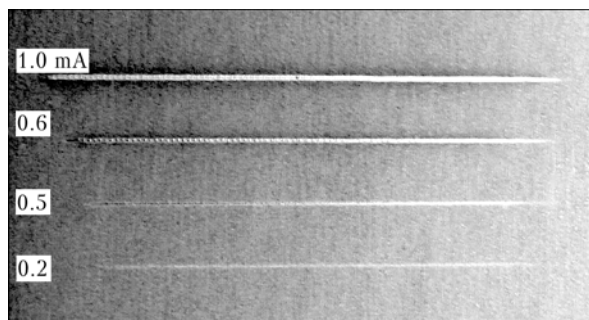


Figure 1. Impact of electron beam moving at the speed of 25 mm/s on the surface of low-carbon steel at different currents (no surface melting at 0.2 mA current)

value used also as the feedback signal of the beam current control channel. The simplest step is connecting a resistor between the ground and «plus» terminal of the accelerating voltage source. In this case no problems of decoupling the control circuits from the high potential are encountered but, in addition to the welding current, also the capacitance leakage currents are flowing through the resistor to the ground of the accelerating voltage source, their frequencies being in the range of 50–300 Hz. While the fraction of capacitance currents is small at full stationary load of the source, at low welding currents and in the transient modes the value of capacitance currents can even exceed the specified stationary value of beam current. For instance, for ELA-60 power source [2] of 60 kW power the value of capacitance currents in the stationary mode is equal to approximately 10 mA, and at transient processes, including pulsed modulation of beam current, it is many times higher than this value. Consequently, the beam current feedback signal has to be filtered, which essentially increases the time constant of the control circuit, and limits the ability of accurately assigning low (≤ 1 mA) setting-up currents.

In order to eliminate the influence of capacitance leakage currents on the accuracy of measuring the beam current in modern accelerating voltage sources the feedback resistance is connected between the «minus» terminal of the source and emission system of the welding gun, and the entire system of beam automatic control is placed under high potential, while the assigned current value is transmitted through the frequency or digital channels with optical decoupling of low- and high-voltage circuits [3]. So far, however, the results of application of such a system were not discussed in publications.

Current pulse shape. At operation of the system of automatic butt following the welding beam is periodically (usually 3 times per second) switched into the mode of probing the surface of the item being welded. Here the following should be taken into account: to prevent violation of weld formation the time of welding process interruption should be minimum, and it should become proportionally shorter with increase of the welding speed. Thus, it is necessary to minimize the duration of the transient processes; not

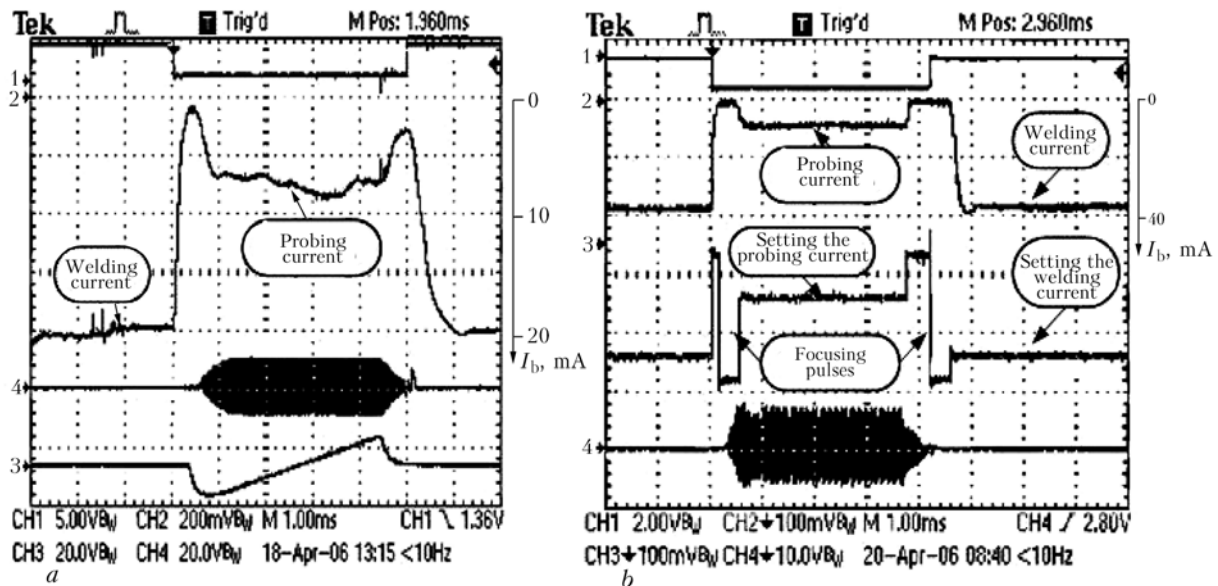


Figure 2. Oscillograms characterizing the operation of analog (a) and microprocessor (b) control of beam current I_b at operation of the system of automatic guidance of the beam to the butt in real time mode for case a: 1 — synchronizing pulse; 3 — beam frame scan current; 4 — beam line scan current; and for case b: 1 — beam line scan current; 4 — synchronizing pulse

less than 3.5 ms are required to generate the information frame proper, i.e. welding zone image, when the probing beam current is equal to 5–10 mA; to prevent damaging of the item surface during welding at a comparatively low rate of increase (~0.5) and decrease (~0.1 ms) of the line scan amplitude, the beam current should be practically zero.

The main factor preventing meeting the above-listed requirements is the distributed capacity of the respective high-voltage cable current-carrying conductors. To prevent development of self-oscillatory processes in the high-voltage circuit, the rate of beam current variation has to be limited, this leading to increase of the current pulse front duration. As is seen from the oscillograms in Figure 2, a, in order to generate a current pulse with the peak duration of 3.5 ms, the overall time of welding process disturbance can be up to 6 ms. The pulse shape in the zero current range leaves much to be desired. Here a flat peak is practically completely absent, thus hindering the timely start of the beam scan generator and, therefore, it is difficult to avoid melting of the item surface during rise and drop of the line scan current.

Considering the above, the purpose of this work is comparison of analog and microprocessor control of electron beam current.

Structural features of beam current control channels. A feature of the considered control channels is their integration into the overall system of computer control of the process of electron beam welding [4] based on Sinumerik 840D NPS system [5], which realizes multicoordinate welding displacements. One of the virtual axes of NPC system is beam current, the instant value of which is rigidly synchronized with the displacements. Type and placing of the respective NPC interface module impose certain restrictions on the structure and characteristics of the channel of beam current control as a whole.

Figure 3 gives two realized variants of beam current control, using the following similar solutions: control signal setting the required beam current is a digital code formed by Sinumerik 840D NPC 1; decoupling of control channel parts which are at different potentials, is performed using fiberoptic pairs 2 located on air–transformer oil boundary in the high-voltage tank of the accelerating voltage source; control voltage of the welding gun emission system is formed by the beam current stabilizer 4, and the beam current feedback signal is read from resistor $R_{f,b}$; maximum value of negative potential of emission system control electrode is set by resistors $R1$ and $R2$.

Differences in the circuits of beam current control consist in application in the first case (Figure 3, a) of a standard digital-analog converter (DAC) of Sinumerik 840D NPC system, and in the second case (Figure 3, b) — building into this system a NPC converter (PWI development) with digital output (DO).

In the schematic shown in Figure 3, a, digital value of the set beam current is converted by DAC into an analog signal, then into frequency signal (Sinumerik 840D NPC system does not include modules capable of direct code-to-frequency conversion) is transmitted through a fiberoptic communication line, then is converted from the frequency (using F–V converter) back into analog signal, filtered through low-pass filter LPF and is fed to the beam current stabilizer. In the schematic shown in Figure 3, b, the digital value of the assigned beam current is converted into analog signal already in the high-voltage tank, directly before the inlet of beam current stabilizer. Microprocessor 3 with its own DAC is used for this purpose.

If we do not consider the characteristics of beam current stabilizer (since this component is the same for both the schematics), it can be seen than in the first case there are at least three links, which have an adverse influence on the reliability of control signal transmission:

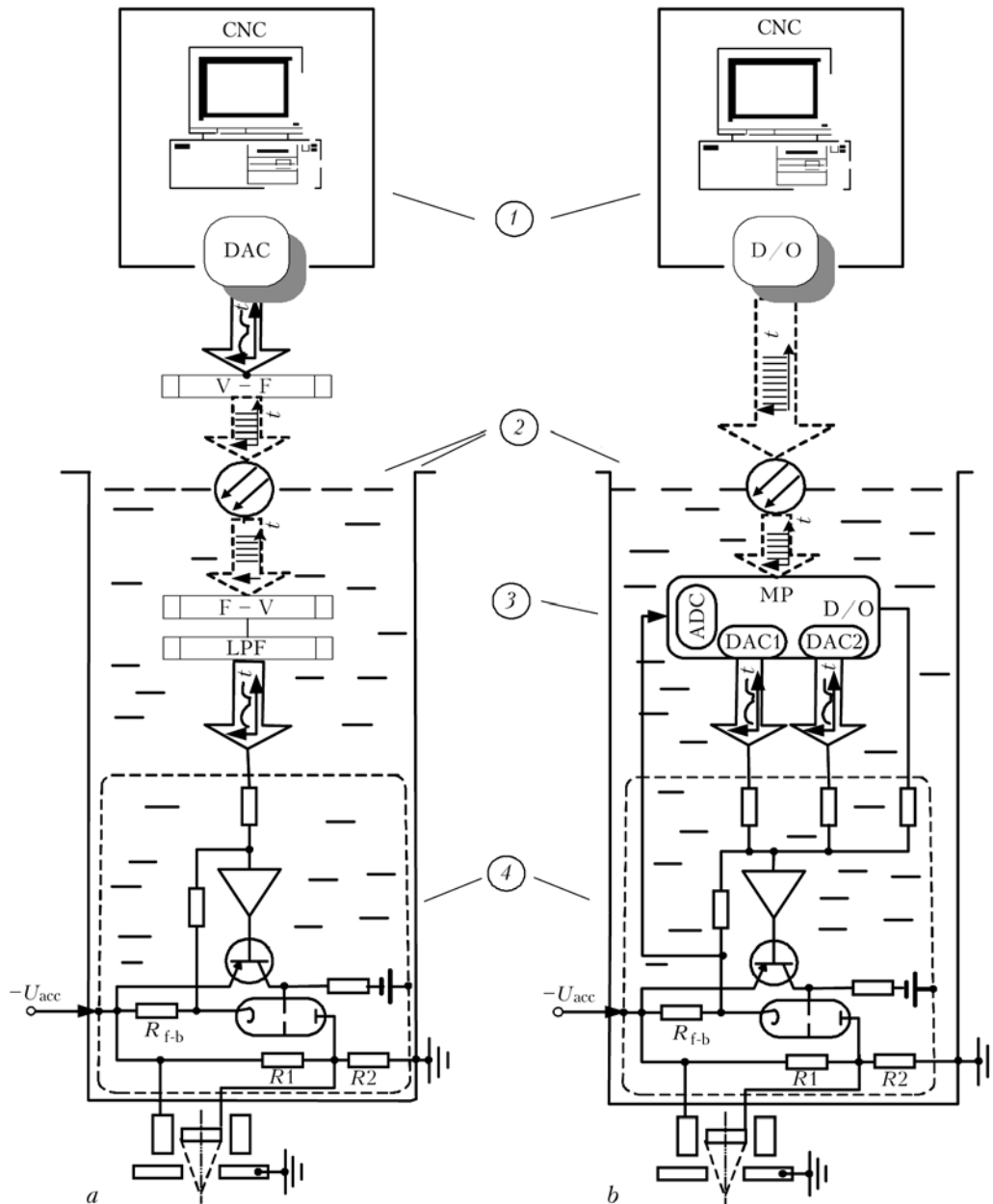


Figure 3. Block-diagram of analog (a) and digital (b) control of beam current: 1 — control computer of Sinumerik 840D NPC system; 2 — fiberoptic decoupling from high voltage; 3 — microprocessor (MP); 4 — beam current stabilizer (DAC — digital-analog converter; ADC — analog-digital converter; D/O — digital interface module; V-F — voltage–frequency converter; LPF — low-frequency filter; $-U_{acc}$ — minus of accelerating voltage source; R_{f-b} — resistor of beam current transducer)

- analog communication channel between the hardware cabinet accommodating the NPC system and accelerating voltage source, of up to 10 m length exposed to the influence of electromagnetic fields;

- «voltage–frequency» and «frequency–voltage» converters ($\leq 0.1\%$ non-linearity at the frequency of 1 μ Hz, temperature instability of $\pm 0.015\%$ /deg at the frequency of 100 kHz, setting time of 11 μ m at the frequency of 100 kHz);
- low-frequency filter.

Although temperature instabilities of «voltage–frequency» and «frequency–voltage» converters are higher than similar DAC parameters, nonetheless, they do not go beyond the maximum admissible values, affecting the welding current parameters. The analog communication channel is the link the most susceptible to electromagnetic noise influence. Therefore, ex-

perimental studies performed by S.A. Shevchuk at PWI showed the need for application of the low-pass filter with the maximum setting time of not less than 0.4 ms that essentially limits both the dynamic capabilities of the beam current control channel, and the stability of the small beam currents (Table). The adverse influence of the low-pass filter cannot be compensated for by application of the known techniques.

In the digital channel of beam current control there is only one link, which affects the reliability of control signal transfer — DAC — incorporated into the microprocessor (see Figure 3). The latter performs only linear operations, and the constants stored in its memory, are independent on time (time spent by the microprocessor for performance of any operations with the input signal is negligibly small).

The microprocessor has the following functions:



Comparison of the characteristics of analog and microprocessor control of welding beam current

Parameter	Analog channel	Digital channel
Linearity, %	0.2	0.05
Temperature coefficient, %/deg	0.07	0.0025
Current setting increment, μA	1000	100
Minimum current, μA	1000	100
Beam current instability in the following ranges, %:		
0.1–1.0 mA	± 100	± 10
1–1000 mA	± 1	± 1
Maximum rate of beam current adjustment, mA/ms	50	200
Duration of interruption of welding process at butt following, ms	6	5

- conversion of the digital setting code into the analog signal of beam current stabilizer control using DAC1;
- implementation of the second adjustment contour in the small current mode using DAC2;
- forcing the process of establishment of the required beam current.

Analog signal of DAC1 converter comes to the main input of beam current stabilizer and ensures the discreteness of assigning the current of $250 \mu\text{A}$ with the execution accuracy of $\pm 125 \mu\text{A}$ for the maximum current of 1 A. If the setting were realized by a beam current stabilizer without errors, such accuracy would be quite acceptable for most of welding purposes. However, the stabilizer, despite the fact that it is included into the analog feedback loop, introduces its own errors and instabilities, dependent on temperature and time, particularly in the initial section of its characteristic. For their elimination, the second feedback loop is included into the control system, which is realized in the digital form as follows.

Resistor feedback voltage R_{f-b} in the current stabilizer lamp cathode is measured by DAC of the microprocessor, constructed so that the bit capacity of conversion in the small signal range is equal to 16, i.e. the increment is equal to several tens of microamperes. The code of the beam current value measured on the feedback resistor is compared with the setting code fed to microprocessor DAC, and then the corrective action on the control signal is generated, which corresponds to the accuracy of the measurement channel. Summing up the main and correcting setting signals further allows, if required, switching to finer setting increments than those which the main DAC1 converter can provide. The latter generates the control signal in a coarse grid, and DAC2 corrects it to the closest value of the fine grid.

Application of a microprocessor allowed improving beam current controllability due to the broad capabilities of the pre-distortion method [6], when in order to control the knowingly «slow» cascade, pre-distortions compensating the insufficient cascade dynamics, are introduced into the control signal to obtain acceptable dynamic characteristics.

In the considered case, in order to cut off the beam current, current stabilizer is switched off by a special discrete pulse and a much higher negative potential is applied to the electron tube control electrode than the one required for complete blocking of the emission system; short time of going out of the repeated blocking mode to the required

current level is achieved by reverting to the current stabilization mode with simultaneous feeding to the stabilizer input of a pulse accelerating the process of reaching the required current.

Comparison of oscillograms characterizing the operation of the considered channels at a jump-like change of current (see Figure 2) confirms the much higher operating quality of the digital channel: duration of welding process interruption is reduced by 20 % --- from 6 to 5 ms; beam current cut-off (its zero level) is clearly registered, this eliminating melting of the item surface during rise and drop of the amplitude of the beam line scan.

The main parameters of electron beam control, when the considered channels are used, are given in the Table. It should be noted that the digital microprocessor channel is characterized by lowering of beam current instabilities by an order of magnitude in the range of low setting-up currents of 0.1–1.0 mA, as well as 4 times increase of the speed of beam current adjustment compared to analog control.

CONCLUSIONS

1. High noise immunity and response of the microprocessor channel of welding electron beam current control make it rational to apply in the new generation units.
2. Results of experimental investigation of the designed microprocessor channel of welding electron beam current control and its application in the production units demonstrated a reliable stabilization of electron beam current with the accuracy of $\pm 1 \%$ in the welding mode and $\pm 10 \%$ in the mode of low setting-up currents of $\leq 1 \text{ mA}$; strict generation of current pulses of the specified shape ensuring operation of the system of automatic guidance of the beam to the butt.

1. Nazarenko, O.K., Shapoval, V.I., Loskutov, G.A. et al. (1993) Observation of electron beam welding process and automatic butt following. *Avtomatich. Svarka*, **5**, 35–38.
2. Nazarenko, O.K., Kajdalov, A.A., Kovbasenko, S.N. et al. (1987) *Electron beam welding*. Ed. by B.E. Paton. Kiev: Naukova Dumka.
3. Mauer, R. *Strahlstromsteuerung fuer eine Elektronenstrahl-Schweissmaschine*. Pat. 24 60 424 Deutsche. Int. Cl. H 01 J 37/24. Publ. 17.03.77.
4. Paton, B.E., Nazarenko, O.K., Nesterenkov, V.M. et al. (2004) Computer control of electron beam welding with multi-coordinate displacements of the gun and workpiece. *The Paton Welding J.*, **5**, 2–5.
5. (2004) *Sinumerik & Simodrive*: Catalogue NC of the Siemens Society.
6. Krotov, N.A., Kozyrev, V.B. (2003) Methods of linearization of amplitude characteristic of power amplifiers. *Radiotekhnika*, **12**.



IMPROVEMENT OF FRACTURE RESISTANCE OF JOINTS OF ALLOY 1420 PRODUCED BY NONCONSUMABLE-ELECTRODE ARGON-ARC WELDING WITH FORCED OSCILLATIONS OF THE WELD POOL

T.M. LABUR, A.G. POKLYATSKY and A.A. GRINYUK
E.O. Paton Electric Welding Institute, NASU, Kiev, Ukraine

Physico-chemical characteristics are compared of the joints of high-strength aluminium alloy 1420 produced by nonconsumable electrode welding in argon by a regular stationary arc and by an arc deflected from the arc vertical axis due to current passing through the filler wire. Values of welded joint strength and bending angle, as well as strength and impact toughness of weld metal, are determined, when batch-produced welding wire SvAMg63 is used. Values of fracture toughness were established, which determine the level of reliability of welded joints in structure service. Features of microstructure of welds and their hardness distribution are analyzed.

Keywords: argon-arc welding, nonconsumable electrode, aluminium alloys, welded joints, arc deflection, pool oscillations, physico-mechanical properties, hardness, structure, fracture resistance

At performance of regular nonconsumable-electrode argon-arc welding of modern superlight high-strength aluminium-lithium alloys, oxide film inclusions form in welds, and pores develop in the zone of weld fusion with the base metal. In addition, presence of lithium which is an alloying element, leads to appearance of brittle precipitations and abrupt increase of stress concentration, which is indicated by low values of fracture toughness characteristics of welded joints [1]. To produce sound welded joints, various methods of impact on the molten metal are applied, which provide optimum thermophysical properties and promote activation of the processes of cathode breaking of the oxide film on the surfaces being welded and removal of gas bubbles from the melt. Methods causing dynamic oscillations of the weld pool molten metal and its intensive stirring during welding, are particularly effective. For this purpose, mechanical oscillations of the electrode are performed, filler wire is fed intermittently, short-time current pulses are applied to the arc, asymmetrical or modulated current is used for powering the arc, and additional magnetic fields are induced.

Molten metal displacements at electrode oscillations become more active due a change of the force impact of the arc on the pool (normal component of arc pressure, inversely proportional to the angle of electrode deflection from the vertical) [2]. Intermittent feed of electrode wire promotes development of liquid metal oscillations as a result of periodical change of the volume of metal, coming to the pool head part [3]. At application of short-time current pulses, oscillations in the melt arise as a result of an abrupt increase of arc pressure during passage of these pulses [4], and in modulated current welding they are due to the difference in the arc pressure during the

welding current pulses and pauses [5, 6]. Application of asymmetrical current also promotes intensive stirring of molten metal, which occurs as a result of arc pressure change at current polarity reversal [7].

When external magnetic fields are used, the intensity of stirring of weld pool liquid metal increases as a result of their interaction with the volume electromagnetic force arising in the arc gap [8-14]. Depending on the direction of the magnetic induction lines, the magnetic field can be longitudinal or transverse, and by the time of action --- constant or variable. A constant magnetic field acting on the arc, causes a change of the arc geometrical dimensions and position, preserving them during the entire time of magnetic field existence. Variable magnetic field periodically deflects the arc column from the vertical position. Direction of arc deflection depends on the direction of magnetic induction lines (longitudinal magnetic field deflects the arc normal relative to weld axis, and transverse field --- parallel to the welding direction). The amplitude and frequency of arc oscillations depend on the magnetic field intensity and frequency of its pole reversal. The simplest method of producing a variable magnetic field is use of solenoids, to which alternating current is applied [15].

To induce mechanical oscillations of the electrode or intermittent feed of filler wire, it is necessary to use specialized devices. Pulsed-arc welding can be performed only with special power sources. The most common methods of electromagnetic impact on the arc make the torch design more complicated, make the assembly process more difficult, hinder arc following, etc.

Passing electric current through the filler wire section can be a promising and simple-to-apply method of effective electromagnetic impact on the arc. As a result of interaction of a variable electromagnetic field, induced around the arc discharge, with a constant or variable electromagnetic field around the filler wire, the arc deviates from the vertical position. De-



pending on the values and polarities of currents passing through the arc gap and filler wire section, the resultant of magnetic inductance will change its value and direction, thus causing a change of the Ampere force acting on the arc and of its direction. Periodical change of current polarities leads to a change of the arc position relative to the vertical axis. The force action of welding arc P_{an} on the pool in this case will change, depending on the angle of its deviation from the vertical α , and will be given by the following formula:

$$P_{an} = KI_a^2 \cos \alpha,$$

where P_{an} is the force of arc pressure in its vertical position (along the normal); K is the coefficient of proportionality; I_a is the current in the arc gap.

Arc deviation from its vertical position causes oscillations of the molten metal of weld pool, changing the conditions of its stirring, degassing and solidification. Application of nonconsumable-electrode argon-arc welding with weld pool oscillations, which are due to current passage through the filler, will allow producing sound welded joints with high fracture resistance values.

Butt joints of sheets ($400 \times 200 \times 4$ mm) of 1420 alloy (Al-5.4Mg-2.1Li) were welded at alternating current of 195 A by automatic nonconsumable-electrode argon-arc welding using MW-450 power source of Fronius, Austria. ASTV-2m unit was used for torch displacement and filler wire feeding. Welding speed was 12 m/h, wire feed rate being 75 m/h, argon flow rate being 15 l/min. Batch-produced welding wire SvAMg63 (Al-6.3Mg-0.6Mn-0.2Zr) of 1.6 mm diameter was used as the filler wire. Main strength and ductility characteristics of base metal by the results of testing 5-7 samples cut out along the rolling direction, are as follows: $\sigma_t = 463.8$ MPa, $\sigma_{0.2} = 352.5$ MPa; $\delta = 5.8\%$; $\alpha = 37^\circ$; $KCV = 11.8$ J/cm².

Prior to welding, sheets and wire were treated by chemical etching in a water solution of NaOH (50 g/l), clarified in 30 % of HNO₃ water solution, washed and subsequently dried. Edges to be welded were mechanically cleaned from three sides to the depth of not less than 0.15 mm. In order to induce oscillations of the weld pool molten metal, direct or alternating current $I_f = 220$ A was passed through the filler wire sections (Figure 1).

After welding, flat samples were cut out of the produced butt joints for determination of their mechanical properties under uniaxial tension, and sections were cut out for investigation of hardness, as well as micro- and macrostructure of welds. The physico-mechanical properties of welded joints at off-center tension were determined by Kahn method, in which flat samples of 36×57 mm size with a deep sharp notch of 0.1 mm radius at its tip [16] are tested. Rate of notched samples stretching at testing was equal to 2 mm/min ($3.3 \cdot 10^5$ m/s). At off-center tension load-deformation (P - f) diagrams were recorded in the oscillograph, which registered the moments of initiation and propagation of cracks in the studied samples up to their complete fracture. Diagrams

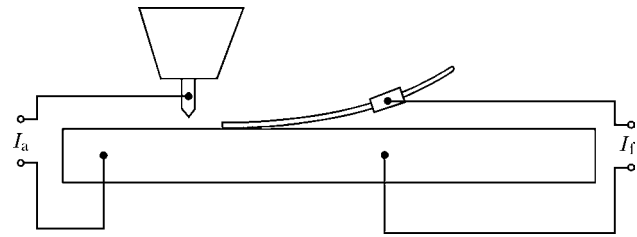


Figure 1. Schematic of the process of nonconsumable-electrode argon-arc welding with weld pool oscillations resulting from electric current passage through the filler wire section

allow quantitative evaluation not only of stress intensity during sample deformation at off-center tension, but also of the extent of the stage of stable metal flow and the work spent by it at individual stages of crack propagation. Testing conditions met the technical requirements of GOST 25.506. Experimental results were obtained at testing five samples in all-purpose RU-5 machine.

Test results were used to determine the values of nominal stress σ_{fr} and critical stress intensity factor K_c , as well as specific work of crack initiation (SWCI) and propagation (SWCP). Values of J_c parameter were evaluated by calculation of the function of variation of deformation energy depending on crack length, using Merkle-Corten relationship [17].

Nature and features of structural changes proceeding in the metal in nonconsumable-electrode argon-arc welding under the conditions of weld pool oscillations, were studied in scanning electron microscope JSM-840 with microanalyzer system Analytic Link --- 860/500 Obtek at accelerating voltage of 15, 20, 30 kV. Analysis results were compared with the data on the nature of variation of fracture relief of joints made under the regular welding conditions. Such a comprehensive approach allowed considering the processes running in the weld metal.

Samples with weld reinforcement produced both by the stationary arc and with weld pool oscillations fail in the fusion zone at uniaxial tension. Tensile strength of welded joints produced by regular nonconsumable-electrode argon-arc welding, is on the level of 326 MPa. Electric current passage through the filler wire section allows improving this index up to 338 MPa.

Strength of weld metal produced by a stationary arc with filler wire SvAMg63 is equal to 322 MPa on average, and with pool oscillations due to direct or alternating current passage through it --- 344 MPa. In this case, however, the weld impact toughness drops from 26 to 12 J/cm², and bend angle of welded joints decreases from 90 to 88°. It should be noted that the values of strength and impact toughness of the metal of welds produced in welding with pool oscillations, are on the level achieved after artificial ageing of the samples (120°, 8 h) welded by a regular stationary arc.

At off-center tension of samples produced by regular nonconsumable-electrode argon-arc welding, the value of breaking stress σ_{fr} of weld metal is in the range of 298-320 MPa, and in the fusion zone it is 279-300 MPa (Table). Critical stress intensity factor K_c , at which spontaneous crack propagation begins, is 18-24 for weld metal, and 17-19 MPa \sqrt{m} for fusion



Indices of fracture resistance of welded joints on 1420 alloy at testing by off-center tension

Studied weld section	σ_{fr} , MPa	K_{Jr} , MPa \sqrt{m}	J_c	SWCP	KCV
			J/cm ²		
Weld metal	298–320	18–24	5.3–6.1	3.0–4.8	5.4–7.3
	379–402	34–50	7.1–12.4	8.3–13.6	8.5–12.0
Fusion zone	279–300	17–19	4.2–5.5	3.9–4.8	4.9–6.3
	345–371	22–24	7.1–7.9	6.3–7.8	6.7–7.8

Note. The numerator gives the values for samples made by regular nonconsumable-electrode argon-arc welding, the denominator --- for samples made with pool oscillations resulting from current passage through the filler.

zone. Current passage through the filler wire during welding allows increasing the level of index σ_{fr} to 379–402 MPa for weld metal and up to 345–371 MPa for fusion zone. Energy values of crack initiation J_c and crack propagation also rise more than 1.5 times in welding with weld pool oscillations compared to regular nonconsumable-electrode welding (Figure 2). Impact toughness index KCV for weld metal increases from 5.4–7.3 up to 8.5–12, and for the fusion zone from 4.9–6.3 up to 6.7–7.8 J/cm².

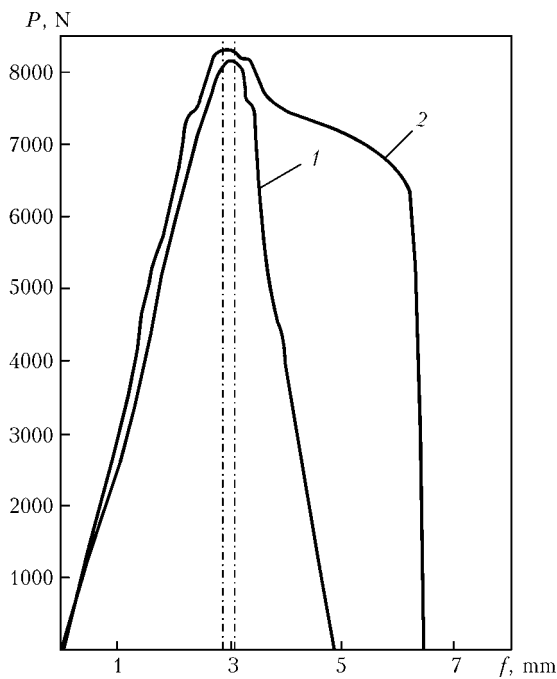


Figure 2. Diagrams of off-center tension testing of welded joints of 1420 alloy produced by a regular stationary arc (1) and with pool oscillations (2)

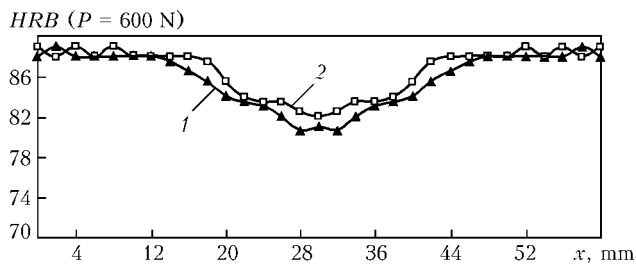


Figure 3. Hardness profile of welded joints of 4 mm thick alloy 1420 produced by nonconsumable-electrode with filler wire SvAMg63 by a regular stationary arc (1) and with pool oscillations (2)

In nonconsumable-electrode stationary arc welding of 1420 alloy the minimum hardness in the weld central part at $P = 600$ N is equal to $HRB 84$, and in the HAZ metal it is $HRB 91$ (Figure 3). Oscillations of the weld pool due to current passage through the filler wire section promote increase of these values up to $HRB 87$ in the weld, and up to $HRB 92$ in the HAZ metal.

Increase of strength and decrease of softening of welds and welded joints as a whole is attributable to refinement of weld structure in welding with weld pool oscillations. The main volume of the weld produced with pool oscillations is made up by equiaxed dendrites of much smaller dimensions than those formed in the welds welded by a stationary arc (Figure 4). Grain refinement limits the microcrack by effective barriers --- boundaries of grains and crystallites. As a result, the initiating microcrack does not go beyond the subcritical sizes or changes its direction at subsequent propagation under the impact of external forces. Such a fracture mode can be related to the fact that fewer defects (dislocations) accumulate along the boundaries of grains (crystallites) in the fine-grained metal [16].

Data of fractographic analysis of sample fractures also confirm the fact that improvement of fracture

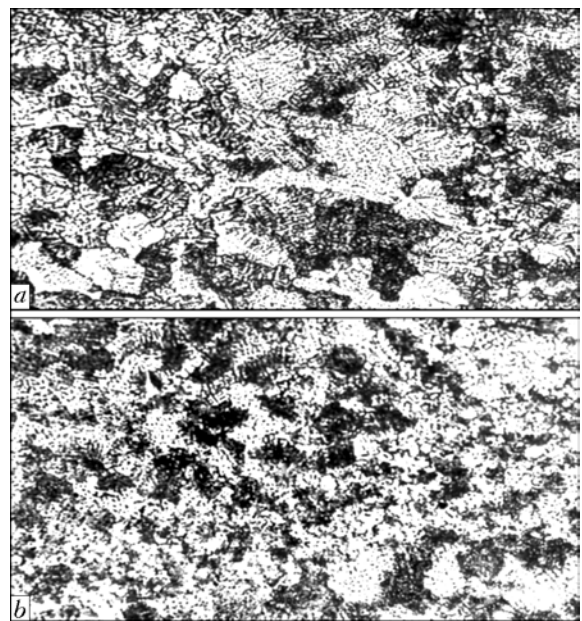


Figure 4. Microstructure of weld metal produced in nonconsumable-electrode argon-arc welding by a stationary arc (a) and with pool oscillations (b) ($\times 100$)

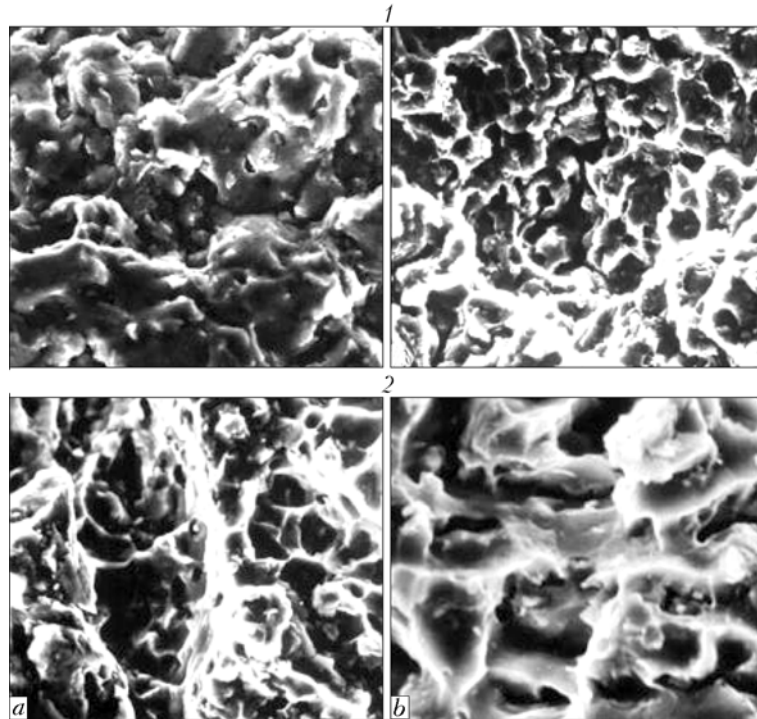


Figure 5. Fractograms of fracture surface of the weld (a) and fusion zone (b) of samples produced in welding alloy 1420 with filler wire SvAMg63 by the regular stationary arc (1) and with pool oscillations (2) ($\times 500$)

resistance values is due to formation of a more uniform finely-dispersed structure in the weld metal and the fusion zone (Figure 5). A greater number of brittle sections is noted in samples produced by a stationary arc, and the share of intercrystalline relief is equal to approximately 50 % of fracture area. Application of welding with weld pool oscillations promotes an increase of the fraction of intercrystalline relief by more than 1.5 times.

A physical prerequisite for improvement of mechanical properties of welded joints are dynamic oscillations of the weld pool arising at current passage through the filler wire during welding. Formation of a fine-crystalline structure of weld metal and fusion zone leads to increase of the total extent of crystal boundaries, this hindering the abrupt increase of stress concentration and thus restraining the propagation of the initiating microcracks.

CONCLUSIONS

1. Oscillations of the weld pool molten metal which are due to continuous variation of arc pressure as a result of its deviation from the vertical position, promote intensive stirring of the base and filler metal, metal degassing, breaking up of oxide film inclusions and formation of a fine-crystalline weld structure, thus providing stable high mechanical properties of welds and welded joints as a whole.

2. Application of nonconsumable-electrode welding with weld pool oscillations, promotes formation of more uniform fine-crystalline structure of welds on alloy 1420, which 2 times increases the level of the critical stress intensity factor, and 1.5 to 2 times increases the metal fracture resistance at the crack propagation stage.

1. Labur, T.M., Ishchenko, A.Ya., Kogut, N.S. (1990) Static crack resistance of welded joints of high-strength aluminium alloys. *Avtomatch. Svarka*, **4**, 9–11.
2. Slavin, G.A. (1980) Formation of disoriented weld metal structure at low-frequency disturbance superposition on the weld pool. *Svarochn. Proizvodstvo*, **6**, 3–5.
3. Zubrienko, G.L., Galkin, N.P., Gaponov, D.A. et al. (1972) Argon-arc welding of aluminium alloys with intermittent filler wire feed. *Ibid.*, **4**, 46–47.
4. Slavin, G.A., Trokhinskaya, N.M., Ryazantsev, V.I. et al. (1986) Optimising the parameters of manual and automatic welding of aluminium sheet alloys with superposition of short-time current pulses on the arc. *Ibid.*, **1**, 14–15.
5. Ishchenko, A.Ya., Poklyatsky, A.G., Lozovskaya, A.V. et al. (1990) Influence of the parameters of low-frequency modulation of alternating polarity rectangular current on weld structure in welding of aluminium alloys. *Avtomatch. Svarka*, **9**, 23–27.
6. Ishchenko, A.Ya., Dovbishchenko, I.V., Budnik, V.P. et al. (1994) Current methods of arc welding of aluminium alloys. *Ibid.*, **5/6**, 35–37.
7. Maruo, H., Hirata, Yo., Makino, H. (1989) Rectangular wave AC TIG arc welding of aluminium alloy. *Quarterly J. JWS*, **1**, 63–69.
8. Chernysh, V.P. (1964) Application of magnetic fields in electric arc welding. In: *Problems of mechanics and machine-building*. Kiev: KGU.
9. Bachelis, I.A. (1965) Magnetic control of welding arc. *Svarochn. Proizvodstvo*, **1**, 17–19.
10. Bachelis, I.A., Varlamov, I.V. (1966) Displacement of electric arc in the magnetic field. *Avtomatch. Svarka*, **5**, 45–48.
11. Mechev, V.S. (1968) Amplitude of electric arc oscillations in alternating magnetic field. *Svarochn. Proizvodstvo*, **3**, 9–11.
12. Jayarajen, T.N., Jackson, C.E. (1972) Magnetic control of gas tungsten-arc welding process. *Welding J.*, **51**(8), 377–385.
13. Wendler, H.D. (1970) Die magnetische Beeinflussung des Schweißlichtbogen. *Wiss. Z. Techn. Hoch. A*, **14**(7), 741–744.
14. Brodyagina, I.V. (1998) Arc welding of aluminium alloys with application of magnetic fields. *Svarochn. Proizvodstvo*, **9**, 48–51.
15. Chernysh, V.P. (1968) Electromagnetic stirring of weld pool and deposited metal quality. *Vestnik KPI. Series Mashinostroenie*, **5**, 61–67.
16. (1976) *Fracture*. Vol. 6: Fracture of metals. Ed. by G.T. Libovits. Moscow: Mir.
17. (1986) *Static strength and fracture mechanics of steels*. Ed. by V. Dal et al. Moscow: Metallurgiya.



INFLUENCE OF PRE-DEFORMATION ON IMPACT TOUGHNESS OF CHARPY SAMPLE IN FRACTURE

V.P. DYADIN

E.O. Paton Electric Welding Institute, NASU, Kiev, Ukraine

An approach is proposed to evaluation of upper shelf impact toughness of Charpy sample depending upon degree of plastic pre-deformation of metal rolled stock. The derived analytical dependencies were analyzed, and main parameters were determined characterizing their change. A simple engineering dependence was proposed, which allowed evaluation of change of the upper shelf impact toughness of a Charpy sample depending upon degree of plastic deformation in fabrication and assembly of the metal structure elements.

Keywords: welded joint, impact toughness, Charpy samples, tough fracture, deformation ageing, upper shelf, plastic deformation

In analytical confirmation of stable connection between values of impact toughness of upper shelf of Charpy and Mesnager samples [1] critical angle of bending of Charpy sample θ_{1c} at the instant of fracture origination was estimated through deformation ε_f corresponding to plastic stability loss of the material ε_t :

$$\varepsilon_t = n / (1 - n), \quad (1)$$

where n is the deformation strengthening of the material.

As it was noted in [1, 2], angle of bending θ_{1c} of Charpy sample may be expressed in this case by the dependence

$$\theta_{1c} = 3\varepsilon_t((1 + 4r/\rho)/K_v^2)^{1/(1+n)}, \quad (2)$$

where ρ is the notch radius ($\rho = 0.25$ mm); r is the distance from apex of the notch, commensurable with a characteristic average size of a structural element ($r = 0.05$ – 0.10 mm); K_v is the concentration factor of elastic stresses in apex of the Charpy sample notch ($K_v = 3.44$) [3]; ε_t is the deformation, corresponding to a conditional tensile strength of the material ε_t .

Good correspondence between experimental and theoretical results was shown on the accepted assumption.

In this article possibility of estimating relative change of impact toughness of the Charpy sample fracture depending upon degree of preliminary plastic deformation of the metal rolled stock is considered. If this issue is solved, practical possibility appears to make corrections in requirements to impact toughness, allowing for its possible reduction depending upon predicted plastic deformation of the structure element, which will allow expending practical application of fracture mechanics criteria [4] in designing and strength calculation of structures, and make more substantiated selection of structural materials in case of occurrence of plastic deformations.

So, for example, it may be useful in estimation of crack resistance of the material of localized damages

in main pipelines, subjected to plastic deformations in the process of assembly, in case of motion of soils, temperature action, etc. [5].

Proceeding from the relations (1) and (2) of [1, 2] and assigning true curve of the material deformation by the power law of strengthening

$$\sigma = \sigma_{0.2}(\varepsilon/\varepsilon_y)^n, \quad (3)$$

specific work of crack propagation a_v^{pr} and fracture origination a_v^{or} of the Charpy sample in static loading may be written in the form

$$a_v^{pr} = ((1 + 4r/\rho)/K_v^2)^{n/(1+n)}(B - L) \times k_2(\sigma_t(1 + \varepsilon_t))^2\varepsilon_t/(4\sigma_{0.2}); \quad (4)$$

$$a_v^{or} = ((1 + 4r/\rho^{or})/K_v^2)(B - L) \times 3k_1(\sigma_t\varepsilon_t(1 + \varepsilon_t))/(4(1 + n)), \quad (5)$$

where ε_t is the deformation, at which a respective conditional yield point $\sigma_{0.2}$ of the material is determined; k_1 is the obstruction factor for a Charpy sample, equal to 1.25 [3]; k_2 is the mean obstruction factor for a standard Charpy sample at the instant of fracture development, equal to 1.26; $(B - L)$ is the height of the sample under notch, equal to 8 mm [1].

Full work of a Charpy sample fracture ($a_v = a_v^{pr} + a_v^{or}$) in this case may be presented in the form

$$a_v = \frac{1 + 4r/\rho_v}{K_v^2} (B - L)\sigma_t\varepsilon_t(1 + \varepsilon_t) [(k_2\sigma_t(1 + \varepsilon_t) \times ((1 + 4r/\rho)/K_v^2)^{-1/(1+n)}/(4\sigma_{0.2}) + 3k_1/(4(1 + n))]. \quad (6)$$

In order to take into account influence of plastic deformations on change of the fracture work of a Charpy sample, let us consider a sample, fabricated from the same material, but preliminary deformed at the value ε in direction of its length.

If we neglect deformation ageing of the material, then proceeding from conditions of the deformation curve (Figure 1), specific work of propagation $a_v^{pr(\varepsilon)}$ and origination $a_v^{or(\varepsilon)}$ of fracture of a Charpy sample may be described in this case by similar dependencies:

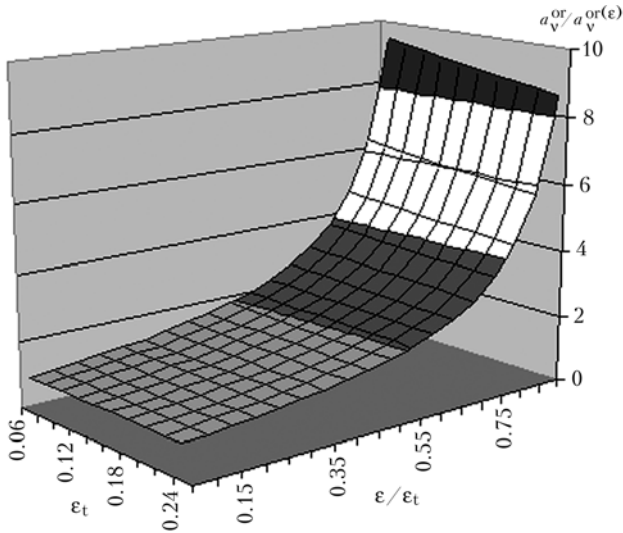


Figure 2. Relative change of work of tough fracture origination of Charpy sample ($a_v^{or}/a_v^{or(\epsilon)}$) depending upon initial value of uniform plastic deformation ϵ_t and value ϵ/ϵ_t

$$\times \frac{k_2 \hat{\sigma}_t (1 + \hat{a}_t) ((1 + 4r/\bar{n})/K_t^2)^{-1/(1+n)} / \hat{\sigma}_{0.2} + 3k_1/(1+n)}{k_2 \hat{\sigma}_t^{(\hat{a})} (1 + \hat{a}_t) ((1 + 4r/\bar{n})/K_t^2)^{-1/(1+n)} / \hat{\sigma}_{0.2}^{(\hat{a})} + 3k_1/(1+n)}$$

Using relations (3), (17) at $\epsilon \geq \epsilon_y$, yield point $\sigma_{0.2}^{(\epsilon)}$ may be expressed in the form

$$\sigma_{0.2}^{(\epsilon)} = \sigma_t^{true} (\epsilon/\epsilon_t)^n = \sigma_t (1 + \epsilon_t) (\epsilon/\epsilon_t)^n \quad (21)$$

In this case, taking into account dependence (21), expressions (19), (20) are additionally simplified:

$$a_v^{pr} / a_v^{pr(\epsilon)} = \left(\frac{1 + \frac{4r}{\rho}}{K_v^2} \right)^{\frac{\epsilon}{(1+2\epsilon_t)(1+2\epsilon_t-2\epsilon)}} \times \quad (22)$$

$$\times \frac{\epsilon_t \sigma_t (1 + \epsilon_t) (\epsilon/\epsilon_t)^n}{\sigma_{0.2} (\epsilon_t - \epsilon)}$$

$$a_v / a_v^{(\epsilon)} = \frac{\epsilon_t}{(\epsilon_t - \epsilon)} \times \quad (23)$$

$$\times \frac{k_2 \left(\frac{\hat{\sigma}_t}{\hat{\sigma}_{0.2}} \right) (1 + \hat{a}_t) ((1 + 4r/\bar{n})/K_t^2)^{-1/(1+n)} + 3k_1/(1+n)}{k_2 \left(\frac{\hat{a}_t}{\hat{a}} \right)^n ((1 + 4r/\bar{n})/K_t^2)^{-1/(1+n)} + 3k_1/(1+n)}$$

As one can see from expression (18), relative change of the work of tough fracture origination in a Charpy sample at static loading is completely characterized by initial uniform deformation capacity of the metal ϵ_t and pre-deformation ϵ . General diagram of relative change of the work of origination of a Charpy sample, depending upon initial value of uniform plastic deformation ϵ_t and value ϵ/ϵ_t , is presented in Figure 2.

Proceeding from dependence (22) it follows that relative change of the work of fracture propagation of a Charpy sample depends upon initial strength characteristics of the metal (σ_t , $\sigma_{0.2}$, ϵ_t), size of zone r , and value ϵ .

In Figure 3 diagrams of the value $a_v^{pr} \sigma_{0.2} / (a_v^{pr(\epsilon)} \sigma_t)$ change from initial value of uniform

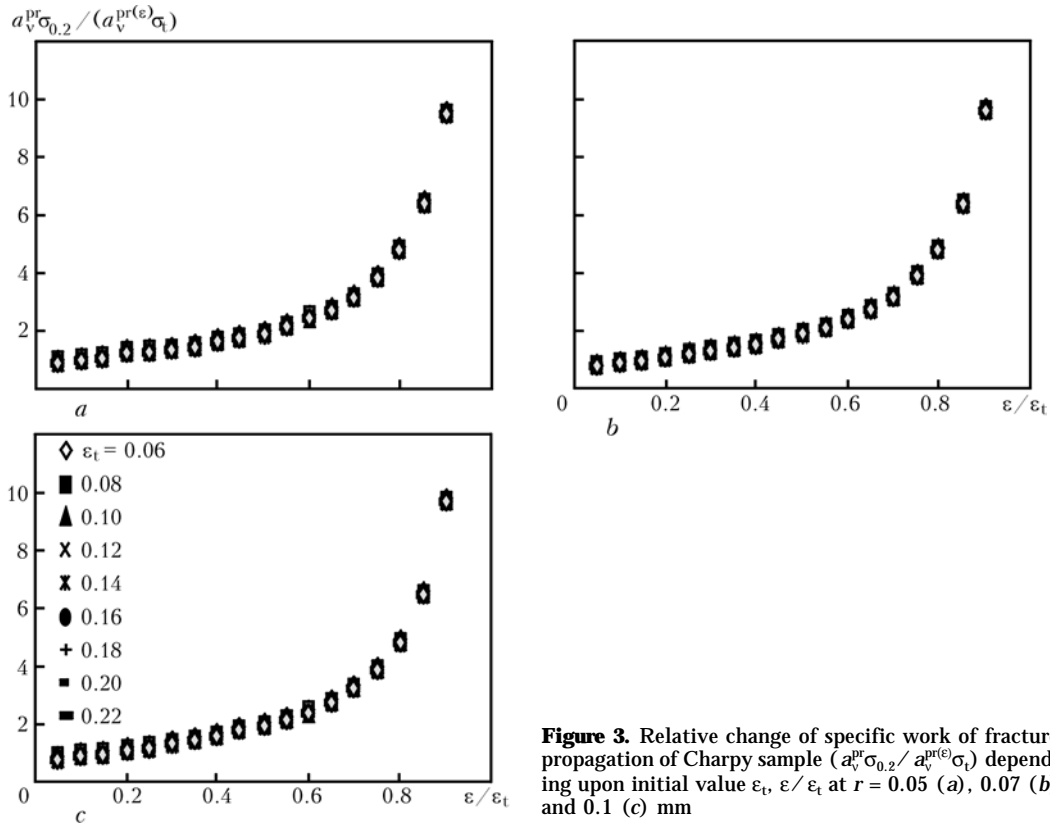


Figure 3. Relative change of specific work of fracture propagation of Charpy sample ($a_v^{pr} \sigma_{0.2} / a_v^{pr(\epsilon)} \sigma_t$) depending upon initial value ϵ_t , ϵ/ϵ_t at $r = 0.05$ (a), 0.07 (b) and 0.1 (c) mm



deformation ϵ_t , value ϵ/ϵ_t and element r , are given. As one can see from the drawing, change of value r within presented range (0.05–0.10 mm) very insignificantly effects values $a_v^{pr}\sigma_{0.2}/(a_v^{pr(\epsilon)}\sigma_t)$, which allows assuming it for simplification of further estimations in a number of cases equal to a certain mean value ($r \approx 0.06$ mm) [1, 2].

Knowing initial strength characteristics of the metal ($\sigma_t, \sigma_{0.2}, \epsilon_t$), equation (23) is quite fit for practical estimation of change of fracture toughness of a Charpy sample depending upon degree of pre-deformation.

It should be noted that direct experimental determination of value ϵ_t in engineering practice is associated with certain difficulties. In particular, when a material is supplied by the manufacturer-plant only minimum values of mechanical characteristics $\sigma_t, \sigma_{0.2}$ are guaranteed, and, as a result, requirements to the degree of homogeneous deformation turn out to be undetermined. In this connection direct application of value ϵ_t in estimation of strength characteristics and designing of structures is not used (in this case in the certificates values are given only of relative elongation, which has limitation from below that allows indirect judging about plastic capacity of the material). In [7] for removal of this shortcoming in establishment of correlation dependence between certificate values $\sigma_t, \sigma_{0.2}$ and value ϵ_t , seven most widely used structural steels with different initial mechanical properties and forms of the deformation curve behavior are investigated. As a result of carried out investigations simplified correlation dependence was obtained (numerical coefficients are rounded off up to hundredth values):

$$n = -0.18 + 0.22\sigma_t/\sigma_{0.2}, \quad (24)$$

where n is determined from expression (1). As follows from (24), index of deformation strengthening in this case has limitation from below, equal to 0.04 ($\epsilon_t \approx 0.041$), which, approximately, corresponds to deformation in determining of conditional yield point $\sigma_{0.2}$ with correction on plasticity of 0.2 %.

Table 1. Strength characteristics of billet being investigated from steel 09G2S-Sh after different kinds of treatment

Deformation degree, %	$\sigma_{0.2}^{(e)}$, MPa	$\sigma_t^{(e)}$, MPa	$\epsilon_t^{(e)}$, %	δ , %	σ_t^{true} , MPa
$\epsilon = 0$	280	450	0.190	39.1	535
$\epsilon = 5$	392	475	0.145	35.6	544
$\epsilon = 7.5$	435	483	0.106	28.6	534
$\epsilon = 10$	474	502	0.096	26.6	550
$\epsilon = 5; 150^\circ\text{C}, 1\text{ h}$	393	471	0.134	34.4	534
$\epsilon = 7.5; 150^\circ\text{C}, 1\text{ h}$	424	474	0.126	32.2	534
$\epsilon = 10; 150^\circ\text{C}, 1\text{ h}$	465	496	0.090	27.9	540
$\epsilon = 5; 250^\circ\text{C}, 1\text{ h}$	421	475	0.115	34.4	530
$\epsilon = 7.5; 250^\circ\text{C}, 1\text{ h}$	465	498	0.106	29.6	550
$\epsilon = 10; 250^\circ\text{C}, 1\text{ h}$	493	512	0.070	23.7	548

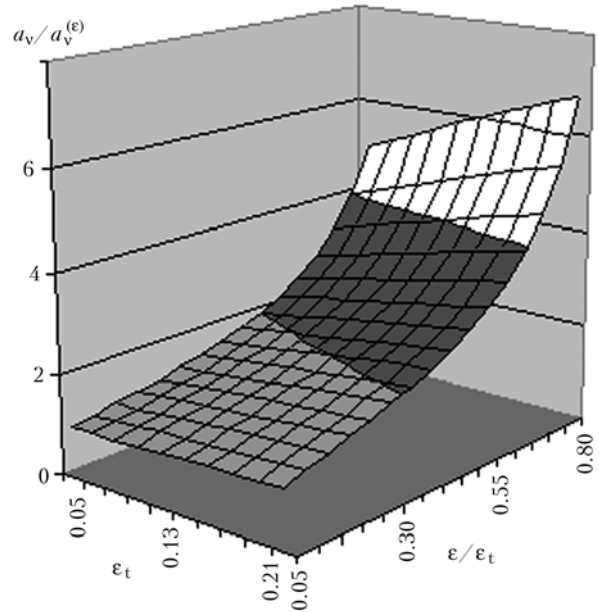


Figure 4. Calculated values of relative change of tough fracture work of Charpy sample, $a_v/a_v^{(e)}$, depending upon degree of plastic pre-deformation ϵ/ϵ_t

Taking into account (24), a possibility appears for graphic analysis of expression (23) depending upon plastic properties ϵ_t and relative plastic pre-deformation ϵ/ϵ_t of the material. In Figure 4 general character of change of dependence (23) is graphically presented, taking into account expressions (1), (13) and (24).

As one can see from Figure 4, when relative pre-deformation ϵ/ϵ_t increases above 50 %, significant reduction of fracture toughness of a Charpy sample is noted. Indirect confirmation of the latter are also experimental data, obtained in [8]. In addition, significant reduction of toughness of a Charpy sample may also take place at low values of plastic pre-deformation of material, ϵ , if the latter has low reserve of plasticity.

As it was noted in [1], quasi-static dependencies, obtained by estimation of fracture works (a_v, a_v^{pr}, a_v^{pr}) of a Charpy sample, may be applied for the case of dynamic loading.

For estimating legitimacy of the assumptions made above and approaches to estimation of fracture work of a Charpy sample [2], experimental check of obtained dependencies was made, using as an example rolled sheet from steel 09G2S-Sh of 70 mm thickness.

In order to exclude influence of inhomogeneity of the rolled metal properties in direction of its thickness, a metal layer of 14 mm thickness, located at the depth 15 mm from the sheet surface, was investigated. Scheme of the cutting-out and location of samples are

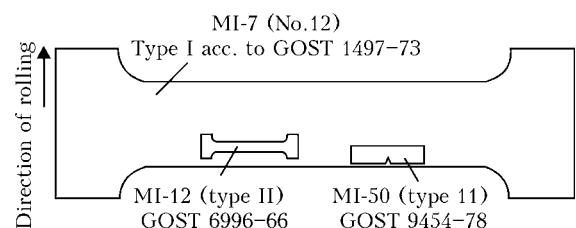


Figure 5. Scheme of cutting-out and location of samples

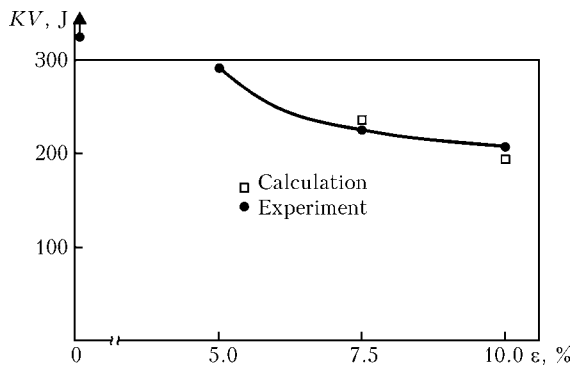


Figure 6. Change of upper shelf impact toughness KV of Charpy sample depending upon degree of pre-deformation

shown in Figure 5. Prepared flat samples MI-7 were subjected to different uniform plastic deformation by 5, 7.5 and 10 %, after which a portion of billets was seasoned in the furnace at temperature 150 and 250 °C within 1 h for determining influence of deformation ageing on strength characteristics of the metal. Then samples for tension (MI-12) and impact toughness (MI-50) tests were made from produced billets.

Time after pre-deformation of flat billets, their seasoning in the furnace, and performance of standard tension and impact bend tests constituted 20 days.

Results of tension tests of samples MI-12, manufactured from the billets being investigated, are given in Table 1. Determination of deformation was performed on 30 mm basis, using displacement sensors.

As one can see from Table 1, true tension σ_t^{true} in the point of plastic stability loss practically does not depend upon pre-deformation and degree of deformation ageing of the metal, which, in its turn, allows later on expanding somewhat area of application of expression (17) (in this case first part of equation $\sigma_t(1 + \varepsilon_t) = \sigma_t^{(e)}(1 + \varepsilon_t^{(e)})$ is meant).

Values of impact toughness of Charpy samples according to lower scatter of data are given in Table 2.

In Figure 6 diagram of change of upper shelf impact toughness KV depending upon degree of pre-deformation ε , and calculated according to formula (23) values, taking into account expression (24), are presented. Due to the fact that impact tests were performed on the impact testing machine with energy reserve 300 J, and upper shelf fracture toughness KV of Charpy sample at $\varepsilon = 0$ % significantly exceeded this value, data, calculated according formula (23), are presented relative experimental data at $\varepsilon = 5$ %.

As one can see from Figure 6, calculated values KV match sufficiently well experimental data, which

Table 2. Results of impact tests of steel 09G2S-Sh

Deformation degree, %	KV, J, at temperature, °C						
	+20	0	-20	-30	-40	-60	-80
$\varepsilon = 0$	>300	>300	>300	240	187.2	165.5	7.2
$\varepsilon = 5$	293.4	>300	216	184.2	175.2	18.6	6
$\varepsilon = 7.5$	224.4	204	213.6	184.2	81.6	4.8	3
$\varepsilon = 10$	201.6	283.8	192	153.6	4.8	4.8	4.8

proves possibility of using this approach for correcting requirements to upper shelf impact toughness in case of possible plastic deformation of metal structure elements.

In addition, detected feeble dependence of true stress σ_t^{true} in the point of plastic stability loss upon pre-deformation and degree of deformation ageing of the metal ($\sigma_t(1 + \varepsilon_t) \approx \sigma_t^{(e)}(1 + \varepsilon_t^{(e)})$) allow later on expanding somewhat area of application of obtained expressions also on HAZ of weld joints.

CONCLUSIONS

1. Analytical dependencies, which allow estimating relative change of specific work of origination and propagation of tough fracture in Charpy samples depending upon plastic deformation ε , ε_t and structural parameter r , are obtained.

2. A simple expression for determining possible reduction of upper shelf impact toughness of a Charpy sample depending upon value of plastic deformation of metal rolled stock is proposed.

1. Dyadin, V.P. (2004) Comparison of impact toughness values of Charpy and Mesnager specimens at tough fracture. *The Paton Welding J.*, **4**, 21–26.
2. Girenko, V.S. (1997) *Widening of applications of fracture mechanics in evaluation of crack resistance of welded structure elements in static loading conditions*. Syn. of Thesis for Dr. of Techn. Sci. Degree. Kiev.
3. Peterson, R. (1977) *Stress intensity factors*. Moscow: Mir.
4. Lobanov, L.M., Girenko, V.S., Dyadin, V.P. (1999) Standard mechanical tests and crack resistance of welded structure elements in static loading conditions. In: *Fracture mechanics of metal and strength of structures*. Vol. 1. Issue 2. Lviv.
5. Paton, B.E., Semenov, S.E., Rybakov, A.A. et al. (2000) Ageing and procedure of evaluation of the state of metal of the main pipelines in service. *The Paton Welding J.*, **7**, 2–10.
6. Rusinko, K.N. (1981) *Theory of plasticity and non-steady creep*. Lviv: Vyscha Shkola.
7. Dyadin, V.P. (1998) *Development of method for evaluation of resistance of materials and welded joints to stable crack propagation in static loading conditions*. Syn. of Thesis for Cand. of Techn. Sci. Degree. Kiev.
8. Potak, Ya.M. (1955) *Brittle fractures of steel and steel parts*. Moscow.



GAS-SHIELDED LASER AND LASER-ARC WELDING OF STEELS

V.D. SHELYAGIN¹, V.Yu. KHASKIN¹, A.V. SIORA¹, A.V. BERNATSKY¹,
E.I. GONCHARENKO¹ and T.G. CHIZHSKAYA²

¹E.O. Paton Electric Welding Institute, NASU, Kiev, Ukraine

²NTUU «Kiev Polytechnic University» Kiev, Ukraine

The effect of argon, carbon dioxide and their mixture on peculiarities of laser and hybrid welding of low-carbon and low-alloy steels was determined. Utilisation of the shielding gas mixture was found to have a positive effect. It is shown that increase of the arc power component in hybrid welding with a laser power of 1–2 kW leads to levelling of the hybrid effect. Stabilisation of the arc and its fixation to the laser beam persists, which allows increasing the welding speed and penetration depth in groove welding.

Keywords: laser welding, low-carbon and low-alloy steels, continuous radiation, decreased power, electrode wire, arc, hybrid process, steel, metallographic examination, structure, hardness

When selecting shielding gases for laser and hybrid laser-arc welding, it is necessary to take into account that the gas atmosphere should provide a reliable shielding of molten and heated metal from air to prevent formation of oxides and nitrides. Also, it is desirable that the flow rate of a shielding gas and its cost should be minimal. The shielding atmosphere and laser plasma formed in it should be as transparent as possible for laser radiation. Plasma consists of a shielding gas ionised by laser radiation and metal vapours flowing out from the keyhole [1]. Formation of the so-called plasma lens that re-focuses the radiation is not permitted.

Based on these conditions, welding of carbon steels is normally performed by using carbon dioxide and, in rare cases, argon. However, the former decreases impact toughness of the weld metal at negative temperatures, which greatly limits its application for welding critical metal structures, whereas argon favours formation of plasma that re-focuses and absorbs a major part (up to 2/3 of the total power) of radiation of CO₂-lasers [2]. This effect is mitigated by using different shielding gas feeding schemes, which are based mostly on purging at a certain angle relative to the radiation axis [3]. In hybrid welding, however, argon promotes a spray-rotational transfer of electrode metal, increase in the welding current and formation of undercuts in the upper reinforcement bead.

For laser and hybrid laser-arc welding, it is desirable to use such gases or their mixtures, which make it possible to avoid the above drawbacks, raise the welding speed, increase the penetration depth and decrease the sensitivity of the weld metal to porosity [4, 5]. First of all, such gases include helium and its mixtures with argon. However, an important drawback of helium is its high cost, especially for welding low-carbon and low-alloy steels. Carbon dioxide also

has a positive effect, as it allows increase in the efficiency of melting of electrode and base metals.

This study is dedicated to investigation of peculiarities of laser and hybrid laser-arc welding of thin-sheet low-carbon and low-alloy steels in an atmosphere of carbon dioxide, argon and their mixture (80 % Ar + 20 % CO₂) [5]. One of the examples of practical application of these welding methods is a large-scale welding of domestic low-pressure (to 2.4 MPa) cylinders. Supposedly, it can replace rotating-arc welding, where the welds have too big reinforcement (2–3 mm) and internal flash. The key requirement to the technology of this welding method is the use of a comparatively inexpensive technological laser. As such, the continuous-wave fast-flowing CO₂-laser with cross-pumping of a mixture was chosen, which generates a power of up to 2 kW with a circular distribution of the intensity in a cross section (e.g. of the «Pluton-2» or ULG-2 type). As established during experiments, the required power is 1.5 kW, allowing for the losses of power during transportation and focusing of the beam using a lens with focal distance $F = 300$ mm onto a workpiece.

A number of comparative experiments were conducted using laser and hybrid laser-arc welding in argon, carbon dioxide and their mixture (80 % Ar + 20 % CO₂) to evaluate the effect of a shielding gas, welding speed and welding current on variations in the penetration depth. Welding was performed by the butt method without groove preparation. The base metal of specimens $\delta = 2$ mm thick, later on welded by laser welding, had the following chemical composition, wt. %: 0.1 C, 0.024 Si, 0.8 Mn, 0.003 S, 0.013 P, 0.03 Cr, 0.03 Ni, < 0.03 Mo, < 0.02 Cu, < 0.02 V. Welding by the hybrid method was performed on specimens of steel St.3ps (semi-killed) ($\delta = 5$ mm).

Laser and hybrid welding procedures are described in [6, 7]. Laser welding was carried out under the following conditions: focused beam power $P_0 = 1.5$ kW, welding speed $v_w = 40$ m/h, focus deep-

Table 1. Results of metallographic examination of laser welded specimens

Shielding gas	Microhardness of structural components of metal of welded joints in low-carbon steel									Grain index	
	Weld			HAZ							
				Coarse-grained region			Fine-grained region			Coarse-grained region	Fine-grained region
	F	P	B	F	P	B	F	P	B		
Ar	250	--	260-290	Traces	--	260-280	189	200-210	--	7	10
CO ₂	190-220	Traces	--	185-190	Traces	--	195	--	230-240	7	10
80 % Ar + 20 % CO ₂	230-260	260-270	290-300	220-240	Same	Traces	190-210	Traces	--	6	9-10

ening $\Delta F = -1$ mm, and consumption of each of the above shielding gases --- 7 l/min. Parameters of hybrid welding were as follows: $P_0 = 1.5$ kW, $v_w = 45$ m/h, $\Delta F = -(2-3)$ mm, 1.2 mm Sv-08G2S electrode wire feed speed $v_f = 400$ m/h, and consumption of each of the shielding gases --- 15 l/min. Welding current I_w for carbon dioxide, gas mixture and pure argon was 200, 250 and 300 A, respectively.

In CO₂-laser welding the used shielding gases were found to have an insignificant effect on the penetration depth. This parameter is strongly affected by the laser radiation power and focus location relative to the specimen surface. In laser welding the use of the gas mixture causes increase in the penetration width, while in hybrid welding it increases the penetration depth. Effect of the welding speed and welding current on the penetration depth in hybrid and arc welding in carbon dioxide using a metal electrode is shown in Figures 1 and 2. To increase the penetration depth in hybrid welding with no increase in laser power, it is necessary to make a V-groove of the butt joints and deepen the focus. As the arc power is increased and the laser beam power is left unchanged and comparatively low, the hybrid effect becomes markedly less pronounced [8].

To conduct metallographic examinations of structure of the welds made by laser and hybrid welding using a different gas shielding, the specimens were etched in 4 % solution of nitric acid in alcohol, and structure of their metal was examined using optical microscope «Neophot-32» at a magnification of $\times 25$ and $\times 500$. Grain indices were measured according to GOST 5639-82. The examination results are given in

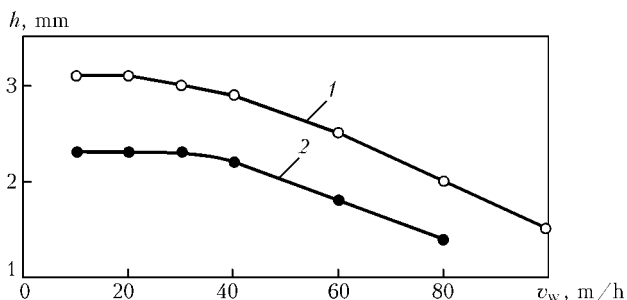


Figure 1. Dependence of penetration depth h on speed v_w of hybrid (1) and arc (2) welding of steel St.3ps ($\delta = 5$ mm) using 1.2 mm diameter electrode wire: 1 --- $I_w = 200$ A; 2 --- 300 A

Tables 1 and 2. Microhardness was measured using the LECO hardness meter M-400 under a load of 0.05 MPa. Curves shown in Figure 3 were plotted on the basis of the measurement results.

Two main regions can be distinguished in HAZ --- coarse-grained region (overheated region) and fine-grained region (re-crystallisation and normalisation region). The rest of the regions normally distinguished in HAZ [9] were not considered, as no visible changes were seen in them.

Consider first the results of laser welding of low-alloy steel ($\delta = 2$ mm) of the above chemical composition. The base metal of the specimens studied was subjected to heat treatment before welding. As a result, it acquired a fine-crystalline structure with grain size equal to 9-10, consisting primarily of ferrite (F) and a small amount of pearlite (P). Hardness of the base metal was HV 210-260.

Microstructure of metal of the welded joints on the specimens made by laser welding is given in Table 1, and the distribution of microhardness in cross section of the joints is shown in Figure 3, curve 1. Note that, unlike specimens made by laser welding in argon and carbon dioxide, structure of the cast zone of a specimen made by the same method in a mixture of 80 % Ar + 20 % CO₂ consists of F, P, bainite (B) and regions of Widmanstätten ferrite (WF). Grain size in its structure is small, which is indicative of substantial overheating.

In laser welding of low-alloy steels, the use of argon (to a greater degree, argon + carbon dioxide

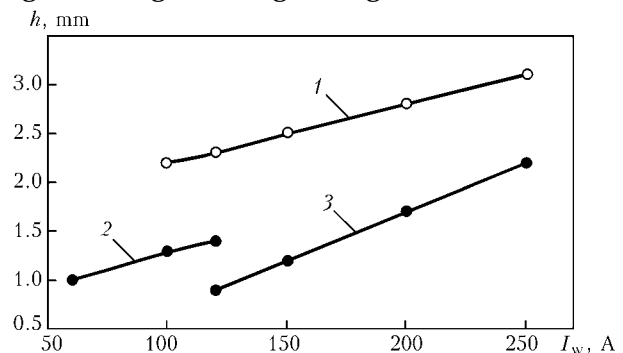


Figure 2. Dependence of penetration depth h on welding current I_w in hybrid welding using 1.2 mm diameter electrode wire (1) and arc welding using 0.8 (2) and 1.2 (3) mm diameter electrode wire at $P_0 = 1.5$ kW, $\Delta F = -(1-2)$ mm, $v_w = 40$ m/h

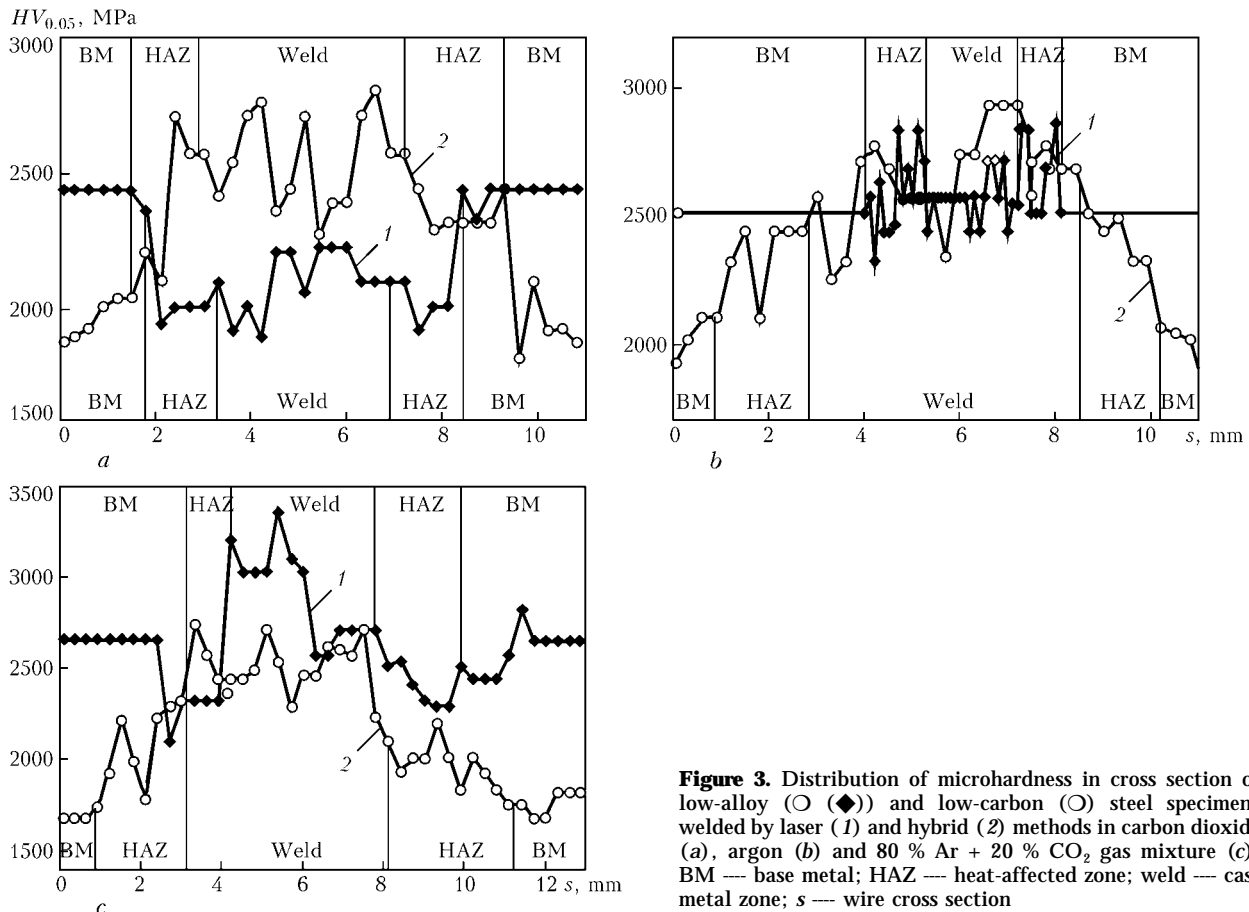


Figure 3. Distribution of microhardness in cross section of low-alloy (○ (◆)) and low-carbon (○) steel specimens welded by laser (1) and hybrid (2) methods in carbon dioxide (a), argon (b) and 80 % Ar + 20 % CO₂ gas mixture (c): BM — base metal; HAZ — heat-affected zone; weld — cast metal zone; s — wire cross section

mixture) leads to increase in hardness of the weld metal, which is caused by increase in the volume content and hardness of the bainite component. In steel under consideration, the growth of hardness is provided by an increased content of manganese (up to 0.8 %). It is likely that increase in hardness is related to some extent to a change in transparency of the plasma plume formed over the keyhole, as well as to conditions of heat transfer when using different gas atmospheres for shielding. So, as the radiation was screened by the plasma plume in the case of using argon, the penetration depth was decreased more than 2 times. In this case, the rate of cooling of molten metal grew, which led to increase in its hardness. The use of the 80 % Ar + 20 % CO₂ mixture leads to some (10–30 %) increase in width of the welds and substantial improvement of formation of the top reinforcement, and eliminates sensitivity to formation of undercuts. The penetration depth does not grow in this case. Most probably, the use of the above gas mixture can lead to increase in the penetration depth only in the case of using a diode laser [10].

Consider now the results of hybrid welding of specimens of low-carbon steel St.3ps ($\delta = 5$ mm). Structure of the base metal in all the cases was a ferrite-pearlite mixture with domination of ferrite (grain index — 7–8, hardness of F — HV 140–170 and that of P — 190–250). Microstructure of metal of the joints on specimens made by this welding method is given in Table 2, and the distribution of microhardness in cross section of the joints is shown

in Figure 3, curve 2. Note that, unlike the laser welding method, in hybrid welding the presence of WF was seen in the majority of the cases. As might be expected, its grain size decreased, i.e. the structure became coarser-grained. In all the cases the HAZ metal has mostly the coarse-grained structure, the fine-grained regions are not clearly defined. In hybrid welding in the 80 % Ar + 20 % CO₂ mixture, hardness of the weld metal decreases to some extent. An important moment in this case is a comparatively small size of ferrite fringes in the weld and HAZ metals. The values of impact toughness here are rather high.

Note that hybrid welding, compared with laser welding, leads to decrease in hardness of metal of the welded joints and provides a more homogeneous structure of this metal. WF is formed in the structure, and hardness of the bainite component decreases to some extent. No effect exerted by different shielding gas atmospheres on structure of the weld and HAZ metal in hybrid welding was revealed, but the effect on the weld formation was detected. Thus, the best weld formation, absence of undercuts in the top bead and decrease in spattering of the molten metal are characteristic of using the 80 % Ar + 20 % CO₂ mixture, whereas in the case of carbon dioxide the weld formation is satisfactory, but spattering of metal from the weld pool grows substantially, and the welding arc is unstable. Using argon as a shielding gas leads to decrease in the penetration depth to 1 mm, like in the case of laser welding. Big undercuts are formed on sides of the top bead, and pores and cracks are

Table 2. Results of metallographic examinations of hybrid welded specimens

Shielding gas	Microhardness of structural components of metal of welded joints in low-carbon steel								
	Weld					HAZ			
						Coarse-grained region			
	F	WF	P	B	Width of ferrite fringe, mm	F	WF	P	B
Ar	230–250	210–220	--	270–290	0.0125–0.0190	205	230	230–245	--
CO ₂	230–250	230–250	Traces	260–270	0.0065–0.0125	190–220	Traces	220–240	--
80 % Ar + 20 % CO ₂	220–230	225–235		245–255	0.0125–0.0170	190–195	--	230	--

Table 2 (cont.)

Shielding gas	Microhardness of structural components of metal of welded joints in low-carbon steel					Width of ferrite fringe, mm	Grain index	
	HAZ						Coarse-grained region	Fine-grained region
	Fine-grained region							
	F	WF	P	B				
Ar	210	--	Traces	--	0.0125–0.0250	4–5	9	
CO ₂	170	--	190	--	0.0065–0.0130	6	9	
80 % Ar + 20 % CO ₂	180	--	220	--	0.0125–0.0235	4–6	8–9	

formed in the cast weld metal. In hybrid welding of carbon steels in the 80 % Ar + 20 % CO₂ mixture the penetration depth grows by about 15–20 %, the welding parameters being the same. In all the cases considered, the presence of argon in the shielding gas raises the sensitivity to cracking of the top part of the welds.

Therefore, compared with carbon dioxide, the use of the argon + carbon dioxide mixture in a proportion of 4:1 in hybrid welding allows the penetration depth to be increased by 15–25 %. Also, this improves the arc stability, decreases metal spattering, and improves the quality of the weld formation. Using the same gas mixture to shield the weld pool in laser welding improves the weld formation and increases width of the welds by 10–30 %, compared with the welds made by carbon dioxide welding, hardness of the weld metal being increased by 20–25 %. Using argon as a shielding gas decreases the penetration depth in all the cases. Undercuts are formed in this case in the top bead in hybrid welding, and hardness of the HAZ metal, compared with the weld metal, grows by 10–20 % in laser welding.

The penetration depth in welding in carbon dioxide or its mixture with argon depends upon the laser radiation power and position of the beam focus relative to the specimen surface. To increase the penetration depth in hybrid welding of the butt joints, it is recommended to make the V-groove and deepen the focus closer to its bottom. Increase in power of the arc com-

ponent in hybrid welding using the 1–2 kW laser leads to decrease in the hybrid effect. Stabilisation of the arc and its fixation to the laser beam persist, which allows a substantial increase in the welding speed or penetration depth when making the butt joints with groove preparation. In hybrid welding, hardness and structure of the weld and HAZ metal when using the argon + carbon dioxide mixture make it possible to increase impact toughness of metal of the welded joints, compared with arc welding.

1. Grigoriants, A.G., Shiganov, I.N. (1988) *Laser equipment and technology*. Book 5: Laser welding of metals. Ed. by A.G. Grigoriants. Moscow: Vysshaya Shkola.
2. Grezev, A.N. (2005) Plasma formation in laser welding. *Svaroch. Proizvodstvo*, **5**, 20–25.
3. Ekoya, S., Tagaki, S., Ogata, T. et al. (2001) Laser welding with shielded gas circulation. *Quart. J. JWS*, **19**(1), 37–43.
4. (2003) Neue gase erzeugen schiankere Naehete. *Produktion*, **30/31**, 15.
5. Voropaj, N.M., Ilyushenko, V.M., Khaskin, V.Yu. (2006) Selection of shielding gas for hybrid laser-arc welding. *Svarshchik*, **4**, 19–23.
6. Shelyagin, V.D., Khaskin, V.Yu., Siora, A.V. et al. (2003) Laser welding of thin-sheet steels using special approaches. *The Paton Welding J.*, **1**, 39–42.
7. Shelyagin, V.D., Khaskin, V.Yu., Garashchuk, V.P. et al. (2002) Hybrid CO₂-laser and CO₂ consumable-arc welding. *Ibid.*, **10**, 38–41.
8. Krivtsun, I.V. (2001) Model of evaporation of metal in arc, laser and laser-arc welding. *Ibid.*, **3**, 2–9.
9. Grabin, V.F., Denisenko, A.V. (1978) *Metals science of low- and medium-alloy steel welding*. Kiev: Naukova Dumka.
10. Danzer, W., Haertl, J. (2002) Diodenlaser zum Tiefschweißen einsetzbar — mit Aktivgas als Prozessgas. *Praktiker*, **2**, 34–35.



PECULIARITIES OF DETECTION OF DEFECTS IN FBW JOINTS ON PIPES BY ULTRASONIC INSPECTION

S.I. KUCHUK-YATSENKO, V.P. RADKO, B.I. KAZYMOV, I.V. ZYAKHOR and A.V. NIKOLNIKOV

E.O. Paton Electric Welding Institute, NASU, Kiev, Ukraine

It is shown that the echo-reflection method involving transducers connected in tandem is an efficient method for ultrasonic inspection of large-diameter thick-walled pipes. For inspection of small-diameter thin-walled pipes, it is expedient to use chord-type TR transducers. Echo signals from defects and interferences in the form of bulges are shown to differ in time of arrival, which allows reliable identification of defects and interferences from the bulges formed as a result of displacement of the weld edges or reinforcement remaining after flash removal.

Keywords: automatic flash butt welding, welded joints, ultrasonic inspection, quality, defects, procedure, false signals, detectability of defects

As specified in regulatory documents, welded joints in pipelines are subject to inspection by in-process and non-destructive methods. The non-destructive test methods, which have received a wide practical application, independently of a welding method, include ultrasonic (USI) and X-ray inspection [1, 2].

Two types of defects, i.e. unclosed craters in the form of discontinuities (Figure 1, *b*) and oxide films (Figure 1, *c*, *d*), may be formed within the joining zone in automatic flash butt welding (FBW). Depending upon the thickness, oxide films can be subdivided into two types, which are substantially different both in structure and effect on mechanical properties of the joints. Oxide films of the first type are films several tenths of a millimetre thick. They are ordinary scales. Defects of this type are called thick oxide films. Oxide films of the other type are fragmented oxide films. In electric arc welding, analogues of unclosed craters are pores, and those of oxide films are lacks of fusion.

Such defects in FBW appear only in the case of gross deviations of the main welding parameters from their set optimal values. These deviations are detected by a computerised monitoring system during the entire welding process [3]. All FBW units developed by the E.O. Paton Electric Welding Institute are currently equipped with such systems. They detect all deviations of the process parameters from their set values, including admissible and inadmissible deviations, and generate corresponding signals, from which the probability of these or other defects is determined. As follows from the data obtained in examination of several thousands of kilometres of industrial pipelines, FBW is characterised by the lowest rate (about 0.2 %) of rejected joints, compared with other methods used for welding of pipes [4]. With FBW, the joints were

rejected mostly because of violation of requirements to preparatory operations for welding, e.g. because of inadmissible size of displacement of the weld edges during alignment of pipes in clamps of the welding machine before welding. The main inspection method in welding of pipelines was and still is the in-process monitoring of welding parameters, the reliability of which is proved by failure-free operation of pipelines for several decades.

Requirements for reliability of welded joints are much tougher in construction of new systems of pipelines designed for operation at increased pressure under severe industrial conditions. Accordingly, requirements to detectability of defects, which may be formed both in pipe metal and in welded joints, thus exerting the negative effect on their properties, also grow.

The purpose of this work was to investigate the efficiency of ultrasonic inspection for detecting the above defects using different methods and types of equipment. The defects may be formed in FBW joints on pipe steels as a result of different violations in the pipe preparation technology, welding and auxiliary welding equipment, or violations in the welding process. They may have a negative effect on mechanical properties of the welded joints. The first stage of the investigations to detect defects was conducted using the criteria common for USI of the electric arc welds.

The investigations were conducted on specimens of welded joints in pipes with a diameter ranging from 114 to 1420 mm and with a wall thickness of 6–18 mm, as well as on welded plates cut from these pipes. All deviations of the main process parameters from the optimal values, which were made to form required defects in the welded joints, were fixed by the computerised monitoring system [3]. After USI, half of the joints of each batch were subjected to standard mechanical tests to tension and bending. The other half of the joints were subjected to forced destruction in the joining zone, for which a notch was made at

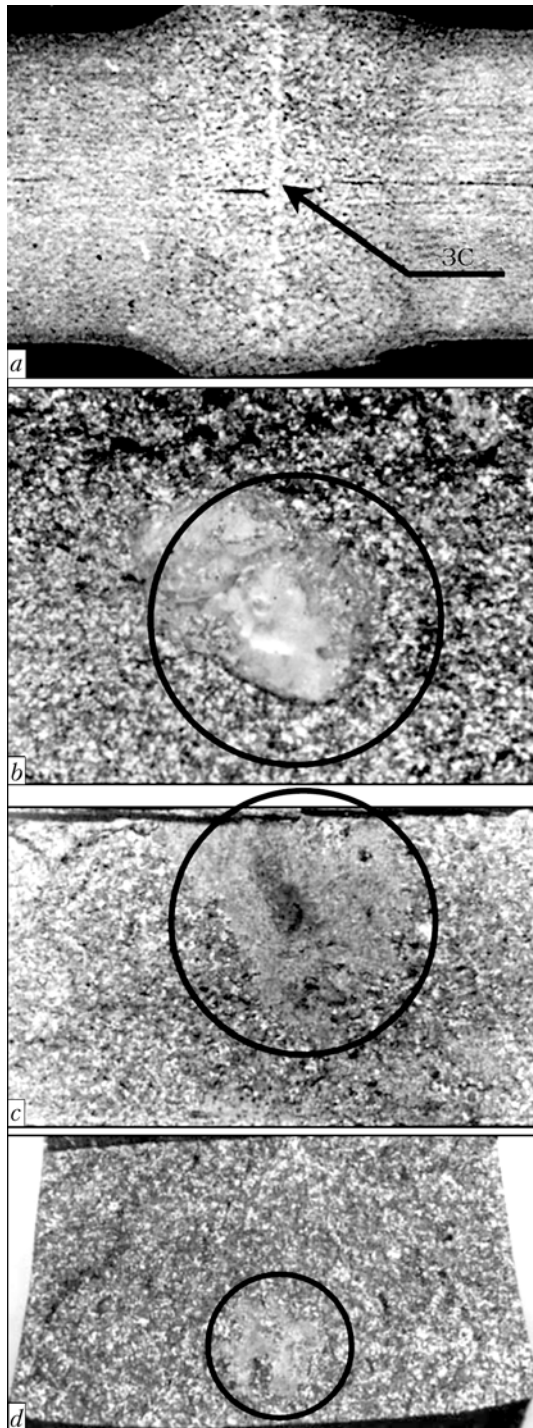


Figure 1. Macrosection of welded joint (a) and characteristic defects on its fracture surfaces: *b* — unclosed crater; *c, d* — thick and thin oxide film, respectively

the joint centre. After the tests, the fracture surfaces of all specimens that fractured were examined to confirm the USI results.

Figure 1, *a*, shows macrosection of the FBW joint. Defects shown in Figure 1, *b–d*, may be formed in the joining zone (JZ). The fracture surface with a defect of the unclosed crater type is shown in Figure 1, *b*. In this case there is a gas cavity in the defect location between the mating surfaces of the pipes welded. Such volume defects can be detected by classic USI methods used to test the arc welds.

Almost identical conditions for the same USI methods are created in detecting thick oxide films. Such a defect is an ordinary scale (Figure 1, *c*). Because of its physical properties, high internal stresses are formed in it after welding in cooling of a welded joint. The stresses destroy it to form numerous macrocracks (discontinuities). Plastic deformation of metal in plane of a joint during upsetting also contributes to this. Cracks can be seen with a naked eye on the fracture surfaces of specimens with such defects. The amplitudes of echo signals from these defects exceed the detection threshold selected on the basis of reference reflectors used to test the electric arc welded joints. The confidence level in detecting them was more than 0.9.

When detecting such defects as fragmented oxide films, where there are no discontinuities (Figure 1, *d*), the classic USI methods have much narrower operational capabilities. Such defects are formed in metal of a welded joint in regions of the pipe ends, where the probability exists of formation of oxide films less than 200 μm in size. Upsetting induces substantial plastic deformation of metal at the pipe ends. As a result, tensile stresses are formed in plane of the joint. They break the oxide film to form a few macrofragments. Metallic bond between the pipes welded is formed in breaking locations. Such defects cannot be detected by the X-ray methods. In USI, the ultrasonic signal dyes away because there is no cavity between the pipes welded. However, its level is higher than the level of structural noises. As shown by the investigations, the most efficient USI method for detection of fragmented oxide films in welded joints 14–32 mm thick is the echo-reflection method, which is realised by using tandem transducers, as well as by means of adaptive selection of the detection threshold on the basis of statistical processing of amplitudes of echo signals emitted from the welding joint over its entire length [1]. This method is particularly efficient with the use of electronic devices. The confidence level in detecting defects by using this technology is above 0.75.

The USI method involving the chord-type TR transducers is employed to detect fragmented oxide films in welding of 114–325 mm diameter pipes with a wall thickness of 4–8 mm. The above transducers provide straight-beam testing of the entire section of the weld, the noises caused by reflection from the reinforcement being almost absent [5, 6]. As shown by the investigations, these peculiarities provide a minimal level of echo signals from probable interferences, compared with signals formed with traditional ultrasonic transducers. This substantially improves the confidence level of the inspection. The chord-type transducers allow testing of welded joints in the TR or combined modes, which makes it possible to identify defects as to their types (volume or plane type) on the basis of determination of shape factors.

Reference reflectors in the form of a flat-bottomed end hole 1.2 mm in diameter were used to adjust the



level of reject sensitivity of the inspection using a chord-type transducer. The set level of search sensitivity for inadmissible defects within the joining zone was 12 dB higher than the reject level.

The high confidence level of USI using the chord-type transducers was proved by testing several batches of welded joints in 114–325 mm diameter pipes with a wall thickness of 6–9 mm, which were produced by using different FBW parameters, including optimal ones and with gross violations. After USI, the joints were deliberately fractured within the joining zone.

When testing sound joints with the flash removed flush with the internal and external surfaces (Figure 2, a), signals only from structural noises can be seen on the flaw detector screen (Figure 3, II, a). Position of upper strobe 1 corresponds to the reject sensitivity level, and position of lower strobe 2 corresponds to the search sensitivity level.

Defects the signals from which are in a range of admissible levels, i.e. between lower strobe 2 and upper strobe 1 (Figure 3, II, b), are most often a structural heterogeneity (different types of inclusions). At the same time, it should be noted that their effect on properties of the welded joints may show up in many different ways. This is evidenced by a scatter of results of mechanical tests of the joints with defects of the above types.

The signal that exceeds the level of the upper threshold (Figure 3, II, c) indicates to the presence of a defect. Comparing the data of USI and results of analysis of fracture surfaces allowed evaluation of the confidence level in detection of restrained defects, which was equal to 0.8–0.9.

False signals may be formed on the flaw detector screen during the inspection process. In addition to structural noises, the main interferences in USI are bulges formed due to displacement of the weld edges (Figure 2, b) and presence of the weld reinforcement remaining after removal of flash (Figure 2, c).

Displacement of the weld edges occurs in welding of pipes that differ in permissible sizes, or in violation of the technology for alignment of pipe ends for welding.

The reinforcement is formed after removal of flash, where a narrow belt remains either in individual regions of a joint, or along its entire length as a result of incomplete removal of metal pressed out in upsetting. The height of the reinforcement depends in many respects upon the flash removal technology. For example, the first welding machines K700 (complex «Sever») comprised a broach-type internal flash remover. In that case the cutting devices were moved following the generating line of a pipe. The drawback of such flash removers was a limited ability of their cutting tools to copy the pipe profile within the welding zone. The ends of pipes during welding are heated to high temperatures. As a result, diameter of a pipe in this region increases due to thermal expansion of metal. That is why the cutting devices cannot copy

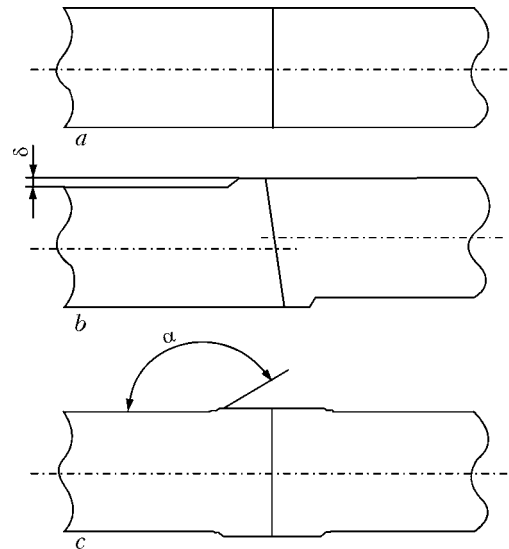


Figure 2. Schematics of FBW joints with removed flash (a), with edge displacement δ (b), and with weld reinforcement (c)

the real actual pipe surface within the welding zone, and cannot provide a complete removal of flash.

This drawback is eliminated in a new generation of the machines due to using the rotor-type flash removers, where the cutting tool of a relatively small size is moved not on the generating line of a pipe, but on its circumference. Such flash removers can remove flash almost completely, i.e. to the level of the internal surface of pipes welded.

Figure 3, II, d, shows an echo signal from an admissible bulge 2 mm high in USI of a sound joint. In this case its level is higher than the reject one set for detection of defects within the joining zone. The amplitude of an echo signal from one and the same bulge may vary with the direction of testing relative to the plane of the joining zone. When the ultrasonic transducers are moved along a welded joint, an echo signal from the bulge may change depending upon the testing direction or reinforcement height.

If the welding zone contains both defect and bulge (of any origin), two signals with a time delay will be seen on the flaw detector screen. When using the chord-type transducers, the front edges of bulges (edges located ahead of the joining zone on the side of placement of the transducers) will generate no noises, as the echo signal from them does not arrive to the receiving transducer. However, edges located outside the joining zone plane may act as interferences in USI. In this case, the first to come is the signal from a defect, and then follows the signal from a bulge (Figure 3, II, e). The interval between them is 4.5 μ s, which corresponds to a difference in distances between the defect and bulge along a beam 7 mm long.

The intensity of echo signals from bulges depends upon angle α between two adjacent surfaces, i.e. the pipe surface and side surface of the reinforcement (see Figure 2, c). As proved, increase of this angle is accompanied by decrease of the echo signal amplitude. The highest interferences in detecting defects within the joining zone occur in testing the welded joints produced with the FBW parameters that create con-

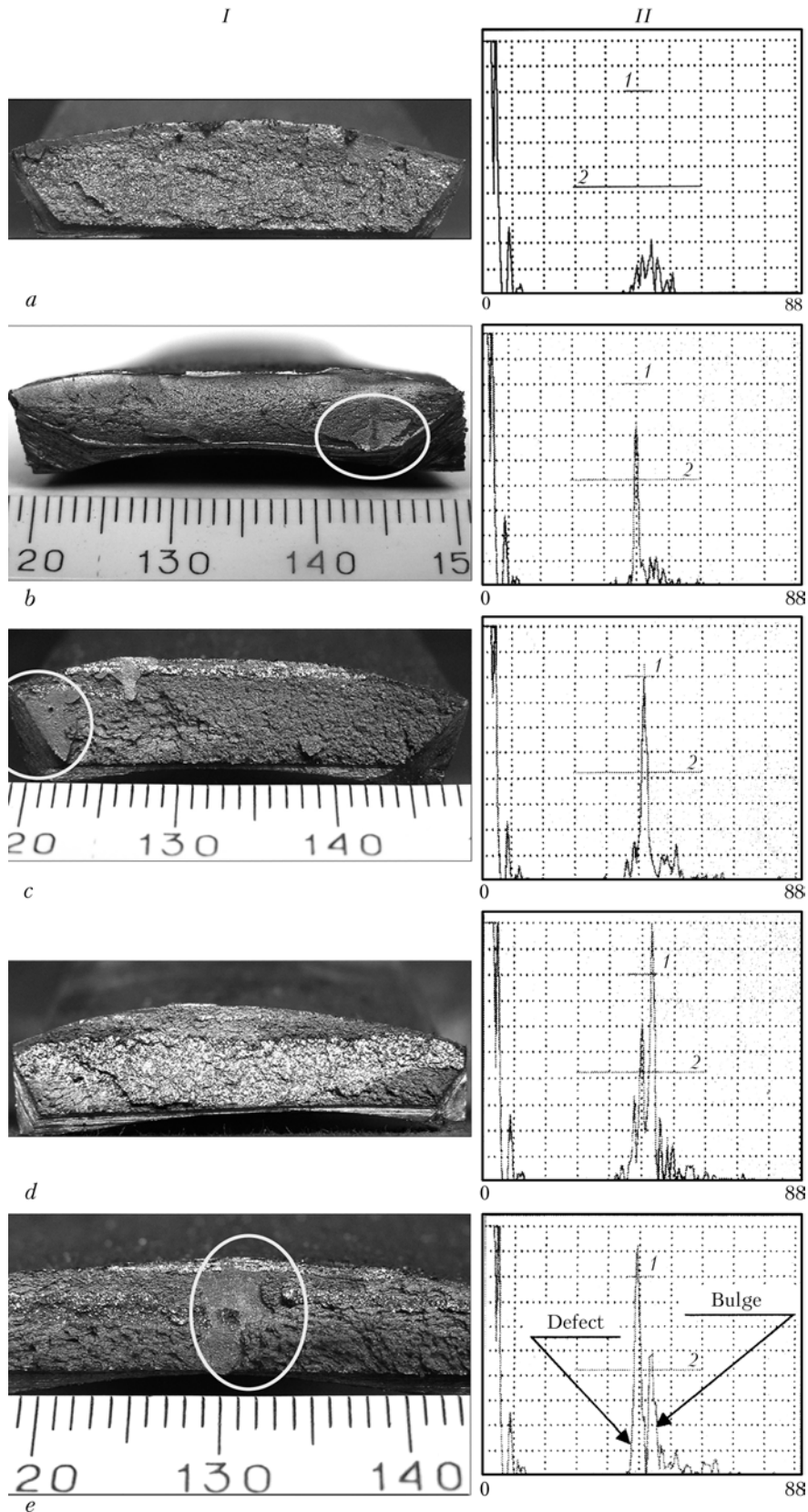


Figure 3. Appearances of fractures (I) and forms (II) of echo signals from metal in the welding zone (a), structural heterogeneity (b), fragmented oxide film (c), bulge (d), defect and bulge (e)

ditions for formation of angle $\alpha = 95-110^\circ$. In this case, there are almost no signals from the reinforcement. These parameters are used for welding large-diameter pipes with a wall thickness of 12–20 mm or more.

Location and type of defects in mechanical test specimens of the welded joints were determined by USI using two methods, i.e. with the inclined-beam TR transducer from the surface of specimens (transverse waves), and with the straight-beam transducer



from specimen edges (longitudinal waves). Defects detected only with the inclined-beam transducer are identified as oxide films, while those detected with the inclined- and straight-beam transducers are identified as discontinuities.

Comparative analysis of the data generated by USI and results of impact tests of a batch of 20 specimens with cross section 10×10 mm showed the high efficiency of the suggested identification method, the confidence level of which was 0.95.

CONCLUSIONS

1. The confidence level in detection of gross defects (unclosed craters and thick oxide films) in welded joints containing no bulges was 0.95. In the presence of bulges on the internal and external surfaces of pipes, especially in the case of formation of edge displacements, the confidence level in detection of defects decreased to 0.8 due to repeated rejection.

2. As established by investigations, the chord-type RT transducers, in which the acoustic axis passes through the pipe body in a plane normal to the vertical axis of a joint, are indicated for testing the welded joints in small-diameter (up to 325 mm) pipes with a wall thickness of 6–8 mm.

3. The investigations show that echo signals from defects and interferences in the form of bulges differ in time of arrival. This makes it possible to reliably identify defects and interferences from probable bulges formed as a result of edge displacement or reinforcement remaining after flash removal.

4. The combined use of straight- and inclined-beam transducers that transmit and receive longitudinal and transverse ultrasonic waves, respectively, allowed identification of defects according to their types, i.e. discontinuities or oxide films.

1. Troitsky, V.A., Radko, V.P., Demidko, V.G. et al. (1986) *Non-destructive testing of welded structures*. Kiev: Tekhnika.
2. (1999) API Standard 1104: Welding of pipelines and related facilities. 19th ed.
3. Kazymov, B.I., Gorishnyakov, A.I., Radko, V.P. (1996) Comprehensive quality control of joints made by pressure welding methods. In: *Proc. of Sci.-Techn. Conf. on Welding in Power Engineering* (Kyiv, Oct. 2–3, 1996). Kyiv.
4. Mazur, I.I., Serafin, O.M., Karpenko, M.P. (1988) Resistance welding of pipelines: ways of improvement. *Stroitelstvo Truboprovodov*, 4, 8–11.
5. Radko, V.P., Troitsky, V.A., Kazymov, B.I. et al. (2006) Study and peculiarities of detection of oxide film type defects by ultrasonic inspection of flash butt welded joints. In: *Proc. of Sci.-Techn. Conf. and Exhibition on Non-Destructive Testing and Technical Diagnostics* (Kyiv, April 10–14, 2006). Kyiv.
6. Giller, G.A., Mogilner, L.Yu. (2000) Ultrasonic chord-type transducers for inspection of welded joints in pipelines. *V Mire Nerazrush. Kontrolya*, 2(8), 18–20.

ECONOMY OF WELDING PRODUCTION

WELDING FABRICATION AND WELDING EQUIPMENT MARKET IN MODERN ECONOMY

V.N. BERNADSKY and O.K. MAKOVETSKAYA

E.O. Paton Electric Welding Institute, NASU, Kiev, Ukraine

Data are given on the state-of-the-art in welding industry, welding equipment market and its sectors, as well as the key factors affecting their development trends. The role of welding in the present-day economy is shown. In particular, the results of comprehensive evaluation of the contribution of welding to the U.S. and German economy are presented.

Keywords: economy, welding, industry, welding equipment market

Welding fabrication, which has an interbranch character, currently is one of the advanced science and engineering components of the world and national economies. Welding fabrication is an independent technology sector, which is to varying degrees integrated into the overall production process in metal-working branches of industry and construction, where welding and allied processes are the base technologies today for joining and treatment of structural materials.

The welding industry at large includes, on the one hand, companies, firms, scientific centers and universities that create innovation product in the form of

technological processes, highly-efficient welding equipment and progressive welding consumables, and on the other hand, branch enterprises and firms — users of welding equipment and technologies, as well as related bodies providing professional training and certification of welding personnel, creation of standard and information support systems and so on.

The most important factor that determines the current activity and future development of welding industry is the availability of developed markets of structural materials and welding equipment, as well as interrelation of these markets. It has been a well-established fact for long that steel has been and remains to be the main structural material for manufacturing welded structures and constructions, while its physical and technical properties and range are constantly per-



ected and upgraded. In 2004 the world steel production overstepped the 1 bln t point, and is expected to reach 1 bln 176 mln t in 2006. The forecast of the International Institute of Cast Iron and Steel (IISI) indicates a continuing growth of real consumption of steel in the world and the demand exceeding the metal product manufacturers' market supply. The apparent consumption of steel products has been constantly increasing by 4–6 % per year for the last years. The apparent world consumption of steel in 2006, by experts' evaluation, will exceed 1 bln t and will reach the level of 1.040–1.055 mln t [1].

IISI analytical studies unambiguously confirm the existence of a direct dependence between the increase of steel consumption and general economic level of the countries, for which a high level of gross domestic product (GDP) growth is typical. The most striking example of this trend is CPR, which over the last years has had the highest and stable rate of GDP growth (8–10 %), it occupies the first place in the world by volume and rates of steel consumption growth. In 2005 the share of this country exceeded 30 % in the world steel consumption. EU countries (25) can be given as one more example, the increase of steel production here being 1–3 %. In 2005, 188.5 mln t of steel were produced in these countries. The dynamics of steel consumption in the countries of the European Union (25) also remains to be positive: in 2005 the volume of steel consumption reached 168 mln t. Such a moderate development of steel consumer market corresponds to moderate growth of GDP in these countries (on average 2–3 % per year).

The trend of interconnection between steel consumption growth and general growth of the economy seems quite appropriate also for evaluation of interrelation between the welding fabrication and welding equipment market development and the volumes of steel and other structural materials consumption. The world experience of welded structure and product manufacturing in different branches revealed that about 2/3 of rolled steel is consumed directly in welded structure fabrication. About 4–6 kg of welding (filler) consumables are used for each ton of consumed rolled stock. High positive correlation is also found between the structures and volumes of applied welding equipment and volumes of steel metal product consumption by the main branches of machine-building production and construction. World and national statistical data on the consumption of metal products can serve as a rather sufficient basic marker in predictive studies and evaluation of development of welding fabrication and basic sectors of welding equipment market. Stable growth of steel consumption allows a substantiated assessment of the favourable prospects for stable and steady growth of the world and national welding fabrications and, correspondingly, of the increased contribution of welding and allied technologies into the economy of leading industrialized countries. Lately these problems have attracted the attention of economists in several countries and have al-

ready been presented on the pages of world welding periodicals.

International exhibition «Welding and Cutting 2005» in Essen (GFR) gave a complete and visual idea of the modern level of world welding fabrication, innovation content of the main sectors of welding market and role of welding fabrication in modern economy at the beginning of the XXI century. Equipment for producing permanent joints (welding, brazing and other) and severing, equipment for surfacing and thermal spraying, technological lasers and laser systems, equipment for adhesion bonding and mechanical joining, welding robots and other automation means, systems for monitoring the welding processes and allied technologies, means and methods of non-destructive testing, welding consumables and fillers (welding electrodes and wires, powders, brazing alloys and other), auxiliary consumables (welding gases and gas mixtures, fluxes, adhesives and other), mechanical equipment, fixtures and tools for welding, means for welder's protection and ecological safety of working environment, were presented in the exposition. Training-methodological materials, training simulators and multi media training tools, software packages for welded structure design, modeling of welding processes, as well as different scientific and technological and standard and reference literature were also displayed at the Exhibition [2].

As the Exhibition showed, novelty and high innovation level is a distinctive feature of modern equipment for welding and allied technologies supplied to the market by leading world development contractors and manufacturers. Today it meets, as a rule, two main demands of customers --- efficiency when used in the industrial process and maximum application of the most recent scientific and technology developments and equipment solutions in it, guaranteeing a high and stable quality of joints. Broad and diverse arsenal of traditional technological processes of welding and treatment of structural materials by the respective equipment with application of welding (filler) materials creates conditions for their competitive selection by the user. Hand in hand with continuous improvement of the existing equipment and technologies for joining and treatment, the equipment for principally new innovation technologies, including friction stir welding (FSW), arc welding with activating flux (A-TIG) and a number of combined processes, is introduced into the market. Combined processes, based on a combination of electric arc or plasma and laser radiation are the most actively developed among them. This earlier known idea is being actively pursued due to application of innovation solutions in the field of electronics, sensors, controls and other. For the last 2–3 years so called hybrid processes (first of all on the base of laser welding) have found wide application in automotive industry, shipbuilding, transport engineering and other.

Today the possibility of comparison and broad selection of different technologies and equipment for



welding and treatment of structural materials of the same class and dimensions is open for a customer in the market. This allows varying the level of expenses for buying the respective equipment, depending on the indices of its efficiency, level of automation and operating reliability, as well as on the criteria of guaranteed quality of the produced joints and compliance of welding technology to ISO 14000 standard.

The peculiarities of the national welding fabrication and welding market can be demonstrated most clearly in the case of Germany. Owing to the efforts of the German Society of Welding and Allied Technologies (DVS), Germany is one of the few countries of the world where economic-statistical data on the volumes of annual production, export and import of a complete list of electrical equipment for welding, brazing and cutting of metallic materials and plastics, different component parts for them, as well as welding consumables and filler materials are open for a wide circle of specialists. This information is based on the official data of Federal Statistical Administration of Germany and corresponds to the classification of the products manufactured by European Union (Statistical Classification of Products by Activity in the European Economic Community --- CPA). Such statistics and its detailed analysis is published annually in the journal «Schweissen und Schneiden», issued by DVS [3]. The enlargement of technological arsenal of joining equipment is accompanied by emergence of new (in addition to welding equipment) sectors of welding market, into which lasers and laser systems, as well as industrial robots should be included. In accordance with the data of [4], the market of German welding equipment had the following structure in 2003:

Market segment	Sales, EUR, mln
Welding equipment (without welding consumables)	1338
Laser and laser systems	340
Brazing equipment	185
Thermal spraying equipment	152
Welding robots	122
Severing equipment	90
Mechanical joining equipment	58
Adhesion bonding equipment	14
Robots for adhesion bonding	7

Taking into account multi-profile structure of the welding market, German specialists introduced a new term for the main types of products: FTB-products --- products for joining (F-Fuegen), cutting (T-Trennen) and coating (B-Beschichten) [4].

The availability of rather full and reliable economic and statistical data on the volumes of production and foreign trade in welding equipment in combination with expert evaluation of sales in other segments of welding equipment and services market, in-

cluding the expenses for personnel training and re-training and other types of services, allowed the economists to evaluate the total volume of the German welding equipment market. In 2004 the total volume of German home welding market exceeded EUR 3.6 bln, while the volume of welding equipment proper (equipment and consumables) made only EUR 1.3 bln the volume of European welding market 3 times exceeds the volume of the German market and is equal to about EUR 11 bln by a conservative estimate of German specialists. In accordance with their, but still more conservative estimate, the world market of welding equipment and services also 3 times exceeds the cost volume of European market --- about EUR 33 bln, or about USD 42 bln [5]. This, in particular, coincides with our tentative evaluation of the volume of world welding equipment and services market by the beginning of XXI century --- about USD 40 bln [6].

The structure of the world and national welding markets undergoes evident changes in the process of development. As it is seen from the example of German welding market, the volumes of innovation equipment sectors grow intensively, being already comparable with sales of the basic sector of equipment for welding and allied technologies. Two relatively new sectors --- «Process lasers and systems» and «Welding robots and robotic stations» are among them, which in accordance with CPA belong to independent groups that are not included into «Welding equipment» group.

Joining and material treatment occupy a dominant position among the main areas of process laser application. The market consumes up to 50 % of the total volume of industrial laser systems for these purposes. The total cost of process laser systems designed for welding industry, will exceed EUR 3 bln in 2006, and its increase up to EUR 5 bln is anticipated by 2010 [7].

Welding robots and robotic stations are the most progressive and effective means of automation of welding and allied processes, they are easily integrated into the general production process. In 2004 the total world park of single industrial robots counted about 850 ths units, of which welding robots made up 254 ths units [8]. In accordance with statistic information of the International Federation of Robotics, 95.4 ths units of industrial robots of about USD 5 bln total cost, were manufactured in 2004. The same year out of the total number of industrial robots, 26.7 ths units of welding robots for the amount of about USD 1.4 bln, were delivered to the world market [9], and about 3 ths units of industrial robots for welding and other technologies (cutting, adhesion bonding, spraying) for the amount of more than EUR 130 mln (USD 162 mln) were delivered to the German welding market. The cited data are indicative of a considerable and continuously growing volume of supply of equipment and systems for new non-traditional technologies and means of automation to the world welding markets, as well as the need to include the products of



these groups into consolidated economic and statistical indices of the world and national welding markets.

Up to now specialists have mainly operated with the total cost of welding equipment produced in the country or with the volume of home welding market, when making direct or comparative evaluation of the general economic value of the national welding fabrications. With such an approach, the real economic contribution made by the manufactured welding equipment to formation of added value at all stages of manufacturing welded products, structures and constructions was ignored. As welding and allied technologies are basic no-alternative technologies in industrial production and construction, a considerable increase of the real contribution of these technologies both into the world and into national economy, in particular into GDP is to be anticipated, as was proved by studies recently carried out in the USA and Germany by the initiative of American Welding Society and DVS.

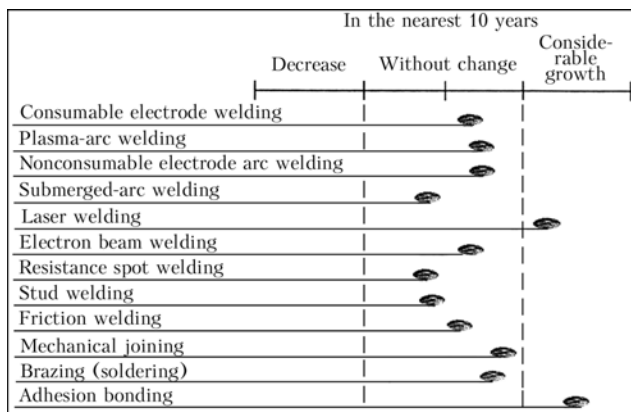
Comprehensive study of welding contribution to the US economy was carried out for seven leading branches of industry (including construction), that are the basis of industrial infrastructure, national defence and prosperity of the country [10]. The total volume of these branches production is a little more than one third of the US GDP. This project was focused on investigation and analysis of general production costs of welding (by all the items of the cost structure). As a result, it was established that in 2000 the total cost of welding exceeded USD 34 bln in the seven investigated branches, while production costs of welding proper were equal to USD 30.7 bln, that, on an average, makes 1.4 % of total production costs in these branches. Extension of the obtained data on the level of economic contribution of welding to such branches as mechanical engineering, mining industry, fuel-power complex and construction, where welding is the key technology, showed that the cost of final product in these branches, produced with application of welding, exceeded 57 % of the total volume of GDP in the USA [11]. By the data of the USA Statistical Department, the number of welders and cutters, including maintenance personnel and operators of weld-

ing and other installations is equal to about 480 ths persons in the above branches [12].

Rhine-Vestfalle Institute of Economic Investigations carried out an evaluation of the actual contribution of welding into German economy in the frame of the project «General economic and branch added value from the manufacture and application of welding equipment». The contribution of welding equipment into general economy added value at all stages of the production process in the branches intensively using welding processes, was studied and analyzed. Here both the direct and indirect added value was taken into account. The results of the study convincingly showed the multiplication effect of increase of added value in manufacturing of welding equipment by 28 times in the process of its future application during the whole industrial cycle (in 2004). The authors of the above-mentioned project showed that general economic added value made EUR 27 bln (USD 33.7 bln) in 2004 or 4.8 % of the added value of the entire German manufacturing sector, taking into account all the added value sources in manufacturing of welding equipment and welding consumables, as well as in welded structure fabrication with application of this welding equipment and technologies. The share of the manufacturing sector was equal to EUR 562.5 bln (USD 703.1 bln) or 33.75 % of GDP. More than 640 ths persons are working with the joining equipment and technology in Germany. In other words, every sixteenth work place in industrial production is connected with welding and allied processes [4, 13].

European manufacturers of welding equipment, attentively following the appearance of scientific and innovation developments in the field of joining equipment and technology, as well as market requirements of different industry and construction sectors for the basic types of welding and joining equipment, worked out corporative evaluation of development tendencies of the welding market and its sectors by the basic technologies [14]. The manufacturers' idea of development of the main joining processes is presented in the Figure.

As it is seen from the Figure, the biggest growth and expansion of production application volumes in the next ten years, is anticipated, first of all, in the field of laser welding, including hybrid processes, as well as in such joining processes alternative to welding as adhesion bonding, mechanical joining (clinchering, caulking, punching and other) and brazing. The tempo of development of the latter is somewhat slower, but it visibly exceeds the development of traditional technologies of electric arc and resistance welding. In the same period, an increase of some market sectors of equipment is anticipated in such innovation attractive processes as friction stir welding, ultrasonic welding, coating and other. Strong growth is retained by market sectors of power sources for fusion welding, automatic control and monitoring systems, diagnostics and non-destructive testing of welded joints. It is typical that the point of view of the European manufacturers of



Technology of joining processes development as presented by European manufacturers [14]



joining equipment practically coincides with the opinion of the users of this equipment, and, in general, it complies with subject directions of scientific studies and technological developments carried out in the national scientific centers, welding institutes and laboratories of higher education institutes.

In conclusion it should be noted that a rather stable development dynamics of both the welding industry and welding market is typical for the industrialized countries that is determined by key nature of welding and joining technologies in different branches of industry and construction, stable growth of structural materials consumption and enlargement of their range, as well as appearance of new progressive technologies and equipment for welding, joining and treatment of structural materials in the market. Development strategies of the national welding industries for the mid-term range practically do not have any drastic differences and are oriented to solving the most urgent tasks: increase of the volumes and widening the areas of welding and allied technologies application, including those sectors of industry and construction where welding was not used before; increase of industrial technological processes efficiency with simultaneous provision of a high quality of the joints; decrease of energy consumption and general production costs for welding and allied technologies; widening the application of new advanced metal, composite and nonmetal materials on the basis of application of new equipment and technologies for their joining and treatment.

Stable and effective development of welding fabrication in industrialized countries is based on the

application of the results of fundamental and applied research, high scientific and engineering potential, qualified labour resources and active transfer of advanced welding technologies and other innovations.

1. (2004) Steel statistical yearbook-2004. In: *International Iron and Steel Institute of Economic Studies*. Brussels.
2. (2005) Internationale Fachmesse «Schweißen und Schneiden» — Stand und Entwicklungstendenz. *Schweissen und Schneiden*, **12**, 1–40.
3. Janben, R., Moos, W. (2005) Schweißen und Schneiden 2004. Schweibtechnik knuepft wieder an hohes Expansionstempo vergangener Jahre. *Ibid.*, **5**, 444–455.
4. Moos, W., Jenben-Timmen, R. (2005) Wertschoepfung und Beschaeftigung durch Produktion und Anwendung von Fuegetechnik. *Ibid.*, **9**, 438–443.
5. (2005) Weltweit fuehrende Plattform fuer Branche. *Stahlmarkt*, **7**, 56–57.
6. Bernadsky, V.N., Mazur, A.A. (1999) State-of-the-art and prospects of the world welding market. *Avtomatich. Svarka*, **11**, 49–55.
7. *Optech consulting. Market report on laser materials processing.* // <http://www.optech-consulting.com/laserprocessing-summary.html>
8. Bernadsky, V.N., Makovetskaya, O.K. (2005) *Economic-statistical data on welding production (SVESTA-2005)*. Kiev: PWI.
9. (2004) *World robotics 2004*. UN Economic Commission for Europe (UNECE) — International Federation of Robotics. United Nations. New York–Geneva.
10. Bernadsky, V.N., Makovetskaya, O.K. (2004) Contribution of welding to economics of USA. *Svarochn. Proizvodstvo*, **5**, 43–50.
11. (2002) Welding's economic impact established. *Welding J.*, **81**(4), 4.
12. Bernadsky, V.N., Makovetskaya, O.K. (2001) *Economic-statistical data on welding production (SVESTA-2001)*. Kiev: PWI.
13. Moos, W. (2001) Wertschoepfung durch Schweibtechnik. *Schweissen und Schneiden*, **9**, 548–551.
14. (2005) Neueste Trends in der Fuegetechnik. *Stahlmarkt*, **8**, 58–59.

TECHNOLOGY AND EQUIPMENT FOR ALL-POSITION AUTOMATIC WELDING OF FILLET WELDS

Automatic welding of fillet welds in all spatial positions is performed in CO₂ with free formation of the metal at welding current of 180 to 300 A; welding speed is 0.08–0.10 m/min. Technology enables performing single-pass overhead welding of fillet welds with 8 to 12 mm leg. Welds form without undercuts or rolls with a smooth transition to the base metal.

Technology provides higher ductile properties of welded joints compared to currently available technologies. Small-sized welding equipment has adequate automation level and provides a high quality of welds, when performed by unskilled operators. Efficiency increases 2 to 2.5 times compared to manual welding.

Technology of welding overhead fillet welds with 8 to 12 mm leg has no analogs in the world practice.

Purpose and application. Technology and equipment are designed for automatic welding in site and on the shop floor in bridge-, ship-building, and when laying tunnels.

Status and level of development. Technology and equipment have passed pilot-production trials and have been introduced in mounting bridges across the Dnieper river in Kiev and Dnepropetrovsk.

Form of co-operation. To be determined during negotiations. Technology, equipment and «know-how» are offered for sale.

Contacts: Dr. Kovtunenko V.A.
E-mail: paton48@paton.kiev.ua

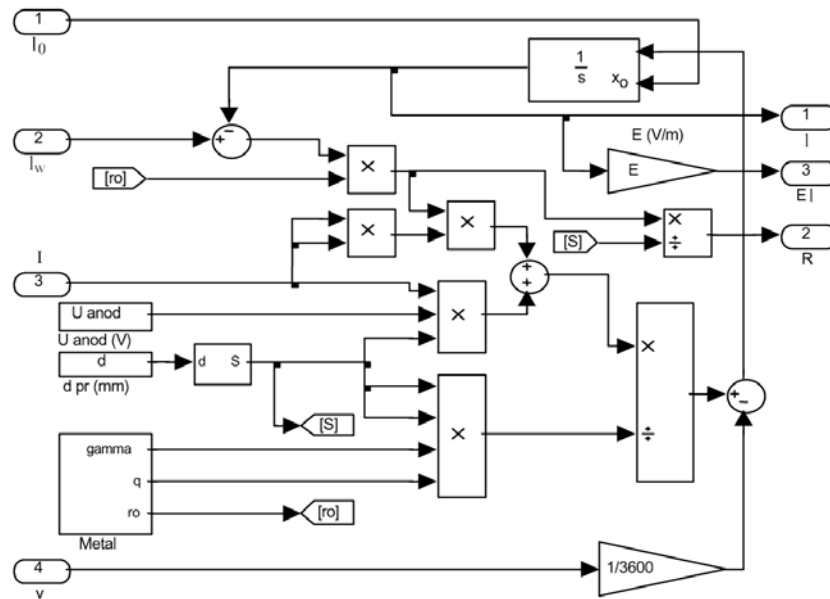


Figure 2. Block simulating consumable-electrode welding arc

ing current polarity) voltage drop, allowing for output potential; i is the instant value of welding current; ρ is the specific electrical resistance of electrode metal; γ , c is the density and specific heat capacity of electrode metal, respectively; T_{melt} is the metal melting temperature; T_0 is the wire temperature at the outlet from the nozzle; λ is the specific heat of metal melting; v is the wire feed rate.

As is seen from Figure 2, «Duga» block includes «Metal» block. This is a parametric block, in which the heat and electrophysical characteristics of electrode wire metal are set. Also calculated in «Metal» block is parameter q ($q = c(T_{\text{melt}} - T_0) + \lambda$ — a constant describing the thermophysical properties of electrode wire metal, which comes to the block output for further use in «Duga» block.

Alongside standard blocks, an additional block « d , S » is also used, which calculates the wire cross-section by its diameter d (see Figure 2).

The kernel of «Duga» block is the integrator-block, which actually solves the differential equation by integration

$$I = \int \left(\frac{SU_{\Delta}i + \rho(I_w - I)i^2}{\gamma S^2 [c(T_{\text{melt}} - T_0) + \lambda]} - v \right) dt + I_0.$$

Input of integrator x_0 is used for setting initial value I_0 .

«Source» block simulating electric circuit is given in Figure 3. Main input of the block is arc voltage drop « Ei », other inputs being parametric. Output is welding current I . Similar to «Duga» block, «Source» block uses standard Simulink blocks: multiplier, divider, summator, scale coefficient. The block which carries the main load, is the integrator with an additional input for entering the initial value. This block solves the differential equation, which describes the electric circuit [1] as follows:

$$\frac{di}{dt} = \frac{1}{L} \left(U_{ps} - R_s i - \rho \frac{I_w - I}{S} i - Ei \right),$$

where L is the inductance of the power source and connecting cables; U_{ps} is the arc power source voltage, which can be both constant and pulsed; R_s is the ohmic resistance of the power source and connecting cables.

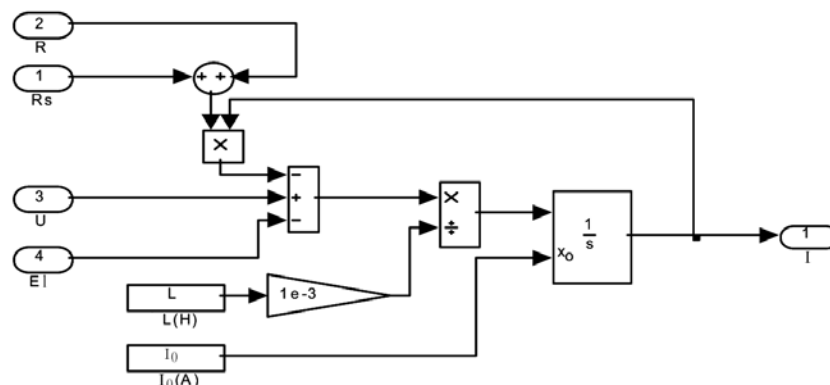


Figure 3. Block simulating electric circuit

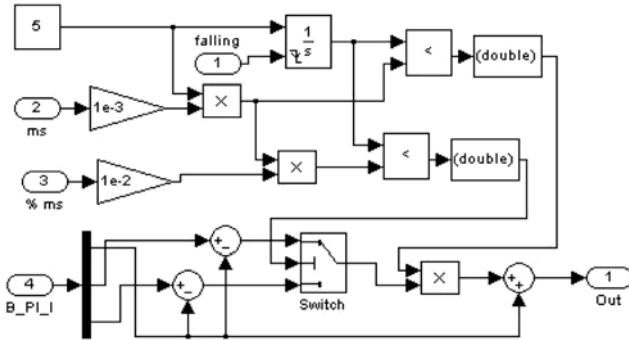


Figure 4. Block simulating power source for pulsed-arc welding

Solving is performed similar to «Duga» block, i.e. differential equation is reduced to integral equation:

$$i = \int \left(\frac{1}{L} \left(U_{ps} - R_s i - \rho \frac{I_w - I}{S} i - EI \right) \right) dt + i_0.$$

If a DC source is to be considered, «U» input is connected to «Constant» block, which assigns open-circuit voltage (see Figure 3). If a power source is studied, in which the output voltage depends on time, this input should be connected to a specialized block. Composition of «I_Source_New» block simulating the power source for pulsed arc welding, is shown in Figure 4.

«I_Source_New» block consists of two parts: former of amplitude and time characteristics of welding current («PI-I» block) and regulator by average value over a period. Regulator integrates the difference between the feedback signal U_{FB} and setting signal U_{Ref} :

$$\int (U_{FB} - U_{Ref}) dt$$

After the signal has achieved zero value, the regulator generates a drop from logical unity to logical zero (rear front). This drop resets the integrator to zero, and also triggers «PI-I» block, which forms the pulses of the high and low level of welding current (in case of a stepped pulse). Equating the integral to zero, the regulator determines the duration, which ensures the stability of a value averaged over a period:

$$\int_0^T U_{FB} dt = U_{Ref}$$

«Constant» block (5) issues a constant signal to integrator input, which is periodically zeroed by the rear front on «falling» input (1). A saw-like signal forms at the integrator output, which by means of two «<» comparators is compared with the levels, which correspond to the durations of the low and high levels of welding current. «Switch» key applies signals corresponding to the amplitude of the low and high level of the pulse to «Out» output (1) of «PI-I» block in the respective time intervals. When the time is

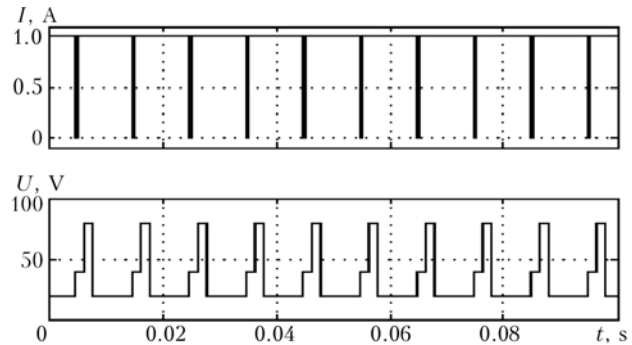


Figure 5. Time diagrams demonstrating the work of the former block

longer than the pulse duration, signal corresponding to basic current, is applied to «Out» output.

Figure 5 gives time diagrams of operation of «PI-I» block for pulsed-arc welding with the following parameters: basic current voltage, pulse voltage of lower and upper level of 20, 40, 80 V, respectively, pulse duration of 3 ms, upper level pulse of 1.5 ms (50 % of pulse) at 100 Hz setting frequency from external generator.

Schematic given in Figure 1, was used at simulation of pulsed-arc sources of arc powering with setting of the pulse repetition rate by an external generator [1]. Similar, but upgraded schematics were used in development of systems for automatic stabilization of average values of arc voltage and welding current with impact on the pulse repetition rate and welding wire feed rate [5].

CONCLUSIONS

1. Experience of MATLAB computer program application at simulation of pulsed-arc systems shows the good prospects for application of this package in development of new welding equipment.
2. When solving the research tasks and during the training process, it is rational to apply the developed block-diagrams for simulation of systems incorporating a consumable-electrode arc, and pulsed power sources, allowing solving non-linear differential equations, which describe the dynamics of arc length variation at electrode melting and of welding current.

1. Sidorets, V.N., Zhernosekov, A.M. (2004) Numerical simulation of the system of power source–consumable-electrode arc. *The Paton Welding J.*, **12**, 9–15.
2. Phillips, C., Harbor, R. (2001) *Feedback control systems*. Moscow: LBZ.
3. Diakonov, V.P. (2003) *MATLAB 6/6.1/6.5 + Simulink 4/5 in mathematics and modeling: Complete user's manual*. Moscow: SOLON-Press.
4. Pavshuk, V.M., Shejko, P.P. *Current source for pulsed-arc welding*. USSR author's cert. 4696750/27. Int. Cl. B 23 K 9/09. Publ. 07.10.91.
5. Zhernosekov, A.M. (2006) *Systems of automatic stabilisation of consumable-electrode pulsed-arc welding process*. Syn. of Thesis for Cand. of Techn. Sci. Degree. Kiev.



LIGHT-WEIGHT WELDED CYLINDERS FOR MOTOR TRANSPORT

M.M. SAVITSKY, A.A. SAVICHENKO, V.M. KULIK, A.F. LUPAN, G.M. MELNICHUK, L.A. CHERTORYLSKY,
N.A. GOLUB and V.A. SUPRUNENKO

E.O. Paton Electric Welding Institute, NASU, Kiev, Ukraine

Design of a welded cylinder for motor transport with a composite skin is described. The possibility of producing light-weight cylinders of different size-types with a specific weight of 0.60–0.65 kg/l is outlined. Guaranteed life of the cylinders is 15–20 years.

Keywords: arc welding, high-strength steel, composite skin, light-weight cylinder, specific weight

Pollution of the environment with toxic fuel combustion products constitutes 70 % of the total pollution in large cities. Utilisation of natural gas (methane) as a motor fuel reduces emissions of CO, hydrocarbons and nitrogen oxides, and eliminates emissions of lead compounds. Moreover, the equivalent amount of gas is 2–3 times as cheap as that of petrol.

Cylinders with a working pressure of up to 19.6 MPa are employed to run cars on compressed methane. Automotive cylinders made from carbon and low-alloy steels with a specific weight of 1.25 and 1.86 kg/l are used currently in trucks and buses in Ukraine. To use cylinders in cars and agricultural machines, their specific weight should be no more than 0.7–0.8 kg/l, which can be achieved through increasing strength of a structural material to $\sigma_t \geq 1275$ MPa by using tubes of nickel-containing steel 20KhN4FA for hot sealing of bottoms and necks. Because of the absence in Ukraine of production of high-quality full-thickness tubes of the required sizes, to manufacture such cylinders it is necessary to turn the

tubes 219×8.5 mm in size both from inside and outside to a size of 215×4.5 mm.

The E.O. Paton Electric Welding Institute developed a design (Figure 1) [1] and technology for the manufacture of combined welded cylinders with a specific weight of 0.60–0.65 kg/l. The gas-tight casing consisting of longitudinally welded skin 1 and two stamped bottoms 4 of the same thickness with butt joints 3 is made from high-strength alloyed steel sheets by TIG welding in argon atmosphere [2]. In sheets 3–6 mm thick the ultimate deviation in thickness is 3–4 times as low as in tubes, and the process of their production at metallurgical enterprises is well-managed. The resulting joints are characterised by a fine-crystalline structure and smooth transition from the weld to base metal at the fusion line. The assigned chemical composition and comprehensive treatment of the longitudinal weld provide its full strength and impart it a high structural and fatigue strength.

Given that stresses in the cylindrical part of the casing are twice as high as in hemispherical bottoms, reinforcing composite skin 2 with a wall of the assigned thickness is formed on it by transverse winding with tensioning of glass fibres impregnated with an epoxy binder and polymerisation at increased temperatures. In the cylindrical part of the casing, the composite skin induces circumferential compressive stresses, which partially compensate for circumferen-

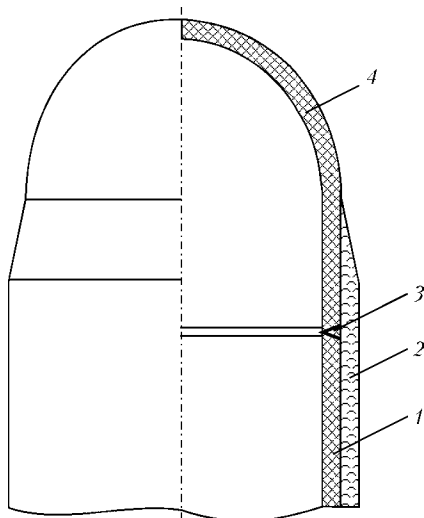


Figure 1. Schematic of combined cylinder with a welded casing made from steel sheets: 1 — shell; 2 — skin; 3 — butt joint; 4 — bottom

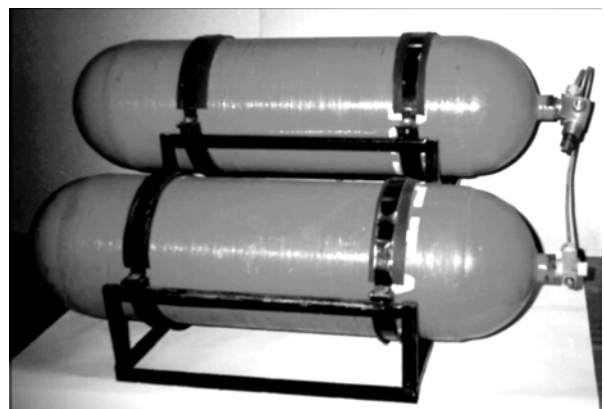


Figure 2. Appearance of combined welded cylinders of different size-types



tial tensile stresses in metal at a working pressure, thus resulting in improvement of performance of a cylinder. Decrease in thickness of the steel casing wall by reinforcing it with the cylindrical composite skin provides decrease in the specific weight of automotive cylinders. This method can be employed to manufacture automotive cylinders (Figure 2) of different size-types in wall thickness, diameter and length, which can be varied both by varying length of a rolled billet and by circumferential welding of several skins.

The combined cylinders with a capacity of 20, 30 and 60 l (610, 845 and 1575 mm long) subjected to hydraulic tests withstand an internal pressure of not less than 52 MPa, which is higher than the working pressure by a factor of more than 2.6. Depending upon the steel casing wall to combined skin thickness ratio, the combined cylinders can have a diameter of 200–400 mm. They can withstand from 15,000 to 24,000 cycles of loading with an internal pressure. The safety factor for strength does not decrease after 15,000 cy-

cles and remains at a level of 2.6. The given quantities of the loading (fueling) cycles provide minimal (15 years) and maximal (20 years) service life of a cylinder [3], based on less than 1000 loading cycles a year.

The technology for manufacture of the combined cylinders with a welded casing, capacity of 28–50 l and diameter of 219 mm was mastered by Kiev enterprises, and is being mastered in Fastov (welded cylinders 335 mm in diameter with a capacity of 50, 70 and 100 l) and in Simferopol (360 mm diameter cylinders). The structural material for the cylinders is a relatively inexpensive sheet steel 30KhGSA, which contains no deficit alloying elements and has been produced in Ukraine for a long time.

1. Paton, B.E., Savytsky, M.M., Kulyk, V.M. et al. *Pressure cylinder*. Pat. 61162 Ukraine. Publ. 2003.
2. Savytsky, M.M., Kulyk, V.M., Lupan, A.P. et al. (2003) *Method of shielded-gas welding of metals and alloys*. Pat. 55385 Ukraine. Publ. 15.04.2003
3. *DSTU UN/ECE R 110-00:2002*.

NEWS

NKMZ FINISHES LARGE-SCALE REDESIGN OF PLATE MILL 2800 AT ALCHEVSK METALLURGICAL WORKS

«One may build future with NKMZ» ---- said chairman of the board of corporation «Industrial Union of Donbass» (IUD) Sergej Taruta when estimating operation of a new state-of-the-art plate mill 3000 (TLS 3000), supplied by producers of Novo-Kramatorsk Machine-Building Works (NKMZ) to Alchevsk Metallurgical Works (AMK). On 7th of November a test rolling was performed on the mill. At present final adjustment works are being terminated. With every passing day new functions are being implemented step by step on the mill, and its operation approaches automatic mode. Design supervision and adjustment of the mill are performed at present by a big group of NKMZ specialists and more than one thousand representatives of other companies. Official commissioning should take place in near future, but in the process of adjustment the mill also produces saleable material.

TLS 3000 is the result of large-scale redesign of its predecessor TLS 2800, for which producers of NKMZ manufactured about 7 thousand of intelligent equipment. Now TLS 3000 corresponds by quality of produced rolled stock, level of possibilities, and automation of technological processes to similar mills, manufactured by known world brands «Fest Alpine» (Austria) and «Mannesmann Demag» (Germany).

Metallurgists, when mastering new possibilities of TLS 3000 and comparing it with the predecessor, get convinced that this is really state-of-the-art rolling complex, one of additional advantages of which is comfortable working conditions.

The customers are satisfied. When sharing his impression after inspection of the mill, Sergej Taruta noted at once how quietly (according to the scale of metallurgists) operates new mill, while near TLS 2800 voice sank in deafening roar. He emphasized that possibilities of new mill in complex with operating line of continuous steel casting, produced by «Fest Alpine» company, will allow Alchevsk metallurgists mastering production of rolled stock of the most special-purpose steels: high strength ones for pipe industry and wear-resistant ones for machine building industry, and getting introduced into new segments of the market.

New mill also impressed member of the board, head of metallurgical sector of «Fest Alpine» Carl Gruber. He said: «TLS 3000 is very successful investment for corporation IUD, which will ensure for it good advantages». Carl Gruber congratulated NKMZ team, which designed new mill, and wished producers of Novo-Kramatorsk further success in their work.



THESIS FOR SCIENTIFIC DEGREE

I.I. Polzunov State Technical University in Altai

V.L. Knyazkov (Joint Stock Research Association «Kuzbass Welding Centre») defended on the 14th of December, 2006, the thesis for a Candidate of Technical Sciences degree on subject «Increasing Efficiency of Manual Modulated-Current Covered-Electrode Arc Welding through Automatic Adaptation of Parameters to the Technological Process».

The work shows that the cause of low productivity and low quality of welded joints in manual covered-electrode welding of relatively thick metal structures (pipelines) in spatial positions other than the flat one is that under the conditions recommended in regulatory documents a welder has no possibility to adjust the heat power of the arc depending upon the thermal-physical situation within the welding zone without interruption of the arc and complete utilisation of the welding-operational properties of basic electrodes.

The model is suggested, describing an electrode metal transfer in modulated-current welding with allowance for the geometry of a plug formed in melting of a covering, as well as one of the main effective forces, i.e. the pressure of gases formed in dissociation of gas-forming components of the covering.

Methods are offered for active control of the heat power of the arc with a pulse modulation of process parameters that realise the «machine-man-technology» concept, at which the modulating parameter is arc voltage U_a (its deviation from set value U_s is no more than 2 V), and the modulated parameters are durations of the main current pulses and main current

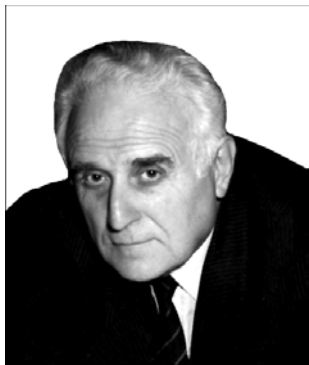
pauses. The procedure was developed for substantiated evaluation of the amplitude value of main and extra current pulses, as well as a set value of arc voltage, U_s , at which the best welding-operational properties of covered electrodes become most apparent.

It was experimentally found that the developed methods for active control of the heat power of the arc allow the volume of the weld pool to be adjusted without interruption of the arc by decreasing a mean value of the welding current, I_{mean} , to 30 A, the operational stability of the process (using 2.5 mm diameter electrodes of the TsU-5 and TsL-39 grade) remaining at the same level.

As experimentally established, frequency of extra pulses, f_{EP} , equal to more than 50 ms and duration of extra pulses, t_{EP} , within 0.5–2.0 ms eliminate the harmful effect on visual function of a welder by light flow pulsations, and, at the same time, provide a high stability of the arc and operational stability of the process in duration of the main pause, t_{pause} .

The performed experimental studies show that, in welding with pulse modulation of the welding current within a range of its mean values equal to that under the steady-state conditions recommended in regulatory documents, the welding-operational properties of electrodes TsU-5 and TsL-39 are not less than 30 % higher, the content of alloying elements in metal deposited with electrodes of the E-09Kh1MF type is higher (C --- 0.015 %, Si --- 0.12 %, Mn --- 0.2 %, V --- 0.05 %), and the content of Cr and Mo in welding with the modulated current depends upon the value of I_{pulse} and does not depend upon the value of I_{mean} .

OUR CONGRATULATIONS

IGOR K. POKHODNYA IS 80

Igor K. Pokhodnya is a known Ukrainian scientist working in the field of metallurgy and technology of metals, materials science and electric welding, a prominent public figure, outstanding organiser of science, academician of the National Academy of Sciences of Ukraine, laureate of State Prizes of the USSR and a State Prize of Ukraine in the field of science and technology, Prize of the Soviet of Ministers of the USSR, Evgeny Paton Prize and N.N. Dobrokhotoy Prize of the NAS of Ukraine, Professor, Doctor of Technical Sciences, and Honoured Worker of Science and Technology of Ukraine. He is a representative of the world-renowned scientific school founded by E.O. Paton and B.E. Paton. Fundamental research into physical-chemical processes of arc welding and development of new high-efficiency processes of mechanised welding and surfacing are related to the name of I. Pokhodnya. He founded a scientific school of metallurgy and technology of welding, made a great contribution to development of the most important aspects of the theory of arc welding, high technologies and advanced welding consumables, and to arrangement of domestic production of welding consumables. He is active in implementation of scientific ideas into specific developments and their wide-scale application to many sectors of the national economy.

I.K. Pokhodnya was born on the 24th of January, 1927, in Moscow. In 1930–1941 he lived and studied in Minsk. During the Second World War he evacuated to the Tambov District (Russia). There he was a manual worker, and then worked as a tractor driver. In 1944 he finished secondary school without attending classes and entered the Kiev Polytechnic Institute (KPI). He graduated from the Institute in 1949, being qualified as a mechanical engineer. In 1950–1952, I. Pokhodnya was working as a welding engineer, managing the welding bureau at the Donetsk Engineering Factory named after the 15th Anniversary of

the Young Communist League of Ukraine. He was in charge of efforts on automation of welding of mining equipment structures. In 1952 he became a post-graduate student and research engineer at the E.O. Paton Electric Welding Institute of the Ukrainian SSR Academy of Sciences. Since then his entire life and activity have been inseparably linked with the E.O. Paton Electric Welding Institute and the National Academy of Sciences of Ukraine.

In 1954 I. Pokhodnya generated the fundamental data on mean temperature of the weld pool in submerged-arc welding, distribution of temperature in the pool, and relationship between temperature of the pool and its chemical composition. These results received international recognition.

I.K. Pokhodnya investigated metallurgical problems of surfacing of high-chromium ledeburite steels, developed alloys and technologies for arc and electroslag surfacing using fluxes and shielding gases, which are still employed by the mining and smelting industry. These investigations formed the basis of his candidate of technical sciences thesis, which Pokhodnya successfully defended in 1955.

In 1956 B.E. Paton initiated the USSR program for development of welding science and technology. And I. Pokhodnya took an active part in the work. The program was approved in 1958 by decision-making authorities of the USSR. Implementation of the program predetermined the progress of welding science and technology in the USSR in the second half of the 20th century.

In 1958 I. Pokhodnya became a laboratory chief, and since 1962 he has been the Head of the Department for Welding Arc Physical-Chemical Processes at the E.O. Paton Electric Welding Institute.

In the 1960-s I.K. Pokhodnya developed an ingenious method for high-speed X-ray filming of fast processes, which allowed generation of the pioneering and reliable data on melting and electrode metal transfer processes occurring in covered-electrode, submerged-arc and underwater welding. The processes of absorption and desorption of gases by molten metal under the arc discharge conditions were studied. The mechanisms of the impact by welding parameters, density and polarity of current on temperature of metal droplets and time of interaction of the droplets with a surrounding atmosphere, as well as of the effect by electrode covering type on melting and metal transfer processes in covered-electrode welding were established.



Results of these studies were generalised in his Doctor's thesis (1968), and in book «Gases in Welds». This work was a major input into the theory of welding processes, and served as a theoretical basis for the development of many new grades of low-toxicity and high-efficiency electrodes. Mass production of these electrodes was arranged. Wide application of low-toxicity electrodes provided a radical improvement in work environment of welders and workers of related professions, as well as a dramatic decrease in the rate of occupational diseases.

For several decades I.K. Pokhodnya has been managing research on metallurgical processes of flux-cored wire welding.

Commercial sample of flux-cored wire requiring no extra shielding of molten metal was developed in 1959. A new, high-efficiency area of arc welding mechanisation was opened up. Development of self-shielding flux-cored wires was a breakthrough in the technology of welding. Their application made it possible to solve the problem of mechanisation of welding processes in site, in open-air shops, under field conditions, and on berth.

Together with associates of the Department, I. Pokhodnya developed a range of gas-shielding flux-cored wires and arranged their commercial production in Ukraine and Russia.

Priority of our scientists was covered by the author's certificates of the USSR, Bulgaria and Czechoslovakia, as well as patents of the USA, West Germany, Great Britain, France, Italy, Austria, Switzerland, East Germany, Hungary and other countries. Domestically produced processing lines, equipment and know-how were supplied to companies in the USA, West Germany, France, Japan, Czechoslovakia, Hungary, Bulgaria, Argentina and China.

Investigations into the main mechanisms of formation of the weld metal, alloying and solidification of the weld pool under conditions of artificial cooling of the weld surface and variable spatial position of the weld pool, conducted under the leadership of I. Pokhodnya, allowed the development of new self-shielding flux-cored wires, advanced technology and equipment for position butt welding of pipes. These solutions were embodied in the specialised «Styk» system. Wide application of the advanced arc welding technology and equipment allowed the welding production to be re-equipped for construction of main pipelines.

In 1965, B.E. Paton launched the project on development of methods and equipment for welding in space. I.K. Pokhodnya took an active part in research to study behaviour of molten metal in arc welding under variable gravity conditions. The studies resulted in the development of a unique method for arc welding in vacuum and in zero gravity. Testing of this method was included into the program of the world's first technological experiment on welding in space, which was accomplished in 1969.

In the 1970-s, I. Pokhodnya was active in developing new ideas on utilisation of flux-cored wires for

out-of-furnace treatment of metal melts. New types of wires containing high-reactivity elements for micro alloying, modification and desulphurisation of steels and cast irons, technologies and equipment for production of large-diameter flux-cored wire were developed. Technologies for treatment of melts by the method of flux-cored wire injection received wide acceptance at the factories of Ukraine, Russia, Belarus and other countries.

The I.K. Pokhodnya's school is characterised by deep theoretical analysis, highly qualified experimental procedures and wide application of up-to-date physical investigation procedures.

New methods were developed for analysis of diffusible hydrogen in the welds. They were standardised in the USSR and included into the national standards of the USA and Japan.

Information-measuring systems were created for statistical analysis of electric and time parameters of the arc welding processes, investigation and monitoring of operational properties of welding consumables and power supplies. The investigation results were generalised in book «Metallurgy of Arc Welding. Arc Processes and Electrode Melting» by I.K. Pokhodnya (1990). This book received international recognition. It was translated into English and published in Cambridge in 1995.

I.K. Pokhodnya was one of the first to apply the methods of mathematical modelling of welding processes. In 1978 he presented his paper «Mathematical Modelling of Behaviour of Gases in Welds» at the IIW Congress. The paper was published as a separate edition, describing results of investigations into peculiarities of growth of a gas bubble in the solidifying weld pool, interaction of molten slag with solidified metal, thermodynamic investigations of high-temperature processes in the «metal-gas-slag» system, kinetic investigations of interaction of low-ionised plasma with molten metal, prediction of structure of the heat-affected zone of a welded joint, and investigations of the kinetics of solid-state interaction of multi-component systems, etc.

The work headed by I.K. Pokhodnya to find effective ways of improving sanitary-hygienic characteristics of welding consumables is in process. Examinations of structure and phase composition of welding fumes, determination of relationship of solubility of a particulate matter of welding fumes and its biological activity resulted in generation of the most comprehensive data needed for hygienic evaluation of welding consumables. Methods for express evaluation of toxicity of welding fumes were developed. Results of these studies were internationally recognised, and they were presented in a book by V.G. Vojtkевич published in Cambridge.

The efforts of the last decade made by I.K. Pokhodnya and his followers have been dedicated to further development of the theory of the arc welding processes and physical materials science of welded joints.

Noteworthy is the work on investigation of liquation of elements in the welds and formation of chemical micro heterogeneity, study of conditions of rational alloying of the weld metal and role of certain elements (nickel, manganese, silicon, phosphorus, copper, chromium and molybdenum) in formation of structure of the weld metal and variations in its cold resistance.

Much consideration is given to addressing the problem of gases in the welds. The physical model of absorption of gases in arc welding developed under the leadership of I.K. Pokhodnya served as a basis for working out of mathematical description of absorption of gases from the arc plasma and computer simulation of this process. Investigations were conducted to study kinetics of absorption of gases, derive the dependence of the flow of an absorbed gas upon the time, temperature of plasma, partial pressure of gases and other factors. Results of these studies were summarised in his book «Metallurgy of Arc Welding. Interaction of Metals and Gases» (2004).

V.I. Shvachko developed, under the leadership of I.K. Pokhodnya, a new model of hydrogen-induced embrittlement of bcc metals. According to this model, atomic hydrogen adsorbed on the surface of iron in the form of negative ions changes the energy state of a sub-microcrack, which initiates in the dislocation cluster during deformation, and then, during the initial period, propagates following the classic Griffith scheme. The new model reveals the physical nature of the effect of hydrogen, and allows its known peculiarities to be qualitatively explained.

New notions of the mechanism of the effect of hydrogen made it possible to develop the experimental procedure to study sensitivity of steels to brittle fracture in the presence of hydrogen. A new criterion was suggested to evaluate resistance to brittle fracture.

The Department headed by I.K. Pokhodnya has close contacts with manufacturers and users of welding consumables in our country and abroad. Advanced welding consumables, i.e. electrodes, flux-cored wires and fluxes, developed by the Department gained wide acceptance and are now applied at thousands of companies and construction sites of Ukraine, Russia, Belarus and other former Soviet Union and foreign countries.

I.K. Pokhodnya is the author and co-author of more than 900 scientific studies, including 28 books, 8 of which were published in the USA, Great Britain, China and Czechoslovakia, 188 inventions, 158 foreign patents, and 6 patents of Ukraine. 38 candidates of technical sciences, among which 6 became doctors of sciences, were trained under his scientific supervision. He was given the title of professor for his active work on training the scientific workers. In 2001 he was elected an Honorary Doctor of the National Technical University of Ukraine «Kiev Polytechnic Institute».

I.K. Pokhodnya was awarded the orders of the USSR and many medals for his fruitful scientific and

practical activities, and for his contribution to development of the national economy. The works on realisation of licenses to produce new welding consumables in the USA, West Germany, France, Czechia and Slovakia, Hungary, Bulgaria, China and Argentina were performed under the leadership of I.K. Pokhodnya.

He took an active part in arrangement of efforts on liquidation of consequences of the accident at the Nuclear Power Station in Chernobyl, being a member of the task commission and chairman of the sub-committee of the NAS of Ukraine for science and technology problems. His role was described in a two-volume edition of the NAS of Ukraine «Chernobyl 1986–1987» and commemorated with Appreciation by the Chairman of the USSR Government Commission, Honorary Medal of Liquidator of Accident at the Chernobyl Nuclear Power Station, and Merit Badge of the NAS of Ukraine «For Scientific Achievements».

For 36 years I.K. Pokhodnya has been conducting a fruitful scientific and organisational activity at the National Academy of Sciences of Ukraine. He made a great contribution to the progress of science and strengthening of international authority of Ukraine. Holding a post of chief scientific secretary at the Presidium of the Ukrainian SSR Academy of Sciences (1970–1983) and first Vice President of the Ukrainian SSR Academy of Sciences (1983–1988), I.K. Pokhodnya devoted much force and energy to improvement of planning, arrangement and coordination of research, strengthening of international scientific contacts of the NAS of Ukraine, promotion of achievements of the Academy institutions, propagation of experience of the Academy in raising the efficiency of research and reducing the terms of its implementation, selection and training of specialists in organisation of research.

Many times since 1988 I.K. Pokhodnya has been elected an academician-secretary of the Department of Physical and Technical Problems of Material Studies at the NAS of Ukraine. Holding this very important appointment, I.K. Pokhodnya pays much attention to arrangement of new areas of research in the field of materials science, coordination of efforts, training of research workers and science organisers, teaching of young scientists, and strengthening of the resource bases of the Academy institutions.

I.K. Pokhodnya is an executive editor and author of books «Modern Materials Science: 21st Century» published in Ukraine and Great Britain, and «Advanced Materials and Technologies» (in 2 volumes). These books were prepared with active participation by prominent materials scientists from Ukraine, Russia, Great Britain, China, Yugoslavia, Poland and Slovakia. The books analyse the state-of-the-art in different areas of materials science and predict trends of its further development.

The Department of Physical and Technical Problems of Material Studies headed by I.K. Pokhodnya plays a prominent role at the NAS of Ukraine.



Igor K. Pokhodnya combines the research and science-organisational activity with an active public work. He was a deputy of the Supreme Soviet of the Ukrainian SSR, member of the Presidium of the Supreme Soviet of the Ukrainian SSR, member of the Trade Unions Council of Ukraine and the Committee of Ukraine at UNESCO, and President of the «Ukraine–Belarus» Society.

I.K. Pokhodnya was awarded the orders of Ukraine «For Service» of the 1st, 2nd and 3rd degrees for his great contribution to the progress of science, development and application of new high-efficiency tech-

nologies, and strengthening of international authority of the national engineering school in the field of welding, and for his many years' scientific and public work.

Igor K. Pokhodnya, an outstanding scientist, teacher and prominent public figure, is noted for his hard-working, enthusiasm for job, adherence to principles, decency, modesty and tactfulness. For these qualities he won the authority and respect among his colleagues and friends.

Igor K. Pokhodnya meets his jubilee with new creative plans and ideas, and works purposefully and energetically to make them a reality.

A.Ya. ISHCHENKO IS 75



Anatoly Ya. Ishchenko, Professor, Doctor of Technical Sciences, Corresponding Member of the NAS of Ukraine, Head of Department for Physical-Metallurgical Processes of Welding Light Metals and Alloys at the E.O. Paton Electric Welding Institute of the NAS of Ukraine, Honoured Worker of Science and Technology of Ukraine, celebrates his 75th birthday in January 2007.

Upon finishing a secondary school in Gorlovka, A.Ya. Ishchenko entered the Kiev Polytechnic Institute. After graduating from the Institute in 1956, he was assigned to the N.D. Kuznetsov Aircraft Engine Works in Kujbyshev.

He has been working at the E.O. Paton Electric Welding Institute since 1961. Here he passed the path from a leading engineer to a department head, and was elected a Corresponding Member of the National Academy of Sciences of Ukraine.

A.Ya. Ishchenko was the first in the world practice to develop and practically apply the high-efficiency process of electroslag welding of aluminium, and in 1967 he defended his candidate of technical sciences degree thesis on this subject. Starting from 1968, his scientific activity has been related to investigations into weldability of high-strength aluminium alloys and development of efficient technologies for welding of aerospace engineering parts. Working in close collaboration with branch organisations, he made a great contribution to the development and practical appli-

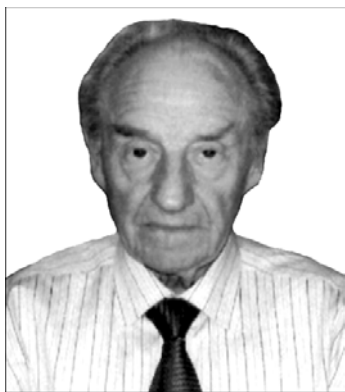
cation of new base materials and welding consumables with different alloying systems. This work cycle was completed with a wide commercial application of technological processes, welding consumables and equipment. It served as a basis for his doctor's thesis, which he successfully defended in 1983. In the next years, he personally and his associates carried out the in-depth investigations of weldability of aluminium-lithium and aluminium-scandium alloys, which received an international recognition. Since 1987, being a Department Head, A.Ya. Ishchenko has been successfully carrying out theoretical and experimental studies of the phenomena occurring within the welding zone in interaction of aluminium alloy components and composite materials with the arc plasma, electron and laser beams, and investigating the mechanisms of primary solidification and formation of structure of the welds under non-equilibrium conditions, as well as their effect on physical-mechanical properties of the welded joints. Significant results were obtained in the development of new, more efficient methods for making of permanent joints in solid state, nanotechnologies for manufacture of base and filler materials having a sub-microscopic structure, which improves technological and functional properties of the joints in advanced high-strength materials, such as heat-resistant alloys, fine composites, intermetallics and dissimilar combinations of materials. The Department, having three doctors and four candidates of technical sciences in its staff, maintains sustained international cooperation and constant creative contacts with many institutions of the National Academy of Sciences of Ukraine.

A.Ya. Ishchenko is an author of three books, over 280 papers and inventions. He is a member of the Scientific Council of the E.O. Paton Electric Welding Institute and Specialised Board on Defence of Theses for Candidate and Doctor of Technical Sciences Degrees, expert of interdepartmental committees of a number of state programs, Chairman of the National Committee «Aluminium» at the International Institute of Welding, and a member of the American Welding Society.

He was awarded as a member of the team of authors the State Prize of Ukraine in the field of science and technology for a cycle of works «Theoretical Principles of Manufacture of Critical Machine Components and Parts from Light Structural Materials» (1995), and Prize of the Council of Ministers «For the De-

velopment and Introduction into Production of High-Efficiency Methods and Devices for Welding Aluminium, Magnesium and Titanium Alloys» (1988). Also, he is a laureate of the Diploma of the Supreme Soviet of the Ukrainian SSR (1984).

F. BLUME IS 80



F. Blume, a well-known German scientist in the field of automation of welding engineering, Doctor of Technical Sciences, Professor, former Chief of the Welding and Assembly Chair at the Dresden Technical University, is 80 in January this year.

F. Blume started his labour activity at the Railway Repair Factory (Reichsbahn) in Halle and Dresden. In 1952 he graduated from the Engineering Institute in Mittweide, and in 1955 he received a welding engineer diploma. In a year he became an auditor in the field of boiler production. Starting from 1957, F. Blume was responsible for training welding engineers and operators for railway companies of the former GDR. In 1970 he defended his Doctor's thesis at the Magdeburg Technical Institute. There he was in charge of the issues of strength of welded joints, allowing for the effect of different defects. His works done in this field were taken into account in the development of different codes on strength design of welded joints. In 1971, F. Blume was awarded the scientific title of Professor and appointed as a Chief of the Welding and Assembly Chair at the Dresden Technical University. He defended his Doctor-Engineer's thesis in 1985.

F. Blume made a great contribution to the development of welding science and technology. The main areas of his activity include simulation of welding processes, automation of assembly-welding processes, surfacing and surfacing consumables, adhesive bonding, and information modelling of the welding technology.

F. Blume is an author of over 120 publications and 150 papers, co-author of 8 books and about 40 author's certificates. He is active in training scientific staff. 320 certified engineers, 76 doctors and 6 doctor-engineers were trained under his leadership. For many years F. Blume has been actively cooperating with the E.O. Paton Electric Welding Institute. He was a GDR delegate of group 15 (Surfacing) of the COMECON Coordinating Board. There he took part in the development of different recommendations in the field of surfacing and surfacing consumables. He intensively collaborated in this area with Department of the Paton Institute, headed by I.I. Frumin, and often visited the Institute. F. Blume took an active part in social life of welding organisations. Thus, from 1968 till 1978 he was elected a Chairman of the Central Board on welding acting under the GDR Chamber of Technology, participated in work of the editorial board of the «Blechnik» Journal (GDR), was a member of the examining board of the Central Welding Institute in Halle for welding engineers, and initiated in 1990 the foundation of the Association of German Welders «DVS DDR».

From 1990 till 1996 F. Blume was a Chairman of the already joined Association of German Welders in Saxony. He has a well-deserved authority and respect with wide circles of welding scientists and engineers both in Germany and abroad. His followers develop the research efforts he initiated, working at different institutions of Germany and abroad, as well as at industrial enterprises.